



THE UNIVERSITY OF
WAIKATO
Te Whare Wānanga o Waikato

Research Commons

<https://researchcommons.waikato.ac.nz/>

Research Commons at the University of Waikato

Copyright Statement:

The digital copy of this thesis is protected by the Copyright Act 1994 (New Zealand).

The thesis may be consulted by you, provided you comply with the provisions of the Act and the following conditions of use:

- Any use you make of these documents or images must be for research or private study purposes only, and you may not make them available to any other person.
- Authors control the copyright of their thesis. You will recognise the author's right to be identified as the author of the thesis, and due acknowledgement will be made to the author where appropriate.
- You will obtain the author's permission before publishing any material from the thesis.

**Seismic Reflection Characterisation and Geomorphology of the Katikati Basin,
Te Awanui (Tauranga Harbour), Aotearoa New Zealand**

A thesis
submitted in partial fulfilment
of the requirements for the degree
of
Master of Science (Research) in Earth Sciences
at
The University of Waikato
by
Erin Mathews



THE UNIVERSITY OF
WAIKATO
Te Whare Wānanga o Waikato

2024

Abstract

Te Awanui (Tauranga Harbour) contains two distinct basins the Katikati Basin in the north, and the Tauranga Basin in the south. The Katikati Basin is not well understood or researched as there is bias towards the Tauranga Basin due to dredging and port activities.

This thesis investigated the Katikati Basin below the surface via a shallow seismic survey and above the surface using historic air photographs and hydrographic charts. No obvious faults were discovered within the seismic survey, therefore the faults found in the Tauranga Basin which are potentially associated with the Taupō rift may not extend into the Katikati Basin. The area surrounding the low gravity anomaly was analysed and there was no clear indication of a caldera therefore the seismic survey did not penetrate deep enough to reach the sediments associated with the low gravity anomaly. The historical air photographs and hydrographic charts showed that most of the changes to the geomorphology occur at the entrance where the tidal inlet has narrowed and deepened and at Waikoura Point on Matakana Island the spit tip changes shape and goes through periods of erosion and accretion especially during a triple-dip La Niña event of the El Niño Southern Oscillation Cycle.

Unfortunately no coring samples were taken within the Katikati basin for this study, therefore the true thickness of the Holocene sediments were not determined however, other studies revealed Holocene sediments up to 20 m in depth which was the depth of this seismic survey therefore I am certain no Pleistocene sediments were reached. There is much more to be researched on the Katikati Basin and this thesis builds as a starting point.

Acknowledgements

Writing this thesis has been a journey in itself. Thank you to everyone who has taught me during my studies at Waikato University and the people I met along the way. I am most grateful to be one of Willem's last master's students at Waikato, and I appreciate all your support in the early stages of my thesis. A massive thank you to Andrew who happily took over the final months of my master's degree as my supervisor to push me over the finish line.

I appreciate everyone who helped fund and collect the field work, without you a major portion of this thesis would not have been possible. A special acknowledgement to Marlena who gave me the first initial push to start the background section of this thesis, your guidance and expertise of the Tauranga geology I appreciated a lot. I would like to recognise the time and effort Ed put in with guiding me tremendously with Petrel and setting up the data. And thank you to Dave for helping me with my seismic maps.

Lastly, to my family, work colleagues, and friends you all supported me through my whole university journey and listened to me rant on about my work, especially this thesis. I couldn't have done it without you.

Table of Contents

Chapter 1: Introduction	9
1.1 Introduction	9
1.2 Study Aim and Objectives	14
1.3 Thesis Outline	15
Chapter 2: Background	16
2.1 Introduction	16
2.2 Regional Geology	16
2.2.1 Volcanism of the Tauranga Volcanic Centre	16
2.2.2 Regional Tectonics	20
2.2.3 Caldera Structures around Te Awanui.....	23
2.3 Te Awanui (Tauranga Harbour)	27
2.3.1 Geomorphology and Landform Evolution	27
2.3.2 Tsunami Erosion Events.....	28
2.3.3 Matakana Island	31
2.3.4 Vertical Land Movement	33
2.4 Sediments	35
2.4.1 Holocene Sediments.....	36
2.4.2 Pleistocene Sediments.....	36
2.4.3 Sediment Sources	37
2.4.4 Sedimentation Rates	38
2.5 Hydrodynamics	39
2.5.1 Wave and Tidal Environment	39
2.5.2 Catchment	42
2.6 Summary.....	43
Chapter 3: Seismic Reflection Characterisation	45
3.1 Introduction	45
3.2 Seismic Reflection Basics	46
3.3 Methods	47
3.3.1 Seismic Field Methods.....	47
3.3.2 Seismic Data Processing	47
3.4 Seismic Interpretation	49
3.5 Structure Contour Maps	51
Seafloor.....	51
Horizon A	51
Horizon B.....	52
3.6 Isopach thickness Maps	56
3.7 Bowentown.....	59
3.8 Low Gravity Anomaly Area	61
3.9 Summary.....	62
Chapter 4: Historical Air Photographs	63
4.1 Introduction	63

4.2 Methods	63
4.3 Historical Air Photographs of the Katikati Basin.....	64
4.3.1 Historical Air Photographs of the Katikati Entrance.....	68
4.4 Hydrographical Charts of the Katikati Basin.....	70
4.4.1 Morphology of the Katikati Basin as Determined from Hydrographical Charts	70
4.4.2 Changes in Morphology of the Katikati Basin as Determined from Hydrographical Charts.....	70
4.5 Changes in the Ebb Tidal Delta and Barrier Spit	73
4.6 Drivers of Change	75
4.6.1 El Niño Southern Oscillation Cycle	75
4.6.2 Triple-dip La Niña Events	76
4.7 Effects of ENSO on Matakana Island.....	77
4.7.1 Changes to the Spit Tip of Matakana Island and Ebb Tidal Behaviour.....	77
4.8 Summary.....	78
Chapter 5: Summary and Discussion.....	79
5.1 Introduction	79
5.2 Seismic Interpretation	79
<i>Stratigraphy.....</i>	79
<i>Faulting.....</i>	80
<i>Low Gravity Anomaly.....</i>	80
5.3 Historical Air Photographs	81
<i>Geomorphology.....</i>	81
<i>Effects of the ENSO on the Katikati Basin.....</i>	82
5.4 Limitations	82
5.5 Summary.....	83
Chapter 6: Conclusion	84
6.1 Summary of Research Findings	84
6.2 Recommendations for Future Work	85
References.....	87

List of Figures

- Figure 1.1.** Satellite image showing the location of Te Awanui (Tauranga Harbour) and major geomorphic features, within the North Island of New Zealand (red dot) created using Google Earth.....10
- Figure 1.2.** Map showing the major physiographic units of the Tauranga Region, other geological units, faults, and major rivers and streams (de Lange et al., 2015).13
- Figure 2.1.** Simplified geological map from Prentice (2023) highlighting the distribution and stratigraphy of volcanic landforms and structures associated with the Tauranga Volcanic Centre (TgaVC). (a) North Island/Te Ika-a-Māui of New Zealand. The red box highlights western Bay of Plenty. (b) Simplified geological map of the TgaVC. Extensional faults associated with the TgaVC are shown as dashed lines, with previously identified non-active faults from Leonard *et al.* (2010) shown as solid lines. (c) Volcanic stratigraphy of the TgaVC. Stratigraphic formation age ranges are shown as coloured bars with dated individual volcanic centres (Minden Rhyolite Subgroup) or defined ignimbrites (Pāpāmoa Formation).17
- Figure 2.2.** Evolution of the Taupō Rift over the last 2 Ma with red lines representing active faults, black lines inactive faults, and dashed circles are the volcanic centres (Villamor et al., 2017). The Tauranga Volcanic Centre is feature 1.....22
- Figure 2.3.** Interpretation of residual gravity anomalies around the Taupō and Bay of Plenty areas. The black thick dashed line represents the old TVZ and the thick black line is the present TVZ. The red lines are the known caldera margins. Low gravity features including sedimentary basins and potential calderas are the smaller black dashed lines. (Stagpoole et al., 2021). ..26
- Figure 2.4.** Map demonstrating the locations of the different morphological shoreline types around Te Awanui, re-drawn from (de Lange et al., 2015; Tonkin and Taylor, 2018).28
- Figure 2.5.** Map of Matakana Island demonstrating the landforms and former shorelines. S1 and S2 are eroded shorelines, S3 is the Kaharoa shoreline, and EHS is the earliest Holocene shoreline, (Shepherd et al., 1997).....30
- Figure 2.6.** Stratigraphy of WAI 1 core taken from the seaward end of Emerton Road at Waihi Beach (Bell et al., 2004).31
- Figure 2.7.** Map of Matakana cores showing the Pleistocene geomorphic features. The dashed line represents the “Relict Pleistocene Marine Cliff”. The P stands for the Pleistocene parabolic dunes, and BGB stand for Blue Gum Bay. Numbers 1 to 5 represent well-log locations (Shepherd et al., 1997).33
- Figure 2.8.** Approximate vertical land movement data for Te Awanui. Retrieved from: <https://searise.takiwa.co/map/6233f47872b8190018373db9/embed>.....34

Figure 2.9. Location of the wave buoy relative to the Katikati entrance in the Bay of Plenty, including isobaths (Macky et al., 1995).	41
Figure 2.10. Location of the permanent Bowentown Wave Buoy (https://envdata.boprc.govt.nz/).....	42
Figure 3.1. Location of seismic lines within the Katikati Basin for the 12 th of October in red and the 13 th of October in blue.	45
Figure 3.2. Deployment of various shallow-water sub-bottom profiling systems used for a seismic survey (Penrose et al., 2005).....	47
Figure 3.3. All seismic lines processed in Petrel. This does not match Figure 3.1 exactly because not all lines were suitable for analysis.....	48
Figure 3.4. A) Uninterpreted seismic line through the main channel. B) Corresponding interpreted seismic line showing the Seafloor, Horizon A, and Horizon B reflectors. C) Location of the seismic line.	50
Figure 3.5. Seismic line from Stella Passage showing MacPherson, et al. (2017)'s interpretation of the seismic reflectors.....	51
Figure 3.6. Map of seismic lines used to create the structure contour maps and isopach thickness maps of the Seafloor, Horizon A, and Horizon B.	52
Figure 3.7. Structure contour map of the Seafloor reflector with depth in meters (m).	53
Figure 3.8. Structure contour map of Horizon A with depth in meters (m).....	54
Figure 3.9. Structure contour map of Horizon B with depth in meters (m).....	55
Figure 3.10. Isopach thickness map showing the thickness between the Seafloor Horizon and Horizon A. The contour interval is 0.5 m.	57
Figure 3.11. Isopach thickness map showing the thickness between Horizon A and Horizon B. The contour interval is 0.5 m.	58
Figure 3.12. A) Uninterpreted portion of seismic line 1400. B) Interpreted portion of seismic line 1400 with the lava flow and rhyolite dome/boulder mapped. C) Location of the seismic line.....	60
Figure 3.13. A) Interpreted seismic line near the boundary of the low gravity anomaly discussed by Stagpoole et al. (2021). B) Location of the seismic line.	61
Figure 4.1. Annotated historical air photograph of the Katikati Basin from 1960. (Image source: Retrolense; https://retrolens.co.nz/).	65

Figure 4.2. Annotated historical air photograph of the Katikati Basin from 1975. (Image source: Retrolense; <https://retrolens.co.nz/>).66

Figure 4.3. Annotated historical air photograph of the Katikati Basin from 1999. (Image source: Retrolense; <https://retrolens.co.nz/>).67

Figure 4.4. Katikati Basin in 2024. (Image source: Google Earth).68

Figure 4.5. Changes to the Katikati Inlet focusing on the shape of Waikoura Point on Matakana Island before and after triple-dip La Niña events during April 1975 to February 1982 and, March 2019 to April 2022 (de Lange, 2023).69

Figure 4.6. Hydrographical chart of the Katikati Basin entrance in 1976. (Data source: <https://paekoroki.tauranga.govt.nz/nodes/view/56207>).71

Figure 4.7. Hydrographical chart of the Katikati Basin entrance in 1993. (Data source: <https://onehera.waikato.ac.nz/nodes/view/1625>).72

Figure 4.8. Hydrographical chart of the Katikati Basin entrance in 2023. (Data source: hydrographical chart NZ5411.72

Figure 4.9. Historical shoreline positions of the spit tip of Matakana Island at the Katikati Basin entrance from 1870, 1901 and 1974 (de Lange, 2023).73

Figure 4.10. Spit tip morphology of Waikoura Point, Matakana Island at the Katikati entrance where A) represents a broad rounded spit, B) rounded spit with notched sides, C) narrow spit with a pointed tip (de Lange, 2023).74

Figure 4.11. Triple-dip La Niña events displayed on a time series graph of the Oceanic Nino Index (ONI), showing a three-month running mean surface temperature anomalies with ENSO (>0.5 = El Niño and <0.5 = La Niña), in the tropical Pacific. This graph was prepared for the northern hemisphere where in the southern hemisphere a triple-dip La Niña event occurs over a four year period over three summers (de Lange, 2023).77

Chapter 1: Introduction

1.1 Introduction

Te Awanui (Tauranga Harbour) is in the western Bay of Plenty (Figure 1.1) and is Aotearoa New Zealand's largest barrier-enclosed, persistent, meso-tidal coastal lagoonal system (Badesab et al., 2017; de Lange et al., 2015). The harbour covers an area of approximately 200 km² and is relatively shallow, with 80% of the area exposed at low tide (Stokes et al., 2009). Extensive and shallow intertidal flats in the central harbour restrict/limit water exchange essentially creating two distinct basins (de Lange et al., 2015): the Katikati Basin at the northern end of Te Awanui; and the Tauranga Basin at the southern end. Both basins have their own tidal inlets which are bounded on either side by the Matakana barrier island and the rhyolite domes of Bowentown and Mount Maunganui (Mauao) respectively (de Lange et al., 2015).

Other geological features of the harbour include Matakana Island which is a Pleistocene/Holocene sand barrier island 24 km in length that encloses the estuary, and the two Holocene tombolo's connecting the Bowentown and Mt Maunganui rhyolite domes to the mainland (Badesab et al., 2012; de Lange et al., 2015). Sediments in the harbour are predominantly sandy, however finer material tends to collect around the margins, particularly within constricted sub-estuaries (Stokes et al., 2009). In Te Awanui, the composition of the surficial sediments are influenced by the surrounding geology of local catchments, therefore sediment composition varies within each basin predominantly within the trace mineral fraction (de Lange, 2023).



Figure 1.1. Satellite image showing the location of Te Awanui (Tauranga Harbour) and major geomorphic features, within the North Island of New Zealand (red dot) created using Google Earth.

The major physiographic units in the area surrounding Te Awanui (Figure 2.2) include the Kaimai Range, Whakamarama Plateau, Mamaku Plateau, and the Pāpāmoa Range (Briggs et al., 1996). These are described below.

Kaimai Range

The Kaimai Range is a series of Late Miocene-Pliocene volcanic rocks with a basaltic-rhyolitic composition representing volcanism of the older Coromandel Volcanic Zone (CVZ). It is an uplifted block that is bound to the Hauraki Fault to the west via erosion of the fault scarp (Briggs et al., 1996; Briggs et al., 2005). The Kaimai Range is dominated by a subgroup of volcanic material including the Pukepunga and Uretara Formations containing andesite to dacite lavas and breccias (Leonard et al., 2010). The Kaimai Range contains exposed volcanic rocks that mark the transition between the CVZ and Taupō Volcanic Zone (TVZ) (Briggs et al., 2005).

Whakamarama Plateau

Ignimbrite sheets are major geological features of the Tauranga region where they form a series of extensive plateaus, including the Whakamarama Plateau (Briggs et al., 2005). The Whakamarama Plateau gently dips at 3-5 degrees to the northeast from the Kaimai Range down to Te Awanui as a result of uplift to the east of the Hauraki Fault. The Plateau consists of the Aongatete Formation and Waiteariki Ignimbrite (Briggs et al., 1996; Briggs et al., 2005).

The Aongatete Formation is a >290 m thick series of pumice-rich ignimbrites that overlie the Kaimai Range; outcropping to the east and ranging from non-welded to densely welded lenticular dacitic ignimbrites and tuffs 3.93 - 3.55 Ma in age (Briggs et al., 2005; Naish, 1990). Drill hole cores determined that there are at least three different ignimbrite units within the Aongatete Formation (White et al., 2008). The source(s) for these ignimbrite units are still unknown but thought to have been within the Coromandel Volcanic Zone (CVZ) due to their age and are not considered to be related to the Tauranga Volcanic Centre (TgaVC) (Briggs et al., 2005).

The Waiteariki Ignimbrite is an extensively welded and widespread ignimbrite found throughout the Kaimai and Tauranga regions (Briggs et al., 1996; Prentice, 2023). It forms the basement rock of Te Awanui where it is encountered in drill holes at 50 - 150 m in depth (Briggs et al., 1996). The ignimbrite is exposed at many localities including the foothills of the Kaimai Range where it underlies the Whakamarama Plateau dipping gently towards Te Awanui and is buried by volcanogenic sediments and younger pyroclastic deposits sourced from the TVZ. (Prentice, 2023).

Pāpāmoa Range

The Pāpāmoa Range is situated south of Te Awanui separating the Tauranga and Maketu Basins (Briggs et al., 1996; Prentice, 2023). The Pāpāmoa Range contains the Ottawa stratovolcano, Pāpāmoa Ignimbrites, and the dacitic to rhyolitic Minden Rhyolite domes that have an NNE-alignment to the south (Prentice, 2023). The two NNE-striking faults that border the Pāpāmoa Range are proposed to control the alignment of these volcanic landforms (Briggs et al., 1996).

The Pāpāmoa Range includes the eroded remnants of the Ottawa stratovolcano, which cover an area of approximately 35 km² to the east of the TgaVC. The lavas produced by Ottawa are basaltic andesite to dacite, with breccias containing hornblende and pyroxene crystals. These lavas erupted around the same time as the Matakana Basalt lava flow on Matakana Island c. 2.95 – 2.54 Ma (Pittari et al., 2021).

The Pāpāmoa Formation is a succession of northward dipping rhyolite to dacite ignimbrites that have been interbedded with fall deposits. Pittari et al. (2021) suggests an age range for the Pāpāmoa Formation of 2.21 ± 0.13 Ma. The sources for these ignimbrites are still unknown, but they are suggested to be local. There are two main Ignimbrite units within the Pāpāmoa Formation where the lower unit is more dynamic containing juvenile andesitic clasts dark grey to brown and white dacitic-rhyolitic clasts. In contrast, the upper unit consists of only white dacitic-rhyolitic clasts (Pittari et al., 2021).

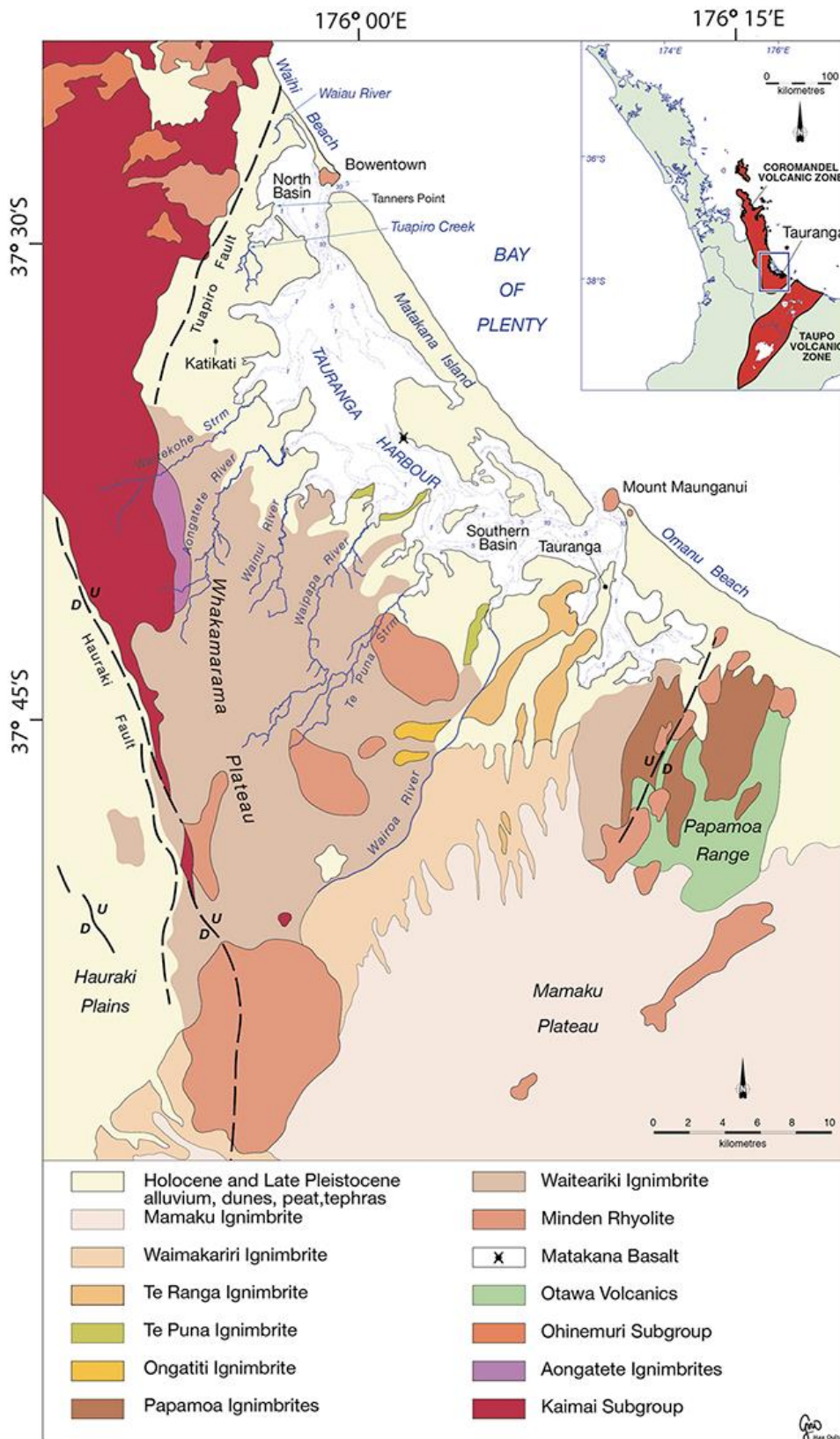


Figure 1.2. Map showing the major physiographic units of the Tauranga region, other geological units, faults, and major rivers and streams (de Lange et al., 2015).

1.2 Study Aim and Objectives

The aim of this study is to determine the thickness of the Holocene sediments deposited since the flooding of the Katikati Basin by Holocene marine transgression and mapping any potential faults by undertaking a shallow seismic survey. The results from this study will help understand the risk of faulting in the area surrounding the Katikati Basin from a hazard standpoint, and any changes to the geomorphology that show areas of rapid change. This will be achieved by:

- 1) Determining the thickness of the Holocene sediments.
- 2) Mapping the thickness and structure of the Katikati Basin using data from the shallow seismic survey.
- 3) Identify any faults and volcanic features of interest.
- 4) Determine any areas of rapid change to the geomorphology of the Katikati Basin using historical hydrographical charts and air photographs.

The seismic survey will determine the thickness and characteristics of the Holocene sediments as well as the geomorphology of the main channel within the Katikati Basin. There is evidence of faulting within the Tauranga Basin (Podrumac, 2016) and Ōmokoroa Peninsula (Christophers, 2015), this study will determine if the faulting (potentially associated with marginal faulting of the Taupō rift) extends into the Katikati Basin. The low gravity anomaly that is associated with a sedimentary basin or caldera in Figure 2.5 (Stagpoole et al., 2021) will also be investigated for ring faults and any indications of a caldera where the seismic survey crosses the boundary of the low gravity anomaly near Matakana Island. The historical hydrographical charts and air photographs will be used to identify the effects of the ENSO cycle has on Waikoura Point on Matakana Island and any areas of rapid change within the Katikati Basin.

1.3 Thesis Outline

Chapter 2: Background

This Chapter will discuss the relevant literature for the Tauranga region as well as the Katikati Basin including the regional geology, Te Awanui (Tauranga Harbour), sediments, and hydrodynamics.

Chapter 3: Seismic Reflection Characterisation

This chapter involves the methods used to obtain and process the seismic data as well as an interpretation of the results.

Chapter 4: Historical Air photographs

This chapter involves the methods used for obtaining the historical air photographs and an explanation of what is observed.

Chapter 5: Summary and Discussion

This chapter will discuss the findings from the seismic survey and the historical air photographs chapters relating back to the literature review.

Chapter 6: Conclusion

This chapter will summarize the main findings from this study relating back to the aims and objectives as well as describe future recommendations for further research.

Chapter 2: Background

2.1 Introduction

This chapter will discuss the literature on the overview of Te Awanui and Katikati Basin within the following subsections: **2.2 Regional Geology** – The volcanism and geological units/structures of the Tauranga region including tectonics. **2.3 Te Awanui (Tauranga Harbour)** – An overview of the geomorphology and vertical land movement with the evolution of Matakana Island and Tsunami erosion events. **2.4 Sediments** – The sediments and sediment sources around and within Te Awanui including the Holocene and Pleistocene sediments. **2.5 Hydrodynamics** – The wave and tidal environment and catchment for both basins, as well as the Katikati inlet. **2.6 Summary** – A brief summary of the main points of the chapter.

2.2 Regional Geology

2.2.1 Volcanism of the Tauranga Volcanic Centre

Volcanism in and around Te Awanui occurred within the TgaVC between 2.95 and 1.95 Ma (Pittari et al., 2021). The TgaVC consists of an eroded stratovolcano (Otawa Formation), the Matakana Basalt, which is a solitary small basaltic lava flow, 17 rhyolite-rhyodacite lava dome complexes known as the Minden Rhyolite Subgroup, and the Omanawa Caldera and associated ignimbrite formations of the Pāpāmoa Ignimbrites, and climactic Waiteariki super eruption (Figure 2.1) (Prentice, 2023).

The TgaVC represents subduction-related silicic volcanism marking the transition between the CVZ (12 - 3.5 Ma) and TVZ (~3 Ma - present) and is the earliest volcanism associated with the TVZ (Prentice, 2023). As the TVZ has migrated eastward the oldest volcanic centres are located on the western margin being the TgaVC and CVZ (Prentice, 2023). The sediments and cover rocks around Te Awanui originated from the TgaVC and landforms are linked to volcanism of the CVZ and TVZ (de Lange, 2023).

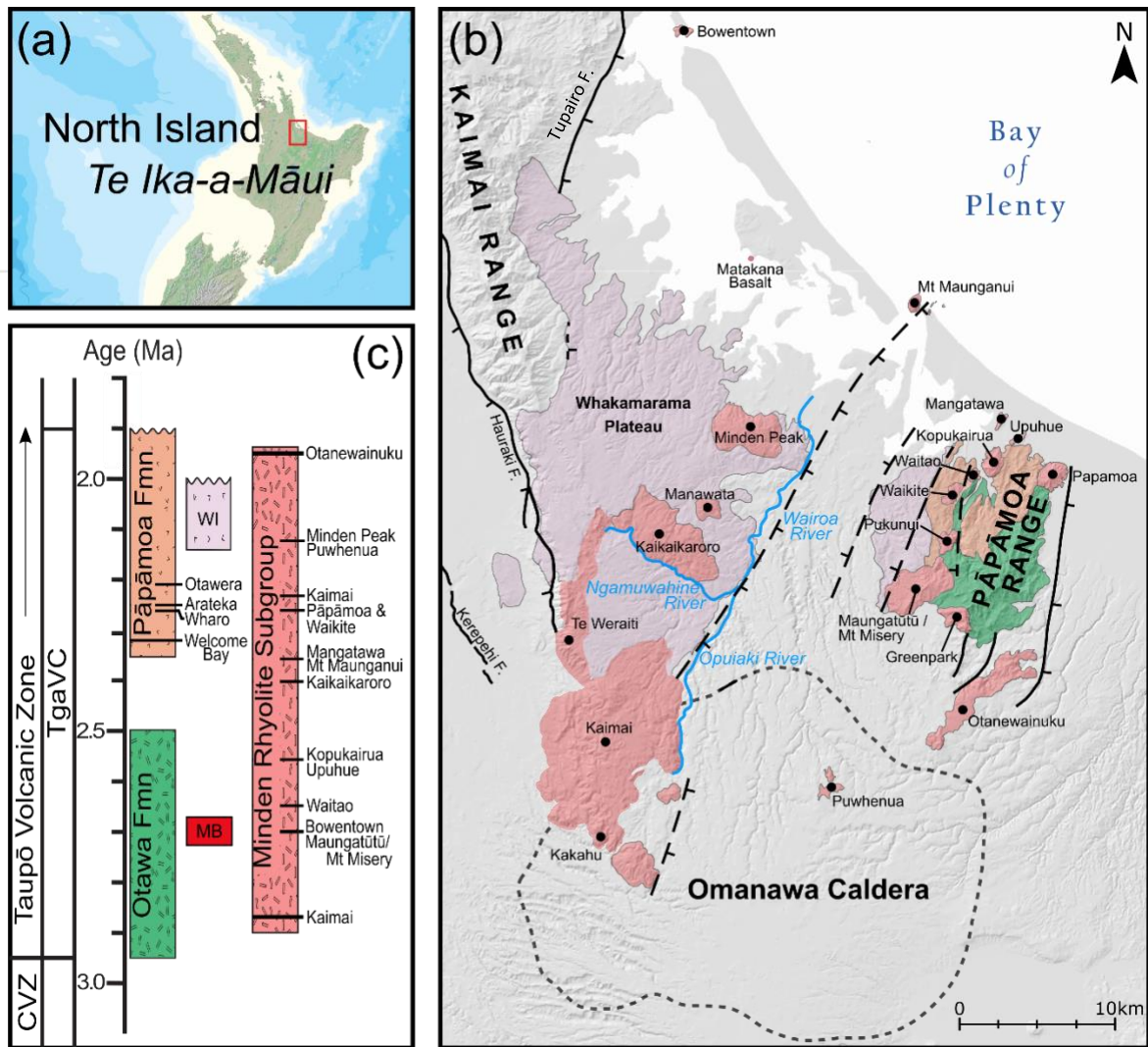


Figure 2.1. Simplified geological map from Prentice (2023) highlighting the distribution and stratigraphy of volcanic landforms and structures associated with the Tauranga Volcanic Centre (TgaVC). **(a)** North Island/Te Ika-a-Māui of New Zealand. The red box highlights western Bay of Plenty. **(b)** Simplified geological map of the TgaVC. Extensional faults associated with the TgaVC are shown as dashed lines, with previously identified non-active faults from Leonard *et al.* (2010) shown as solid lines. **(c)** Volcanic stratigraphy of the TgaVC. Stratigraphic formation age ranges are shown as coloured bars with dated individual volcanic centres (Minden Rhyolite Subgroup) or defined ignimbrites (Pāpāmoa Formation).

Matakana Basalt

The Matakana Basalt is a solitary outcrop of basaltic lava with pseudo-pillow structures and forms a small island on the harbour side of Matakana Island (Briggs *et al.*, 2005; Prentice, 2023). This basalt is the only occurrence of basalt in the Tauranga region and is K-Ar dated at 2.7 ± 0.1 Ma (Briggs *et al.*, 2005). A high gravity anomaly underlies Matakana Island and could represent a lava flow with a buried structure beneath the island (Prentice, 2023).

Minden Rhyolites

The Minden Rhyolites are a sub-group of 16 Miocene-Pliocene age rhyolite-rhyodacite lava domes and dome complexes north of the TVZ in the Bay of Plenty and Coromandel regions (Prentice, 2022). The dome complexes consist of the Minden Peak, Mt Maunganui, Mangatawa, and Mount Misery groups (Briggs et al., 2005).

Briggs et al. (2005) classified the Minden Rhyolites based on their spatial distribution, mineralogy, and geochemistry into assemblages of high, intermediate, and low SiO₂, K₂O, and Zr concentrations. However, Prentice (2023) simplified the groupings of the dome complexes into either high or low ⁸⁷Sr/⁸⁶Sr isotopic concentrations, linked to compositional differences of TgaVC magmas erupted east and west of the Wairoa River. It was inferred that this was associated with a fault near the Wairoa River (Figure 2.1) (Prentice, 2023).

The low ⁸⁷Sr/⁸⁶Sr group is lavas with ratios of ⁸⁷Sr/⁸⁶Sr below 0.705800, and include the Mt Maunganui and Minden Peak complexes, and the domes of the Pāpāmoa Range to the east. The high ⁸⁷Sr/⁸⁶Sr lavas have ⁸⁷Sr/⁸⁶Sr ratios above 0.705900 and include the Mangatawa and Mt Misery dome complexes to the east of the Wairoa River (Prentice, 2023).

Most of the Minden Rhyolite domes are aligned parallel to inferred NNE-trending faults associated with the opening of the Taupō Rift (Prentice, 2023). While volcanic activity associated with these domes occurred throughout the history of the TgaVC, several lavas were erupted within two relatively short periods of activity between 2.5 - 2.3 and 2.2- 2.1 Ma (Figure 2.1).

An exception to the simplified Minden Rhyolite grouping, is the Bowentown rhyolite dome within the Katikati Basin. Although this dome has geochemical and mineralogical similarities to the Minden Peak and Mount Maunganui dome complexes, it is spatially removed from, and not compositionally linked to, the other domes of the TgaVC (Prentice, 2023). Age estimates for the Bowentown dome range between 2.09 ± 0.34 Ma (Cook, 2016). However, Prentice (2023) suggests an age of 2.7 Ma as this is consistent with the ages of the other domes in the general area. Although the Bowentown dome occurs within the broader boundaries of the TgaVC, its inclusion in the TgaVC along with the Matakana Basalt is provisional (Prentice, 2023).

Waiteariki Ignimbrite

The Waiteariki Ignimbrite is a thick, extensive, crystal and pumice-rich, densely welded dacitic ignimbrite that underlies the Whakamarama Plateau and forms the basement rock of Te Awanui. (Prentice, 2023). The age of the Waiteariki Ignimbrite was determined at two sites: being 2.18 ± 0.031 Ma at Aongatete River; and 2.09 ± 0.029 Ma at McLaren Falls (Prentice, 2023). Due to its widespread nature, Prentice (2023) has correlated the Waiteariki Ignimbrite with the newly defined Omanawa Caldera located to the southeast of the Kaimai Range, buried beneath the Mamaku Plateau (Figure 2.1). The caldera is identified by variations in ignimbrite thickness, textural characteristics and numerous lava domes together with a negative gravity anomaly that is found at the end of an asymmetrical rifted graben within the Mamaku Plateau at the northern end of the Taupō Rift (Prentice, 2023).

Prentice (2023) presented new evidence relating to the origin of the Waiteariki Ignimbrite. The ignimbrite belongs to the TgaVC, where it represents a magnitude 8 eruption ejecting 1470-1506 km³ of material from the Omanawa Caldera. The Waiteariki Ignimbrite's estimated minimum distribution is concentrated along a small zone that stretches over 200 km from Katikati in the NW to the northern Hawke's Bay region with a NNW-SSE orientation (Prentice, 2023).

Matua Subgroup

The Matua Subgroup is an intercalation of all terrestrial and estuarine sediments that have deposited and formed after the deposition of the Waiteariki Ignimbrite (c. 2 Ma) and predating the Hamilton Ash at 0.35 Ma (Briggs et al., 1996).

The Matua Subgroup contains fluvial pumiceous and rhyolitic silts, sands, gravels, diatomaceous lacustrine and estuarine muds, peats and sediments reworked from ignimbrites, lava flows and domes from the TgaVC and distal TVZ (Prentice, 2023). Several primary pyroclastic deposits found throughout Te Awanui include distal ignimbrites originating from younger volcanic centres throughout the TVZ also belong to the Matua Subgroup including the Kidnappers and Te Ranga Ignimbrites (Prentice, 2023) .

Pahoia Tephra's

The Pahoia Tephra sequence includes at the base non-welded pumiceous deposits of the Kidnappers Ignimbrite, and a series of clay-rich halloysitic tephra beds that are highly weathered and divided into a lower and upper Pahoia Tephra's due to one distinct paleosol. These deposits are overlain by the Hamilton ashes which are younger in age (c. 0.35 to c. 0.05 Ma) and highly weathered (Kluger et al., 2020). The age range for the Pahoia Tephra's are from c. 2.18 to 0.35 Ma. These tephra's are exposed throughout coastal sections and terraces of the Harbour including Matakana Island, Pahoia Peninsula, Mt Maunganui, and Ōmokoroa (Briggs et al., 1996; Kluger et al., 2022). The Pahoia Tephra's are split into an upper and lower layer where the lower layer is a highly sensitive layer due to spheroidal halloysite clay and responsible for the Ōmokoroa flow side at Bramley Drive in Te Awanui and active erosion around peninsulas within Te Awanui (Kluger et al., 2022; Kluger et al., 2020). Te Awanui contains a series of NNE-trending terraced peninsulas that extend into the harbour (Mason et al., 2023). The Matua Subgroup and Pahoia Tephra's are generally mapped at lower elevations within the NNE-aligned terraces around Te Awanui and overlain by the Hamilton Ashes of the TVZ (Mason et al., 2023).

Kidnappers (Te Puna) Ignimbrite

The Kidnappers Ignimbrite is described as a non-welded, buff brown ignimbrite with grey fibrous pumice at 15 - 20% with a mineral assemblage of plagioclase, quartz, hornblende, orthopyroxene, Fe-Ti oxides and biotite. Lithic clasts include rhyolites and minimal charcoal, obsidian, and fragments of the Ongatiti Ignimbrite (Prentice, 2023). This ignimbrite's known exposures are restricted to Te Awanui and is thought to have either erupted locally, or be linked to unidentified ignimbrites from the TVZ (Briggs et al., 2005). However, $^{40}\text{Ar}/^{39}\text{Ar}$ dating provides an age of 0.929 ± 0.012 Ma, making it younger than all TgaVC eruptives and considered to be derived from a distal source of the TVZ. The Kidnappers Ignimbrite is found outcropped in cliff sections along the Wairoa river, Ōmokoroa, Pahoia Point and Matakana Island (Prentice, 2023).

2.2.2 Regional Tectonics

Active faults at depth are generally defined as gentle to broad-scale warps and folds of the ground surface where the age of the warped surfaces are between at least 70,000 – 128,000 years old (Van Dissen & Heron, 2023). No active faults have been traced through the Katikati Basin, recent studies have found evidence of potentially active faults in the Tauranga Basin (Podrumac, 2016). However,

the geomorphology of the region reveals key evidence for past faulting including the localisation for volcanic vents (Minden Rhyolites), rivers predominantly flowing towards the NNE, the alignment of terraced peninsulas also towards the NNE (Briggs et al., 1996), and offsets on key geological units (Prentice, 2023).

The Taupō rift (Figure 2.2) has evolved over time and began in the western Bay of Plenty region where it formed in continental crust via subduction of the Pacific Plate under the Australian Plate in the Havre Trough back-arc Basin (Villamor et al., 2017). A series of NNE-striking normal faults are located in central areas of the Tauranga region which have been linked to the Taupō Rift where the close association between faulting and volcanism suggests the rift was active in the Tauranga region from c. 2.5 Ma. During the early stages of rifting, the pattern of fault activity is hard to determine due to thick extensive ignimbrite sheets varying in distribution around the rift have buried most of the faulting record (Villamor et al., 2017). Overtime, the location of the Taupō rift has shifted eastward and narrowed to form the Modern Taupō Rift (Villamor et al., 2017).

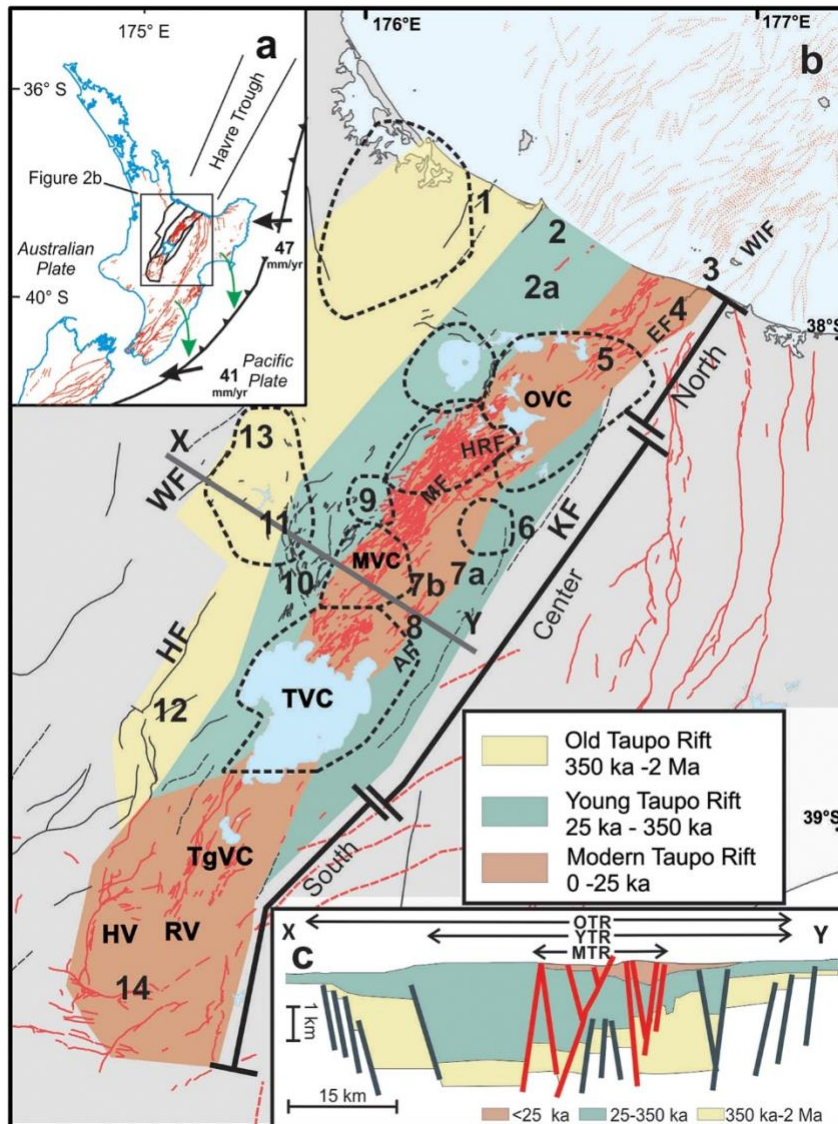


Figure 2.2. Evolution of the Taupō Rift over the last 2 Ma with red lines representing active faults, black lines inactive faults, and dashed circles are the volcanic centres (Villamor et al., 2017). The Tauranga Volcanic Centre is feature 1.

Northwest of the Taupō Rift is a major fault that runs through the Katikati end of Te Awanui known as the Tuapiro Fault (Figure 2.1). This concealed fault is buried beneath volcanic rock and sediment and its location is inferred via the presence of warm springs and a sharp gradient in Bouguer gravity data. Tuapiro Fault is deemed inactive as it has not shown movement by rupturing the surface in the last 128,000 years (Lee & Villamor, 2018).

The interpretation that there are no active faults within Te Awanui was based solely on there being no evidence of surface rupture in the past 128,000 years. However, Podrumac (2016) undertook a thesis where potential faults within the western channel and Ōmokoroa were discovered by

undertaking shallow seismic surveys in the Tauranga Basin. Deformation in the seismic profiles at three sites indicated that there was folding, fracturing, and potential faulting near the transects. Cores were sampled to show ground proof data of the faults identified in the seismic data. Their data from the coring showed that CS3 was uplifted and contained finer darker sediment that is presumed to be older, and CS4 was downthrown and contained only Holocene sands. These cores were taken between Motuhoa Island and Ōmokoroa Peninsula in Te Awanui. These faults within the sediments from the last glacial extend into the Holocene sediments indicating there has been movement in the last 128,000 years and may therefore be considered active (Podrumac, 2016).

Christophers (2015), undertook a thesis focusing on Ōmokoroa Peninsula within the Tauranga Basin and found evidence of uplift and potential faulting around Ōmokoroa. They inferred displacement between the cliffs and surrounding intertidal flats of Ōmokoroa due to evidence of stratigraphic relations between the geological units at the coastal sections and within cores taken at the intertidal flats. Evidence includes a sharp discontinuity of the Pahoia Tephra's on the western margin of cliff sections at Ōmokoroa indicating vertical displacement. Also, cores taken at the western and eastern margins of Ōmokoroa revealed different sediment sequences. The eastern margin contained a thick sequence of marine sediments that underlie more recent sediments deposited during the present-day environment. Whereas, the western margin contained a thin layer of more recent sands overlaid Pleistocene sediments and no evidence of marine deposits. This provided evidence of vertical land movement within the Pleistocene sediments at Ōmokoroa (Christophers, 2015).

Although no faults had been previously mapped along the Ōmokoroa Peninsula, Christophers (2015) states that the series of NNE-aligned trending faults speculated within the Tauranga Basin (Briggs et al., 1996), likely also control the alignment of Ōmokoroa Peninsula. The timing of vertical movements is unknown but inferred to have followed the deposition of Te Puna ignimbrite dated at 0.93 Ma (Christophers, 2015).

2.2.3 Caldera Structures around Te Awanui

Stagpoole & Miller (2021) define calderas as collapsed craters formed due to large voluminous eruptions ejecting a significant amount of material from the subsurface. The underlying magma reservoir becomes drained after an eruption causing the overlying strata to slump and collapse leaving behind large topographic depressions that infill with volcanic deposits and other sediments. A recent example of a caldera is Lake Taupō (Stagpoole & Miller, 2021).

Gravity anomalies use the principle of gravity where a force is generated between two objects, attracting them to each other with a force that is proportional to their masses. An area that has a negative gravity anomaly has a lower density forming a deficit of mass. Whereas an area that has a positive gravity anomaly has a higher density forming a mass excess. Gravity anomalies tend to be given as Bouguer gravity anomalies which account for the difference in elevation between the location of measurement and sea level, impacts of local terrain including the mass of rocks that form the terrain, including mountains and valleys which can cause minor changes to the local gravitational acceleration (Stagpoole & Miller, 2021).

Calderas are identified on gravity maps as low gravity anomalies as they are filled with low-density volcanic material whereas, high-gravity anomalies are areas of dense materials including consolidated volcanic material or basement units (Stagpoole & Miller, 2021). The Omanawa Caldera is now recognised via a negative gravity anomaly at the northern end of the Taupō rift (Prentice, 2023).

In the area offshore of Te Awanui, there is a circular low gravity anomaly that is speculated to be a potential caldera (Figure 2.3). Other onshore rhyolitic calderas in the Bay of Plenty are similar in magnitude to the one speculated offshore. This potential caldera has been linked to a basement ridge with normal faulting around thick sediments. There is another speculated caldera offshore within the old TVZ that is also associated with normal faulting around thick sediments (Stagpoole et al., 2021). Neither have been investigated enough to be certain that these anomalies are indeed calderas.

Figure 2.3 also demonstrates a negative anomaly within the Katikati Basin which is inferred to have been related to the Coromandel Volcanic Centre (Stagpoole et al., 2021). Christophers (2015) argues that the belt of Pleistocene sediment between Ōmokoroa and Matakana Island forming the ridge between the two basins within Te Awanui, also marks the boundary between two calderas that once formed the Katikati and Tauranga Basin's in the past. These calderas have then been infilled by recent Holocene sediments (Christophers, 2015). However, a volcanic centre has not yet been identified at this location. It is speculated that the anomaly may be associated with a sedimentary basin and not a caldera, but both theories have neither been proven nor disproven at this time (Stagpoole et al., 2021).

There is also an unknown offshore circular low gravity feature in Figure 2.3 near Te Awanui which may be linked to a linear feature of back arc structures of the Tonga-Kermadec subduction Zone and the Ngatoro Basin in particular. The Ngatoro Basin is a NNE-trending aligned graben structure located northeast of Mayor Island within the Bay of Plenty (Cole, 1978; Cole & Lewis, 1981). This basin

represents a south-westward extension of the Havre Trough and is linked to back arc structures of the Tonga-Kermadec subduction zone (Cole, 1978; Cole & Lewis, 1981). Pantellerites are minerals associated with tensional graben structures as seen within the East African rift (Cole & Lewis, 1981). The presence of Pantellerites in lavas on Mayor Island is therefore indicative of rifting within the Havre Trough and Ngatoro Basin extending south-westwards onto the continental shelf, and these unique lavas are found nowhere else within the North Island (Cole & Lewis, 1981). The trend may also continue onshore towards Te Awanui as there is an unknown anomaly in Figure 2.3 and Cole & Lewis (1981), state that if the trend were to continue towards Te Awanui then it would be marked via three aligned magmatic anomalies potentially due to basaltic dykes. Cole (1978) also states that Te Awanui tends to be slightly subsiding in areas compared to Maketu and Waihi coastlines, therefore further indicating the unknown anomaly may be due to the extension of rifting within the Havre Trough of the Ngatoro Basin.

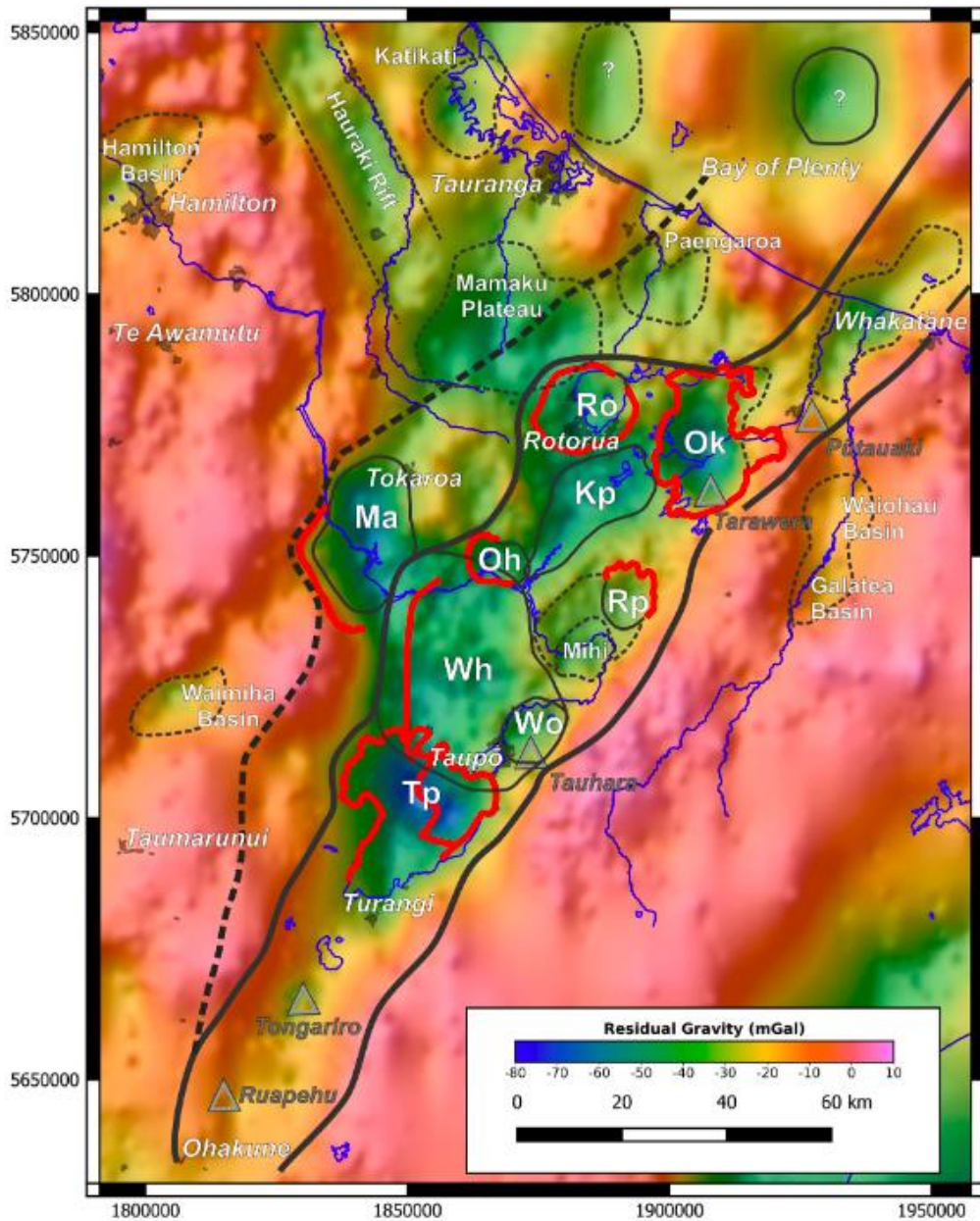


Figure 2.3. Interpretation of residual gravity anomalies around the Taupō and Bay of Plenty areas. The black thick dashed line represents the old TVZ and the thick black line is the present TVZ. The red lines are the known caldera margins. Low gravity features including sedimentary basins and potential calderas are the smaller black dashed lines. (Stagpoole et al., 2021).

2.3 Te Awanui (Tauranga Harbour)

Te Awanui began forming 2-4 million years ago via subsidence, and more recently barrier spit development on Matakana Island that commenced following the Postglacial Marine Transgression (c. 7000 cal BP) around c. 6000 cal BP, combining with the stabilising effects of the Mt Maunganui and Bowentown rhyolite domes (Betts, 1996; Davis & Healy, 1993; Shepherd et al., 2000). The following sections will outline the geomorphology and landform evolution, sedimentation, and hydrodynamics of Te Awanui.

2.3.1 Geomorphology and Landform Evolution

The geomorphology of Te Awanui includes a series of tombolo's (Bowentown and Mt Maunganui), a barrier island (Matakana Island), and low terraces and sand dune complexes around the harbour formed during the Pleistocene and Holocene (Briggs et al., 1996; Briggs et al., 2005). Tonkin and Taylor (2018) separated the harbour shorelines into three different morphological types:

- I. Consolidated cliffs around the harbour that can be vertical with eroding faces, stable slopes that are highly vegetated, or even completely bare. Low banks are considered to be consolidated shorelines.
- II. Unconsolidated shorelines are uncommon in the harbour and are mainly characterised by beach ridges.
- III. Non-eroding shorelines, usually flanked by mangroves and salt marshes define the low-lying estuarine areas. These shorelines usually occur within the upper areas of the harbour that are more sheltered.

Type I shorelines are generally erosional, while Type II can be erosional or depositional depending on sediment supply, and Type III are depositional shorelines. Motuhoa Island, Rangiwaea Island, and Ōmokoroa are examples of consolidated cliffs with medium to high erosion rates in Te Awanui (Figure 2.4). The lithotypes of the consolidated cliffs tend to include the Matua Subgroup, and Holocene fluvial and estuarine deposits and minor non-welded ignimbrites. Ongare is a sheltered unconsolidated shoreline near Katikati with minor erosion. Te Puna is an unconsolidated shoreline with high long-term erosion rates. Eroded sediment is lost from the upper beach system and transported offshore, it does not settle and deposit in either basin. An example of a non-eroding shoreline is the Matua Saltmarsh in Figure 2.4 (Tonkin and Taylor, 2018).

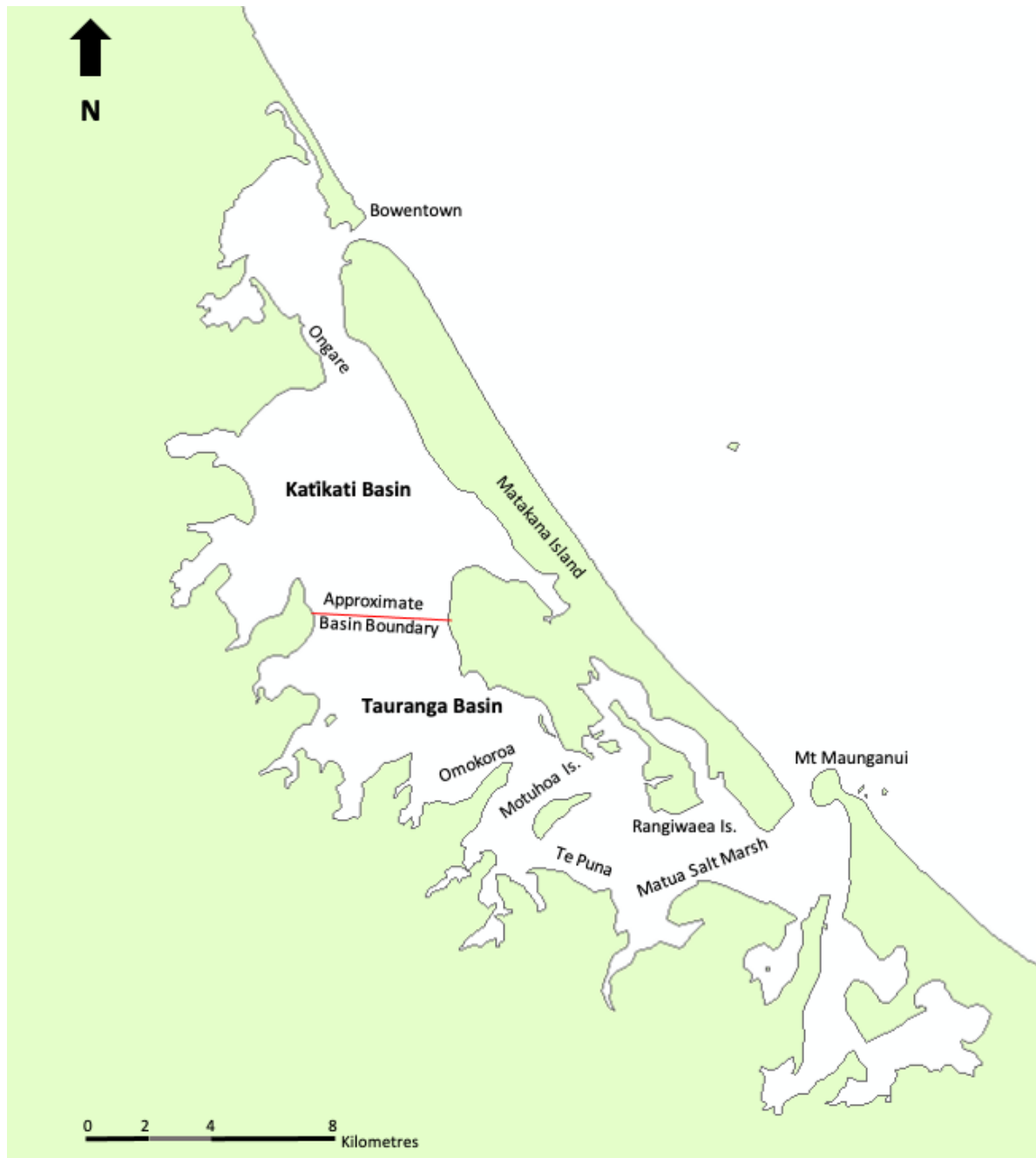


Figure 2.4. Map demonstrating the locations of the different morphological shoreline types around Te Awanui, re-drawn from (de Lange et al., 2015; Tonkin and Taylor, 2018).

2.3.2 Tsunami Erosion Events

There is evidence of two large tsunami events that affected the east coast within the Waihi mires over the last 3 ka (Gardiner, 2023). The older event occurred approximately 2.5 ka and has been linked to deposits in Ōmokoroa ($1,652 \pm 20$ cal BP), and near the Wairoa River near the south-eastern end of the Te Awanui. Evidence suggests that this tsunami event occurred due to a small, localised earthquake within the Tauranga area. The second tsunami occurred around 582 ± 66 cal y BP, and

compared to the first event it was a much larger regional event. This tsunami caused extensive spit erosion of Matakana Island at each end, where the eastern end (Panepane Point), was truncated to the Purakau Shoreline (Figure 2.5) (de Lange et al., 2015).

Figure 2.5 shows the truncated shorelines at Waikoura Point, western end of Matakana Island (Katikati Entrance). The S1 shoreline formed during the Holocene High Stand (peak Holocene sea level for New Zealand around 4.5 - 3.5 ka), however, the actual age of the shoreline is unknown. Whereas the S2 shoreline is dated at approximately 1750 cal y BP suggesting that it could have been eroded by the older tsunami event (de Lange et al., 2015). The S3 shoreline is the youngest and is associated with the erosional Purakau Shoreline that extends across the whole island (de Lange et al., 2015; Shepherd et al., 1997).

Waihi Beach Tsunami Cores

The tsunami hazard report for the Bay of Plenty undertaken by Bell et al. (2004) highlights the tsunami events mentioned above in cores taken from Waihi Beach. Figure 2.6 demonstrates two possible tsunami inundation events during AD1302 - AD1435 and 2500 years BP. Poor diatom presence in deposits inhibited accuracy when dating the tsunami events (Bell et al., 2004).

The unique Loiseles Pumice is present in the younger event which helped determine the timing of this event. Markers of this event include a unique coarse sand unit with diatoms. Subsidence is inferred and stated that it seems possible but is unlikely. However, this ~1 m subsidence coincides with the tsunami deposits found at Ōmokoroa and the lower Wairoa River in Te Awanui. This also points to a local earthquake (potentially along the Tuapiro Fault), that generated a tsunami affecting all of Te Awanui and surrounding areas (Bell et al., 2004).

A chaotic unit containing coarse sand, shell, and shell hash marks the older event (pre- Taupō) in Figure 2.6. This tsunami event coincides with another inundation event south of Tauranga in a small valley by the Wairoa River. A site 7 km inland at Hopping Farm dated the bark of an old tree from the inundation which produced an age of 2962 ± 52 years BP (Bell et al., 2004).

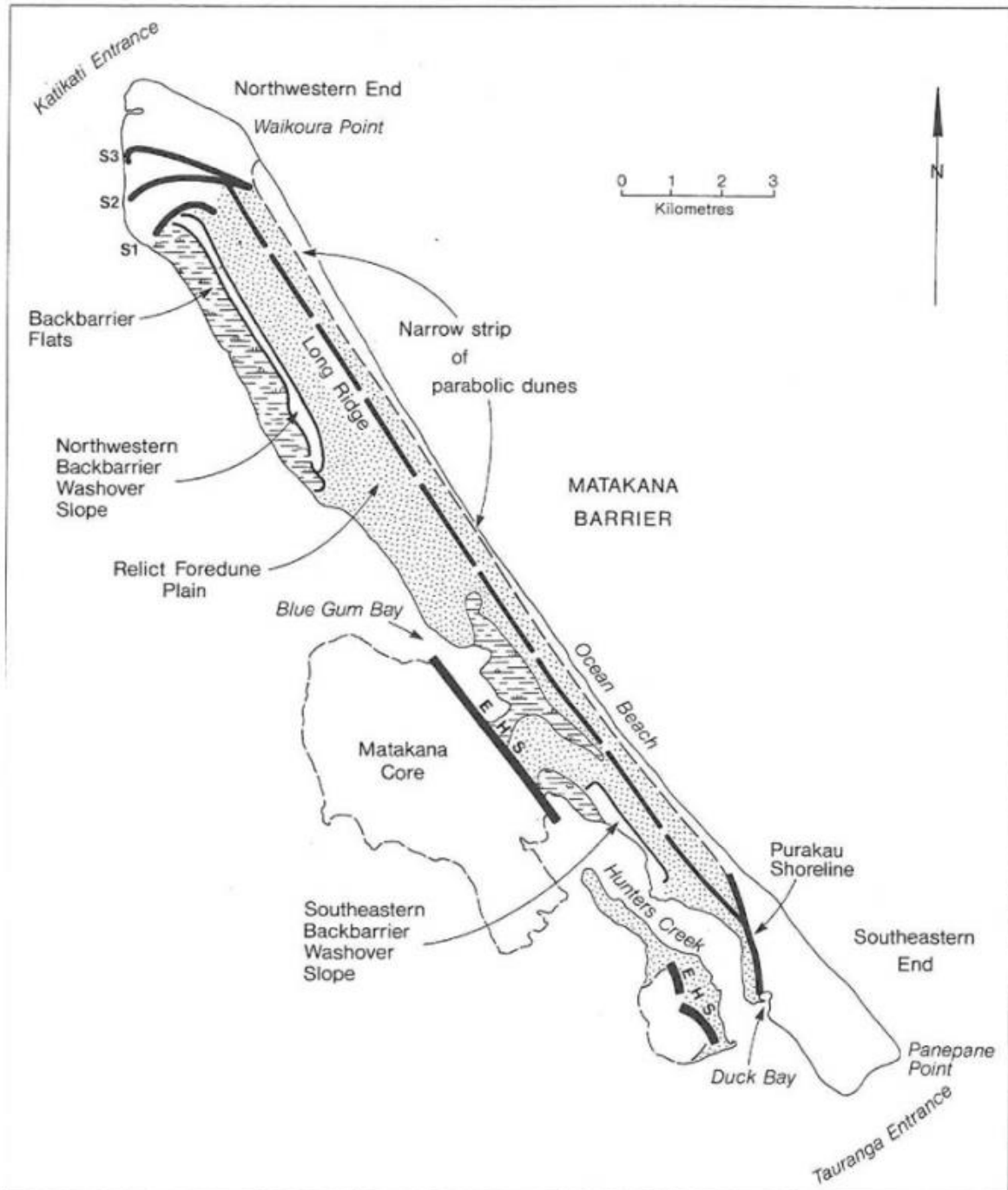


Figure 2.5. Map of Matakana Island demonstrating the landforms and former shorelines. S1 and S2 are eroded shorelines, S3 is the Kaharoa shoreline, and EHS is the earliest Holocene shoreline, (Shepherd et al., 1997).

Waihi Beach - Core WAI 1
Chronology

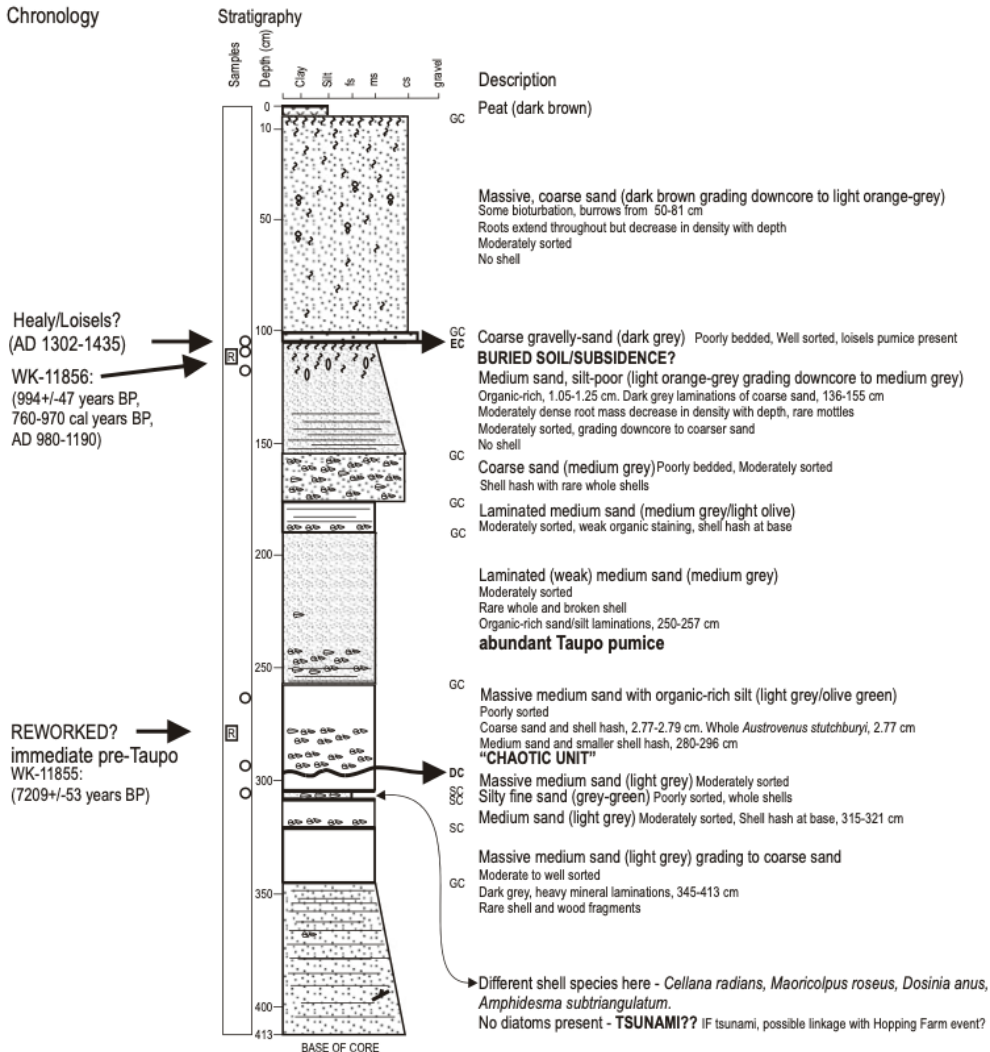


Figure 2.6. Stratigraphy of WAI 1 core taken from the seaward end of Emerton Road at Waihi Beach (Bell et al., 2004).

2.3.3 Matakana Island

Matakana Island forming the seaward border of Te Awanui, is New Zealand's largest barrier island at 24 km in length. The development of Matakana Island alongside the two tombolo's resulted in the formation of Te Awanui during the Holocene (Shepherd et al., 1997). Archaeological evidence indicates that large settlements of Māori people occupied the island in the past as the island has optimal soils and weather conditions for gardening and foraging, and food sources from the sea (Shepherd et al., 1997; Rorke, 2011). At present, Māori hapū of Ngāi Tuwhiwhia and Ngāti Tauaiti, which are sub-tribes of Ngāi Te Rangi, populate the island, although numbers have decreased in recent years (Nation, 2015; Rorke, 2011). The island is used for farming, horticulture, and timber operations (Rorke, 2011).

Betts (1996) undertook research of the Late Quaternary evolution of Matakana Island and identified the main stages of formation. Matakana Barrier Island has two distinct parts: being the older Pleistocene terraces comprised of tephra's (Matakana Core), and a Holocene sand barrier (Matakana Island) on the seaward side. There is a linear feature between Matakana Core and the Holocene Sand barrier and is identified as a "Relict Pleistocene marine cliff", formed during the end of the last interglacial around 6500 years BP and is the earliest Holocene shoreline. Figure 2.7 includes well-logs taken at 5 sites where it was found that there is over 10 m of Pleistocene tephra material buried beneath the sand and it is likely that marine material underlies the terraces around Matakana Core (Shepherd et al., 1997).

The lowermost Pleistocene terrace of Matakana Island formed during the last interglacial high sea level stand c.125 000 years ago. The Holocene Matakana Island barrier began to form from the end of the Postglacial Marine Transgression when sediments on the shelf were reworked and moved on shore. The sediment accumulated as a series of small barriers between c.7 000 cal BP to c.5 200 cal BP. From c.5 200 cal BP to c.4 500 cal BP, the barriers coalesced and tidal deltas, including at both present-day entrances of Te Awanui and two flanking the Matakana Core (Blue Gum Bay and Hunters Creek) began to mature due to rapid onshore sediment movement extending the sand barrier. From c.3 750 cal BP to c.1 750 cal BP was a significant period of development for the sand barrier when tidal inlets such as at Blue Gum Bay were closed, and a single Matakana Island Barrier formed between the two present-day inlets. Larger foredunes on Matakana Island formed during this period as the closing of Blue Gum Bay inlet, increased the tidal flow at the Katikati Entrance, enlarging the channel and the Katikati delta ebb tidal delta. Although the progradation rates for the Matakana Island seaward shoreline slowed, continued growth extending the barrier south-eastward (Betts, 1996).

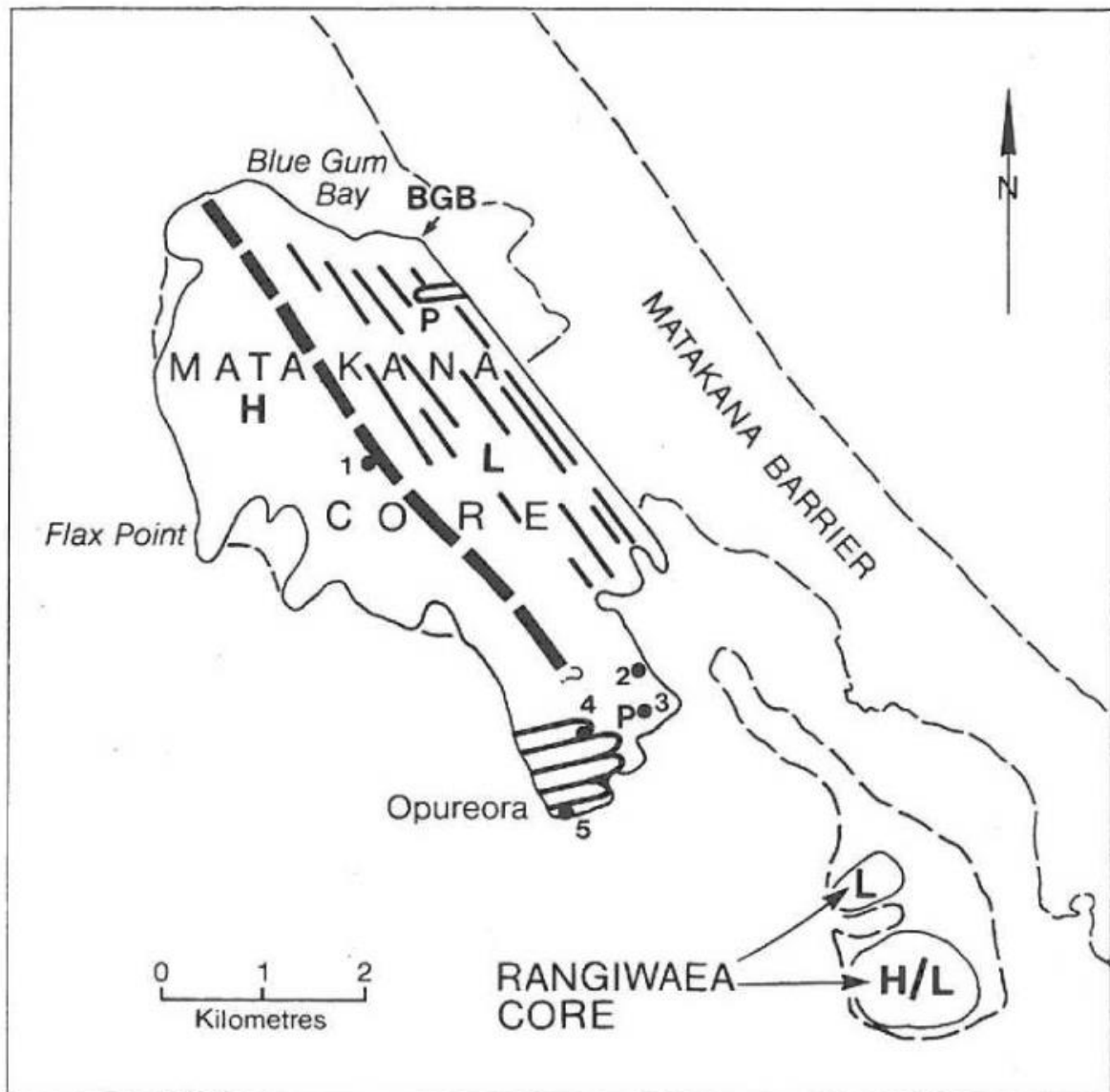


Figure 2.7. Map of Matakana cores showing the Pleistocene geomorphic features. The dashed line represents the “Relict Pleistocene Marine Cliff”. The P stands for the Pleistocene parabolic dunes, and BGB stand for Blue Gum Bay. Numbers 1 to 5 represent well-log locations (Shepherd et al., 1997).

2.3.4 Vertical Land Movement

Data from the NZ SeaRise program using satellite InSAR (Interferometric Synthetic Aperture Radar) estimated the rates of vertical land movement around New Zealand coastlines. The data for Te Awanui and the surrounding areas, including Katikati is shown in Figure 2.8. Noting that there is no data for Matakana Island and other smaller surrounding islands. Katikati appears to be stable to slightly uplifting however, the Bowentown Tombolo and some tidal creeks are sinking. In comparison, the Tauranga Basin that is mostly uplifting. However, the InSAR data only covers 8 years, and should not be considered as representative of long-term trends (Hamling et al., 2022).

A more recent Google Earth KMZ file obtained from Hamling et al. (2024) was used to determine the recent vertical land movement around Te Awanui at 1 km spaced intervals. The data shows that the majority of the Katikati Basin tends to be relatively stable however, some areas tend to be slightly subsiding more than others. Bowentown tends to be slightly subsiding ranging from -0.5942 mm/yr at the seaward side and -0.5922 mm/yr on the harbour side to the west at Shelly Bay (Hamling et al., 2024).

Beavan & Litchfield (2012) documented the changes of land elevation around coastlines of New Zealand over the last 125,000 years. Uplift and subsidence tend to be driven by tectonic activity and can be measured using InSAR as mentioned above, continuous GPS, and Geodetic Surveys. It can also be inferred from relative sea level (RSL) measured by tidal gauges. They found that Te Awanui ranges from stable to slightly uplifting due to its location near the active subduction plate boundary of the Pacific plate causing the land to steadily rise over time (Beavan & Litchfield, 2012).

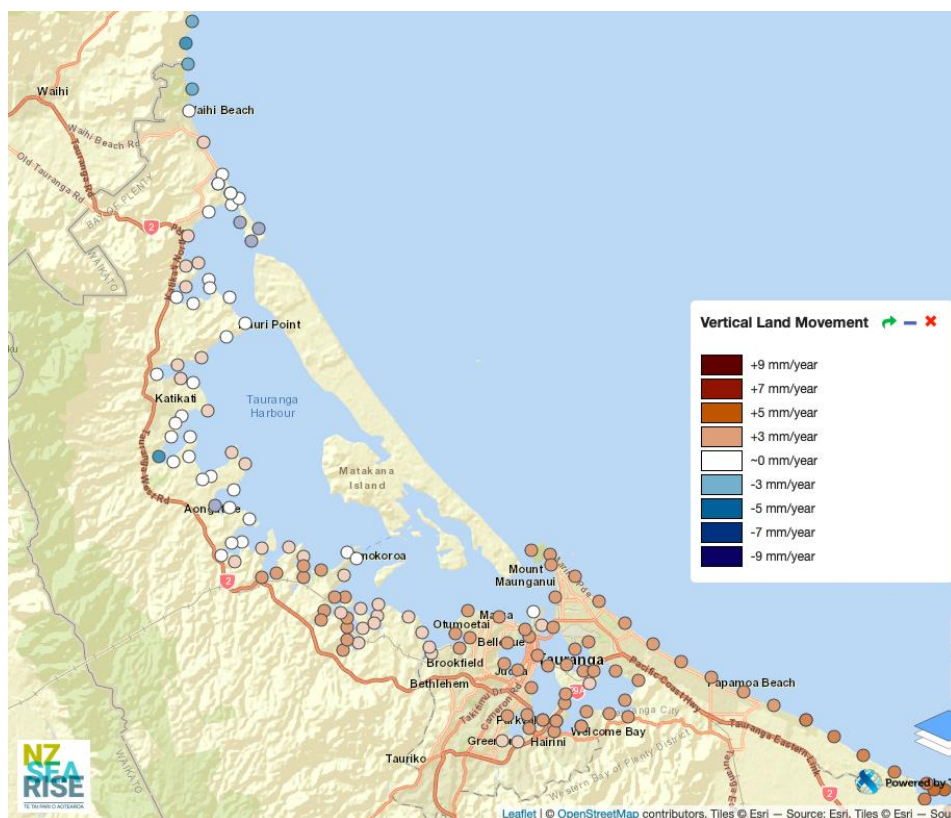


Figure 2.8. Approximate vertical land movement data for Te Awanui. Retrieved from:

<https://searise.takiwa.co/map/6233f47872b8190018373db9/embed>.

2.4 Sediments

Te Awanui is Pleistocene in age covering an area of around 200 km². A period of rapid subsidence caused partial infilling of the harbour following the Waiteariki Ignimbrite eruption (Briggs et al., 1996). Sediments that infilled the basin include terrestrial and estuarine interbedded with volcanoclastic material including distal ignimbrites and tephra's via airfall (Burns & Cowbourne, 2003; Briggs et al., 1996). The basement rock of Te Awanui is the Waiteariki Ignimbrite, and the main river draining into the basin is the Wairoa River located between the Whakamarama and Mamaku Plateaus which is structurally controlled following the major fault marking the boundary between the two Plateaus (Prentice, 2023).

Te Awanui contains sediments from the Holocene from around 7,500 years ago, underlain by Pleistocene deposits with complex topography (de Lange et al., 2014). Seismic surveys and other sedimentation studies have been biased towards the Tauranga Basin due to dredging for shipping channels, so there is little data for the Katikati Basin. However, there is little terrestrial input, so most sediment is derived from offshore as mentioned above. Hence, it is likely that the nature of sediments and deposits are similar for the two Basins.

Magnetic minerals in the coastal environment can be used to determine sediment transport, sources, and depositional processes (Badesab, 2012). Badesab (2012) looked at the distributions of magnetic minerals within Te Awanui and found that the dominant minerals within the estuarine and riverine sediments are titanomagnetite and titanium oxides ilmenite/hemoilmenite. The Tauranga and Katikati Basins differ in the concentrations and types of magnetic minerals. The Tauranga basin contains high concentrations of multi-domain magnetite and titanomagnetite grains and high values of magnetic susceptibility and saturations of isothermal remnant magnetisation. Whereas, the Katikati Basin contains lower values reflecting lower magnetic mineral concentrations and has relatively higher concentrations of titanium rich iron oxide minerals (Badesab, 2012).

Badesab (2012) also found a trend where magnetic mineral concentrations increased and sediment grain size decreased in the riverine sediments draining into Te Awanui from the northwest to the southeast, indicating a variability between the rate of sediment input, transport mechanism and source materials between the two basins. The variability in the terrigenous sediment input also suggests that the local hydrodynamics and regional topography play a major role in controlling the sediment distribution for the two basins within Te Awanui (Badesab, 2012). Therefore it can be

concluded that there is little mixing between the two basins as the concentrations, grain size, and amount magnetic minerals differs for Katikati and Tauranga.

2.4.1 Holocene Sediments

The uppermost Holocene sediments within Te Awanui are composed of clays, silts, sands, gravels, and calcareous materials (mostly shell). The two tombolo's Bowentown and Mt Maunganui are connected to the mainland via a system of progradational dune ridges that are either fixed or moving sand dunes. The progradational dune ridges were formed during the post-glacial marine transgression during the Holocene starting 6500 years ago (Briggs et al., 1996).

Davis & Healy (1993), conducted a study on the Holocene sediments within the south-eastern end of Te Awanui and found three main lithofacies which include in ascending order a pumiceous sand and gravel unit, a shelly mud unit, and a shelly sand unit. The pumiceous sand unit was interpreted as a reworked fluvial and fan deposit (in a terrestrial setting) as a result of volcanic activity during the Late Quaternary period (Davis & Healy, 1993). This unit was dated at 9420 ± 100 yr BP using a wood fragment deposited within the unit and described to be of Pleistocene to early Holocene in age. The shelly mud unit was interpreted to represent a low-energy normal estuarine marine environment within a valley-like setting due to the constrained geometry of the unit (Davis & Healy, 1993). This unit was dated at 8100 ± 80 yr BP. Finally, the shelly sand unit is described as an extensive unit containing shell beds and shell fragments and was deposited during dominant wave shoreface conditions similar to present day when the sea level reached its current level around 6500 years ago. This unit was dated to be between 6000 and 7000 yr BP (Davis & Healy, 1993).

2.4.2 Pleistocene Sediments

The Pleistocene deposits are of mainly volcanic origin. There are two main units recognised, which include a silty pumiceous unit that originates from a distal ignimbrite, and a stiff green mud with an unknown origin. These two units were deposited during the interglacial period around 120,000 - 125,000 BP. Although the green muds origin is unknown, it is suspected to have been deposited during the early Holocene around 7,000 - 10,000 BP via estuarine sediments (de Lange et al., 2014). A common feature within the Pleistocene deposits is the ridge and valley morphology via erosion that are orientated in a sub-parallel nature to the open coast shoreline at present. The Holocene deposits overlying the Pleistocene deposits tend to be thinner over the ridges and thicker in the valleys (de Lange et al., 2014).

There is around 500 m of Pleistocene sediment deposited in the Tauranga Basin. It is unclear the extent of this sediment in the Katikati Basin. The upper beds of the Pleistocene sediment include tephra's and non-welded ignimbrites (mid-late Quaternary), that are overlying and interbedded with sediments of marine to aeolian origin, including fluvial, lacustrine and marine sediments (Shepherd et al., 2000).

During the last Pleistocene interglacial period (the Eemian Interglacial), Te Awanui was a sediment sink for sediments of fluvial, marine, and estuarine origin. Surrounding valleys channelled streams into the harbour dissecting the Pleistocene sediments that were situated below the current sea level. The postglacial marine transgression drowned these ancient valleys to form the Te Awanui (Shepherd et al., 2000).

2.4.3 Sediment Sources

Q-Maps of the Rotorua area published by Leonard et al. (2010) were used to determine the surrounding geology as sources of sediment for the Te Awanui and the Katikati Basin.

The terraces surrounding the harbour contain Holocene alluvium forming a unit known as the Tauranga Group. The lower parts of the terraces within the estuary contain a mixture of alluvial sands, silts, gravels, muds, and pumice clasts Holocene in age. Whereas the upper terraces contain volcanic rich alluvium with pumice, ash rich sediments, and reworked ignimbrites of Pleistocene age (Leonard et al., 2010).

Matakana Island and Matakana Core contain a range of sediments. Matakana Island is a Holocene sand barrier consisting predominantly of the Tauranga Group, with active and stable dune deposits and minor gravel. In contrast the major units at Matakana Core are Pleistocene alluvium and Matakana Basalt, a basaltic scoria cone within the Hewson Formation (Leonard et al., 2010).

The Whakamarama Plateau is a major unit surrounding Te Awanui. This unit originates from the CVZ and is comprised of the Waiteariki Formation, a crystal-rich, welded, dacite ignimbrite (Leonard et al., 2010).

The Kaimai Range contains a range of units. The Kaimai Subgroup contains the main Uretara Formation and the Pukepunga Formation. The Uretara Formation has alternating andesite-dacite lava flows, pyroclastic breccias, epiclastic sediments and minor dike intrusions from the Omahia Formation. The Pukepunga Formation is an andesite-dacite jointed lava flow with autobreccias (Leonard et al., 2010).

The Waipupu Formation of the Waiwawa Subgroup containing andesite breccias, lava flows, and minor epiclastic sediments also forms the Kaimai Range. The Aongatete Formation of the Whakamarama Group is a minor unit in the Kaimai Range consisting of an andesite lava with subordinate dacite-rhyolite ignimbrite and tephra (Leonard et al., 2010).

de Lange (2023) highlights that the provenance of sediments is dependent on the geology of the local catchment. Catchments contributing sediments around Te Awanui produce extremely similar mineral compositions for the Katikati Basin and Tauranga Basin, however there are slight differences between the two (de Lange, 2023). Badaseb et al (2017) focused on the magnetic heavy metal mineral concentrations of sediments entering Te Awanui from rivers and streams across transects within the two basins. For the Katikati Basin, sediments contain high proportions of ilmenite which is derived from andesites of the Kaimai Ranges. Whereas for Tauranga Basin, sediments contain high proportions of titanomagnetite derived from rhyolites of the Whakamarama and Mamaku Plateaus (de Lange, 2023).

2.4.4 Sedimentation Rates

Sedimentation rates for Te Awanui are biased towards the Tauranga Basin as there is little to no data for the Katikati Basin. According to Tonkin and Taylor (2018), the major freshwater sediment source in the harbour is from the Wairoa River. However, 95% of the finer sediments are not retained within the harbour and are discharged into the ocean, as there is no extensive area of low energy sediment sinks where it can be deposited. The intertidal flats within both basins is are subjected to sufficient wave action to remobilise any fine sediment that may be deposited in calm conditions (Tonkin and Taylor, 2018). Within Te Awanui, sedimentation rates are low compared to other estuaries in New Zealand with an annual average of 0.75 to 1.57 mm/yr obtained using measurements on the intertidal flats (Hancock et al., 2009). Along fringe embayment's within the Harbour are where the sedimentation rates are highest. (Tonkin and Taylor, 2018).

2.5 Hydrodynamics

Te Awanui is defined as a shallow mesotidal estuarine lagoon and is characterised by a semi-diurnal tide ranging from 1.2 – 1.6 m (de Ruiter et al., 2019; de Lange, 2023). The shallow estuary has an average water depth of around 3 m. Intertidal flats are a common feature making up approximately 65% of the estuary where they contribute to the estuaries well mixed nature and are exposed during low tide. These tidal flats divide the estuary into two basins the northern Katikati Basin and southern Tauranga Basin (de Ruiter et al., 2019).

During the Holocene, the harbour's coastline was unprotected and exposed while sediment was brought into the area via longshore and onshore transport. Over time, this sediment accumulated and began constructing the present-day tombolo's and barrier island Matakana Island. These enclosed the Te Awanui lagoon apart from the tidal inlets, restricting marine sediment input and developing the hydrodynamic and sedimentary regime we see in the harbour today (MacPherson et al., 2017).

2.5.1 Wave and Tidal Environment

Due to its location on the east coast, Tauranga has a lower wave energy compared to most other New Zealand coastlines. The waves are generated by a combination of distant swell from storms in the North Pacific Ocean, and locally generated waves due to onshore north easterly winds. The wave conditions can be defined as a mild meso-energy swell wave environment as the locally generated waves are dominated by the swell waves with a significant wave height of 1.5 m and 0.6 m (Shepherd et al., 1997).

Both the Katikati and Tauranga tidal inlets are tidally-dominated due to their morphology and vast ebb-tidal deltas influencing both entrances large tidal prisms ($95.8 \times 10^6 \text{ m}^3$ at Katikati and $130.8 \times 10^6 \text{ m}^3$ at Tauranga), relative to the moderate wave energy at the coast. These ebb-tidal deltas store extensive amounts of sediment with a volume of $30 \times 10^6 \text{ m}^3$ at Katikati and $47 \times 10^6 \text{ m}^3$ at Tauranga. The deltas provided sediment to Matakana Island during its development, and they also modify the incoming waves by refraction and energy dissipation due to their presence (Shepherd et al., 1997).

Wave Environment at the Katikati Inlet

NIWA installed a directional wave measuring buoy 8 km off the Katikati inlet at 34 m in water depth (Figure 2.9) during February 1991 to study sediment movement around the area as well as wave climate and characteristics data (Macky et al., 1995).

Macky et al (1995) summarised the first three years of data from the buoy for the Katikati inlet. What they found was that storms give the highest significant wave height where in June and October 1992 the significant wave height was 4.3m. For 70% of the time, mean wave heights were less than 1 m and the mean wave height for the three year period was approximately 0.8 m and the significant wave period had a mean of 6 s. Data from the longshore component of wave energy flux at the breaker line showed that most of the wave energy from major storms arrived from the east moving sediment to the north-west. They also found that long persistent periods of low energy waves from the north caused littoral transport of sediment to the south-east (Macky et al., 1995).

Overall, the net longshore transport rate due to storms was 72 000 m³y⁻¹ North-westwards and fluctuated in direction and magnitude per storm compared to the overall longshore transport of the area of over 1 000 000 m³y⁻¹. It is important to note that the study period from 1991-1994 was measured during El Niño conditions and may not represent the long-term effects of the wave climate of Katikati (Macky et al., 1995).

A new permanent wave buoy was installed and is operate by the Bay of Plenty Regional Council located 7 km off the Bowentown Heads in 30 km of water Figure 2.10. The buoy measures significant wave height, significant wave period, wave direction, and sea surface temperature (sensor is located approximately 0.5 m below the sea surface). Daily data is available for anyone to access on the Bay of Plenty Regional Council Environmental Data Portal.

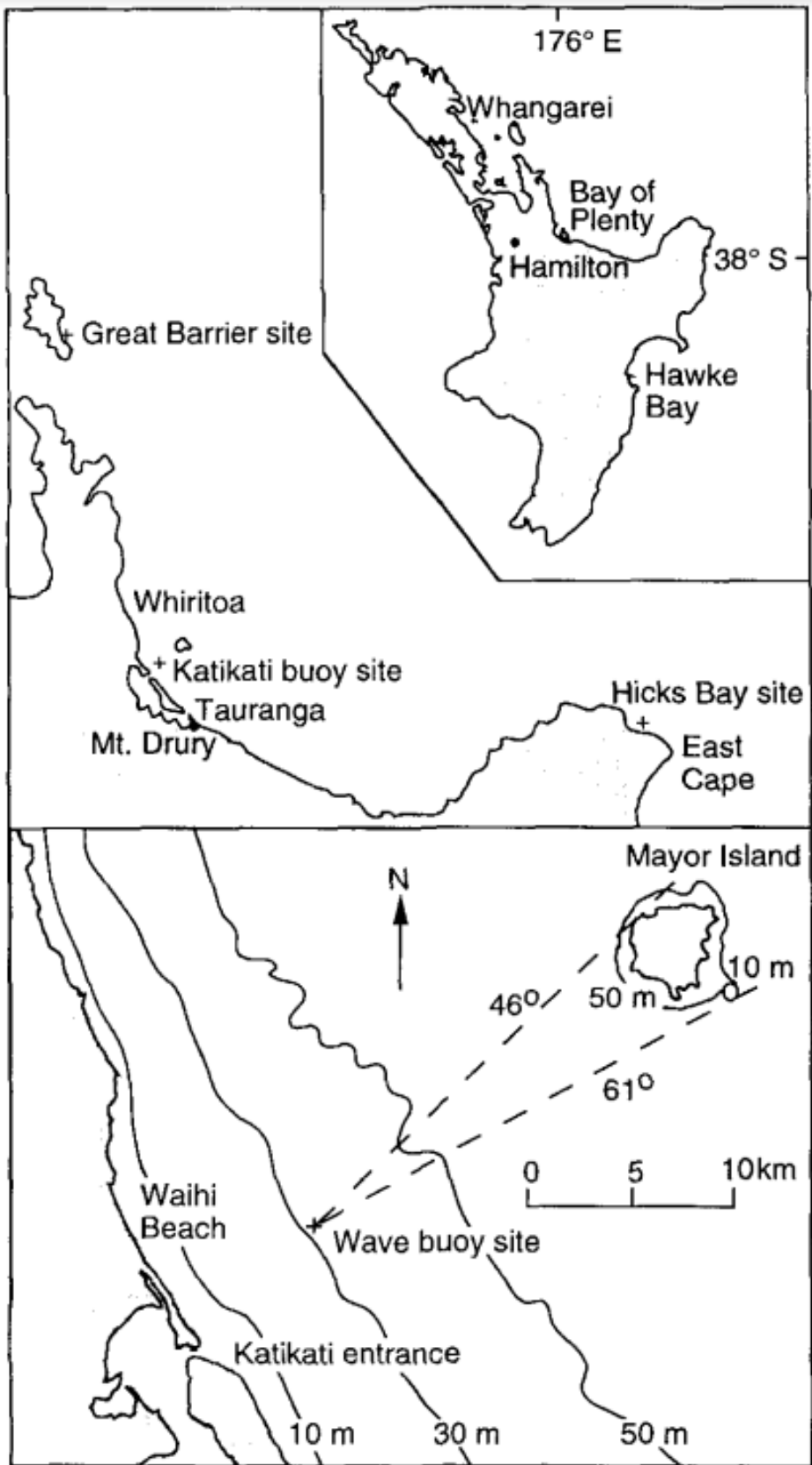


Figure 2.9. Location of the wave buoy relative to the Katikati entrance in the Bay of Plenty, including isobaths (Macky et al., 1995).

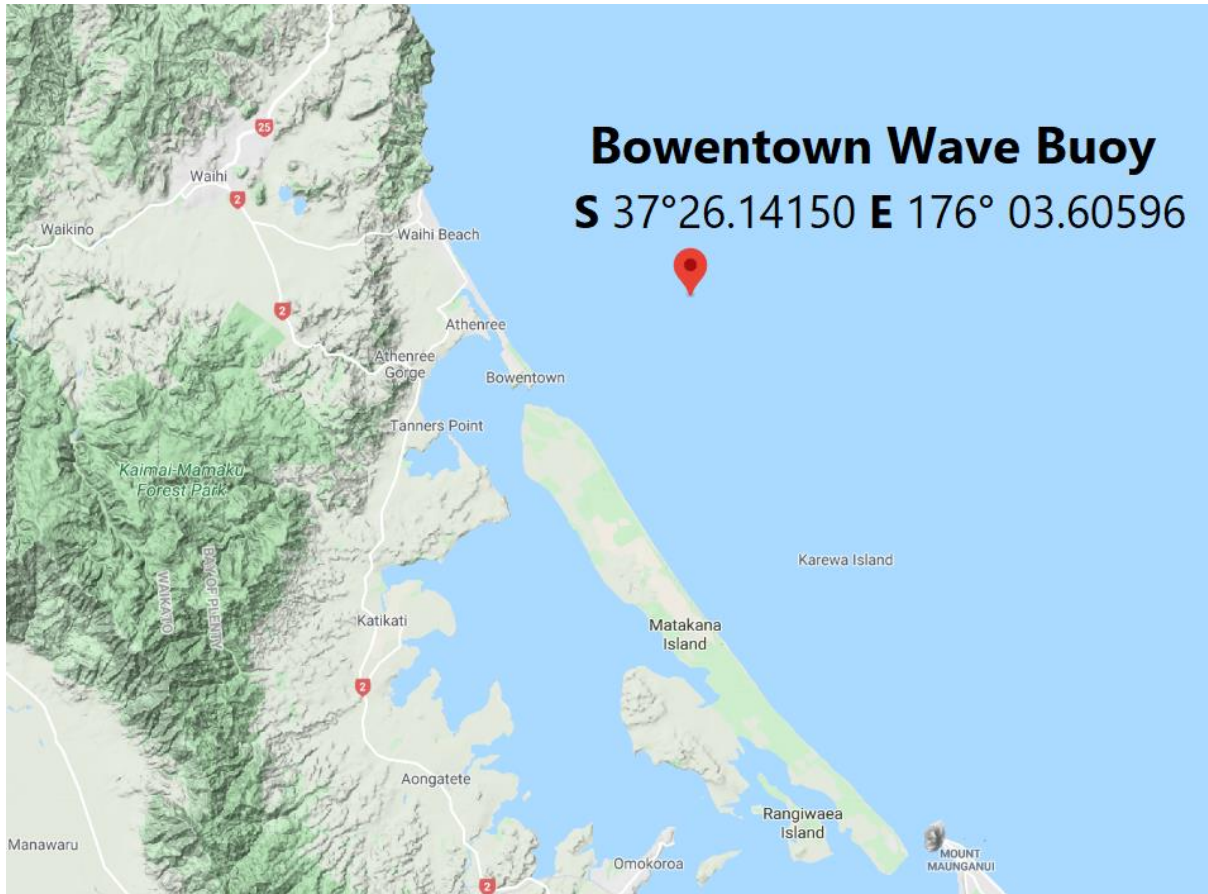


Figure 2.10. Location of the permanent Bowentown Wave Buoy (<https://envdata.boprc.govt.nz/>).

2.5.2 Catchment

Shallow intertidal flats in the centre of Te Awanui separate the harbour into two basins in terms of hydrodynamics and fluvial inputs: Katikati Basin in the northwest; and Tauranga Basin in the southeast (de Lange et al., 2015). These lagoonal basins are independent of each other as they have their own drainage channel systems and bays. Katikati Basin is shallower, and calmer compared to the larger Tauranga Basin which is more energetic (Badesab et al., 2017). However, dredging in the Tauranga Basin through Stella Passage has caused the current speeds to be significantly lower compared to the shallower areas that have not been dredged (Watson, 2016).

For Te Awanui the total catchment area is $\sim 1300 \text{ km}^2$. The catchment for the Tauranga Basin is 1030 km^2 with a mean annual freshwater inflow of $30.5 \text{ m}^3/\text{s}$. The catchment for the Katikati Basin is 270 km^2 with a mean annual freshwater inflow of $4.1 \text{ m}^3/\text{s}$, demonstrating that it is a much smaller basin than the Tauranga Basin (Badesab et al., 2017).

Small rivers that are a source of freshwater inflow for the Katikati Basin include the Tuapiro, Uretara, and Aongatete Rivers. The Aongatete River has the largest catchment area of all the rivers flowing into the Katikati Basin of 78 km², and forms the largest sub-estuary, entering the southeast area of the basin. The other two main catchments are the Uretara and Tuapiro rivers. The Uretara River catchment covers an area of 77 km² and the river flows down into the central area of the Katikati Basin from the Kaimai Ranges. The Tuapiro River Catchment has an area of 60 km² and the river flows into the southwest Katikati Basin from the Kaimai Ranges (Badesab et al., 2017).

2.6 Summary

In summary, Te Awanui is in the western Bay of Plenty and is Aotearoa New Zealand's largest barrier-enclosed, persistent, meso-tidal coastal lagoonal system covering an area of approximately 200 km² with two distinct basins the Katikati Basin in the north and the Tauranga Basin in the south (Badesab et al., 2017; de Lange et al., 2015; Stokes et al., 2009).

The sediments and cover rocks found around Te Awanui originate from the TgaVC and the landforms are linked to volcanism of the CVZ and TVZ (de Lange, 2023). It is suggested that the opening of the Taupō rift causes NNE-aligned trending faults in the Tauranga region and controls the alignment of the Minden Rhyolite subgroup, local rivers, and terraced peninsulas (Briggs et al., 1996; Prentice, 2023). The Waiteariki Ignimbrite forms the basement rock of Te Awanui (Prentice, 2023). The Tuapiro Fault flows through Katikati and is deemed inactive as it has not shown movement in the last 128,000 years (Lee & Villamor, 2018). Two thesis studies on the Tauranga Basin found movement of faults through the Holocene sediments (Podrumac, 2016) and displacement between sediments at the cliffs within Ōmokoroa Peninsula (Christophers, 2015). There is a low gravity anomaly within the Katikati Basin that is speculated to be a caldera or sedimentary basin (Stagpoole et al., 2021).

The geomorphology of Te Awanui includes the two tombolo's Bowentown and Mt Maunganui, consolidated cliffs, unconsolidated shorelines, and non-eroding shorelines (Briggs et al., 1996; Briggs et al., 2005; Tonkin and Taylor, 2018). There was a local tsunami that affected Te Awanui found in deposits at Ōmokoroa and an eroded shoreline on Matakana Island (Bell et al., 2004; de Lange et al., 2015). Matakana island began forming during the last interglacial high sea level stand c.125 000 years ago and contains two distinct parts including the older Pleistocene terraces (Matakana Core) and a Holocene sand barrier on the seaward side (Matakana Island) (Betts, 1996). InSAR data shows that the vertical land movement of the Katikati Basin is relatively stable to slightly uplifting due to its location

near the active subduction Pacific Plate boundary (Beavan & Litchfield, 2012; Hamling et al., 2022; Hamling et al., 2024).

Te Awanui is Pleistocene in age and a period of subsidence caused partial infilling of the harbour following the eruption of the Waiteariki Ignimbrite via terrestrial and volcanic sediments (Briggs et al., 1996; Burns & Cowbourne, 2003). Holocene and Pleistocene aged sediments are deposited in the Katikati Basin (de Lange et al., 2014). The Holocene sediments are composed of clays, silts, sands, gravels, and calcareous materials (Briggs et al., 1996). The Pleistocene sediments are mainly of volcanic origin with a silty pumiceous unit and a stiff green mud unit (de Lange et al., 2014). The difference in magnetic minerals between the Katikati Basin and Tauranga Basin means they have different sources of sediments via local topography and hydrodynamics (Badesab, 2012).

Te Awanui is defined as a shallow mesotidal estuarine lagoon and is characterised by a semi-diurnal tide ranging from 1.2 – 1.6 m and an average water depth of approximately 3 m (de Ruiter et al., 2019; de Lange, 2023). Due to its location on the east coast, Tauranga has a lower wave energy compared to most other New Zealand coastlines with locally generated waves and a significant wave height of 1.5 m and 0.6 m (Shepherd et al., 1997). There is a permanent wave buoy located 7 km off the Bowentown Heads that continuously measures significant wave height, significant wave period, wave direction, and sea surface temperature. The catchment for the Katikati Basin is 270 km² with a mean annual freshwater inflow of 4.1 m³/s, and is a much smaller basin than the Tauranga Basin (Badesab et al., 2017). Small rivers that contribute to freshwater inflow for the Katikati Basin include the Tuapiro, Uretara, and Aongatete Rivers where the Aongatete River has the largest catchment area of all the rivers flowing into the Katikati Basin of 78 km² (Badesab et al., 2017).

Chapter 3: Seismic Reflection Characterisation

3.1 Introduction

A shallow seismic reflection survey was carried out in Te Awanui within the Katikati Basin and Katikati entrance on October 12th and 13th 2023 to identify key stratigraphic interval from the seafloor into the subsurface (Figure 3.1). This Chapter will discuss the findings within the data using interpreted seismic lines and a series of structure contour and isopach thickness maps.

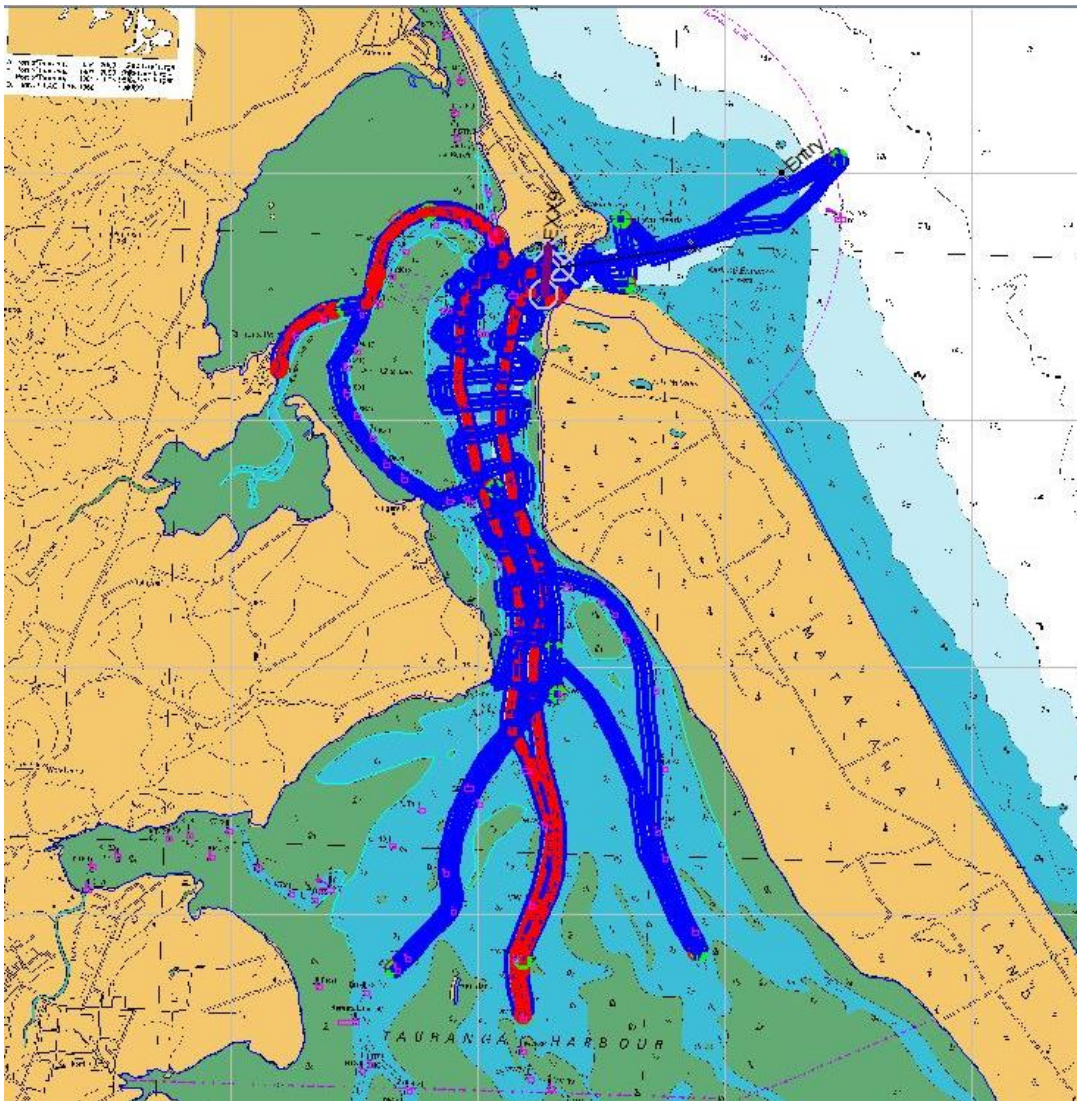


Figure 3.1. Location of seismic lines within the Katikati Basin for the 12th of October in red and the 13th of October in blue.

3.2 Seismic Reflection Basics

In marine seismic surveys, artificially generated sound waves interact with the geological features beneath the seafloor via reflection and refraction at stratigraphic interfaces generating an “image” of the subsurface. Seismic reflection involves artificially generated compressional waves called P-waves that travel down into the Earth reflecting off of geological boundaries and features that travel back to the surface and are recorded. A marine seismic survey involves towing of a controlled seismic source (a series of cables or Sub-Bottom Profiler) within the water just below the surface generating seismic waves which are then processed by generating seismic images revealing the nature of the subsurface geology including faults, lithological boundaries, unconformities etc (Figure 3.2). (Crutchley & Kopp, 2018). Each layer has its own acoustic impedance (Z) which is dependent on the wet bulk density of the sediments (ρ) and the compressional wave velocity (c) (Penrose et al., 2005), shown as:

$$Z = \rho c$$

The seafloor is the first and strongest reflection due to the contrast in physical properties of the water column and seafloor sediments (Crutchley & Kopp, 2018). Reflections below the seafloor can be strong or weak depending on the velocity and density differences of the stratified sediments and underlying strata (Crutchley & Kopp, 2018). The returning sound waves are recorded by a hydrophone or a transducer/transceiver where an acoustic receiver resolves the pulses of energy with the shallower reflectors arriving first and are displayed in a real-time continuous profile of the bathymetry and boundaries between the subsurface strata (Penrose et al., 2005).

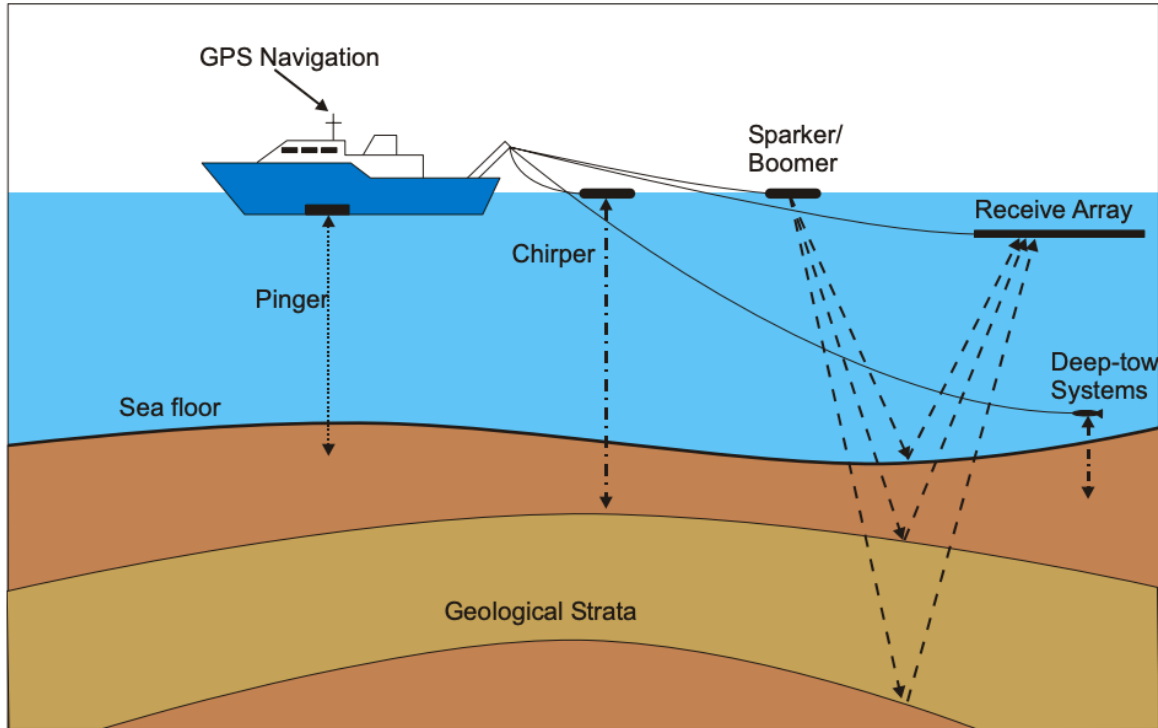


Figure 3.2. Deployment of various shallow-water sub-bottom profiling systems used for a seismic survey (Penrose et al., 2005).

3.3 Methods

3.3.1 Seismic Field Methods

The shallow seismic survey was undertaken using a Knudsen Pinger Sub-Bottom Profiler (SBP) with a 3.5 kHz chirp signal. The SBP was secured to the boat by a pole. A GPS receiver was also used to record co-ordinates alongside the seismic data from the SBP. The pulse length was adjusted depending on the depth of the water where 0 - 2 m needed no adjustment, Tx1 represented 2 - 3m in depth, Tx2 3 - 4.5 m, Tx3 4.5 - 7 m, and Tx4 7+m. The SBP was connected to a computer running through the KNUDSEN SounderSuite Windows application that produced real time data of the bathymetry and subsurface strata. The data was saved in 10 minute segments to simplify the analysis on Petrel and saved to a USB.

3.3.2 Seismic Data Processing

The GPS data was processed through Google Earth and Excel, and the seismic data was processed through ArcGIS into SEG-Y files then loaded into Petrel. The seismic segments ranged from 100 m to

~1550 m in length. The sound velocity the SBP assumes is approximately 1500 m/s. Correlating the seismic data began with mapping the sea floor reflector on all the seismic profiles. Through the central area of the Katikati Basin two other reflectors were correlated and mapped as Horizons A and B. All identified reflectors through the central area of the Basin were made into composite lines which were then used to create structure contour maps and isopach thickness maps.



Figure 3.3. All seismic lines processed in Petrel. This does not match Figure 3.1 exactly because not all lines were suitable for analysis.

3.4 Seismic Interpretation

The main prominent reflector within all the seismic profiles was interpreted to be the sea floor, two slightly less prominent reflectors were labelled Horizons A and B through the main channel of the study area within the Katikati Basin. Figure 3.4 shows a seismic profile through the main channel of Katikati Basin with the three main reflectors. All three reflectors tend to follow a similar shape through the channel however the middle section of Horizon B the reflector drops into a U shape.

The Seafloor reflector is interpreted as the upper layer of the Holocene sediments. Horizon A is interpreted as the base of Holocene sediments. Horizon B is interpreted another layer of sediments of unknown age, possibly also Holocene. I interpret all three reflectors to be of Holocene origin as Figure 3.5 represents a seismic line through the Stella Passage in the Tauranga Basin where there are reflectors at similar depths to the seismic line in Figure 3.4 for this study, and the reflectors through the Stella Passage are of Holocene origin and labeled as a Holocene sand and silt unit up to 20 m thick in depth (MacPherson et al., 2017). The thickness of the sediments through the seismic profiles of the three identified reflectors ranges up to about 15 m, and the depth of the seismic profile overall for this study reached up to approximately 23 m (Figure 3.12).

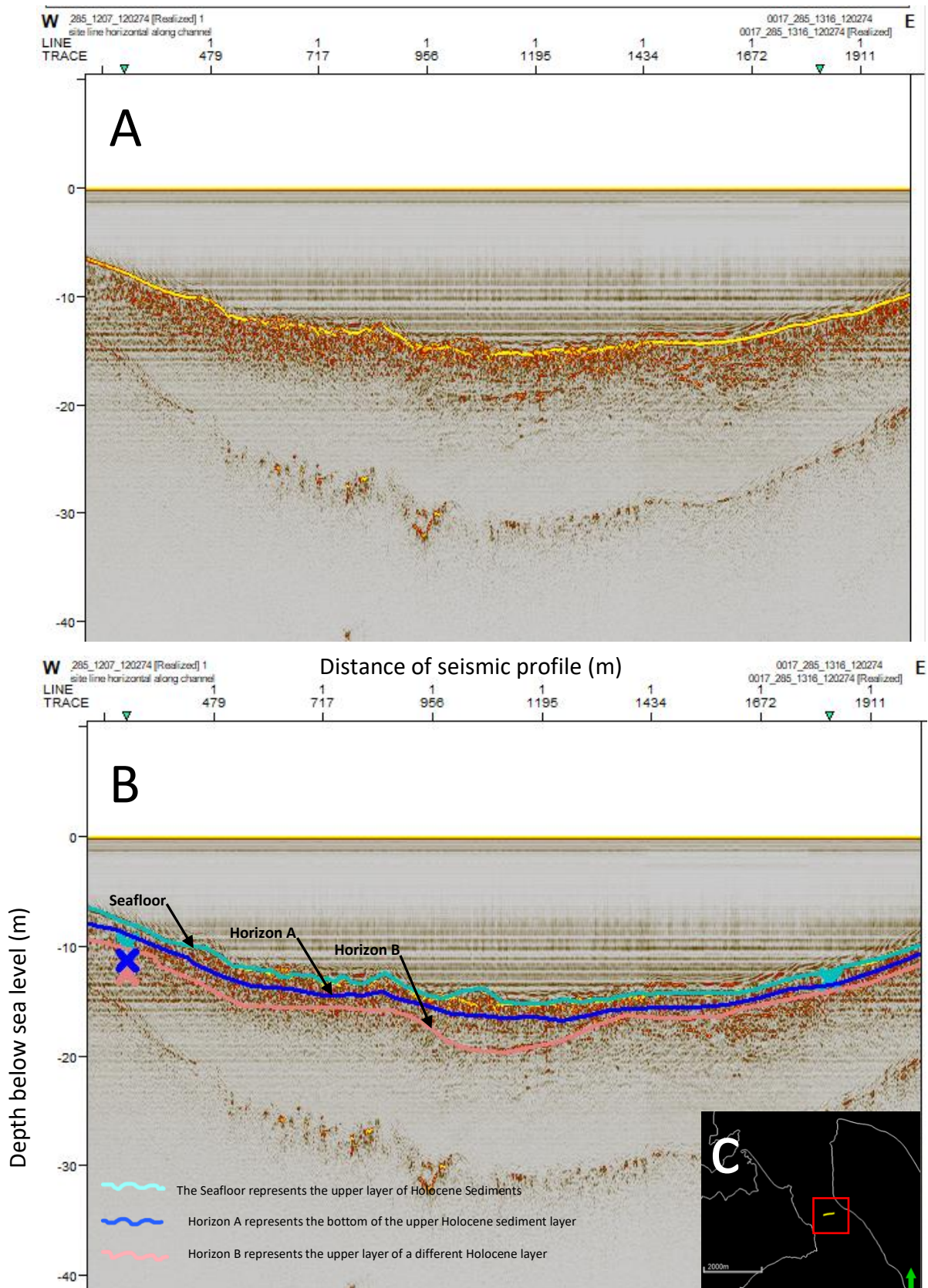


Figure 3.4. A) Uninterpreted seismic line through the main channel. B) Corresponding interpreted seismic line showing the Seafloor, Horizon A, and Horizon B reflectors. C) Location of the seismic line.

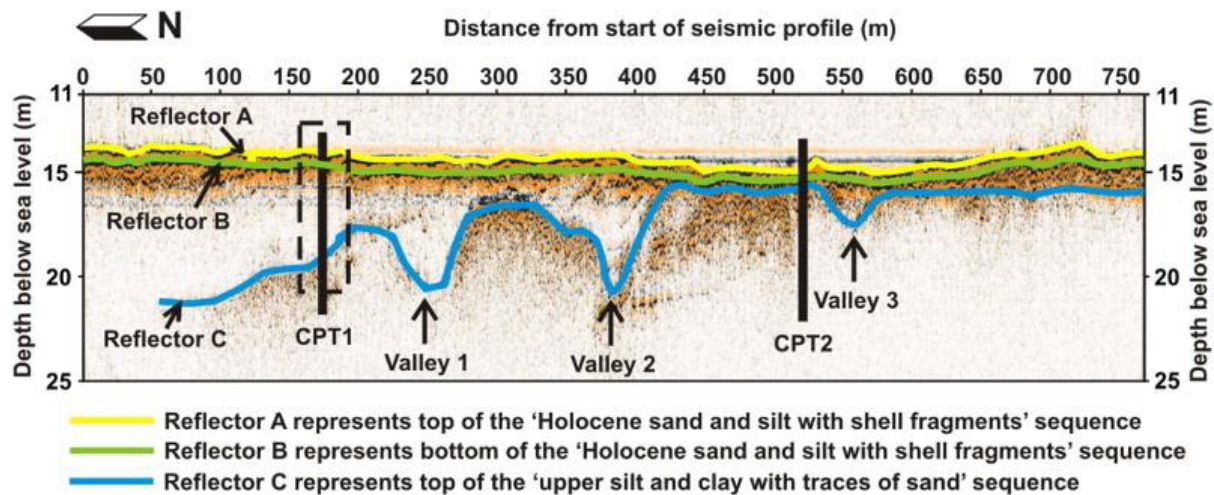


Figure 3.5. Seismic line from Stella Passage showing MacPherson et al. (2017)'s interpretation of the seismic reflectors.

3.5 Structure Contour Maps

Structure contour maps of the Seafloor, Horizon A, and Horizon B were created using the seismic lines in Figure 3.6 to determine the geomorphology of the main channel and bathymetry below the surface. Overall, the three contour maps show similar stratigraphic patterns.

Seafloor

The Seafloor structure map in Figure 3.7 shows that the depth of elevation ranges from 0 m to -16 m. The deepest area at -16 m is the main channel through the narrow part of the basin where it then tapers off and becomes shallower from -2 m to -10 m to the south. The area surrounding the main channel range from approximately 0 m – 8 m in depth. Further north, there is no clear channel running through the basin and this area comprises mainly shallow peaks (lighter colours) and troughs (darker colours).

Horizon A

Horizon A in Figure 3.8 has a depth of between -2 m and -20 m. Similar to the Seafloor reflector in Figure 3.7, Horizon A has a deeper main channel through the narrowest part of the basin at -20 m depth and tapers out becoming shallower further south. The area surrounding the main channel ranges from approximately -2 m to -12 m in depth. To the north, there is minimal evidence for shallow peaks and troughs where the area is smoother at generally -8 m in depth.

Horizon B

Horizon B in Figure 3.9 has a depth that varies from -2 m to -22 m. The main channel in this contour map is not as well defined as the channel in Figures 3.7 and 3.8 having a lumpier shape rather than smooth and continuous across the whole map and ranges from approximately -12 m to -22 m in depth. The areas surrounding the main channel are not as well defined and range from approximately -2 m to -12 m in depth. The northern end of the contour map is similar to Figure 3.8 where the area is generally quite smooth mainly around -10 m in depth.



Figure 3.6. Map of seismic lines used to create the structure contour maps and isopach thickness maps of the Seafloor, Horizon A, and Horizon B.

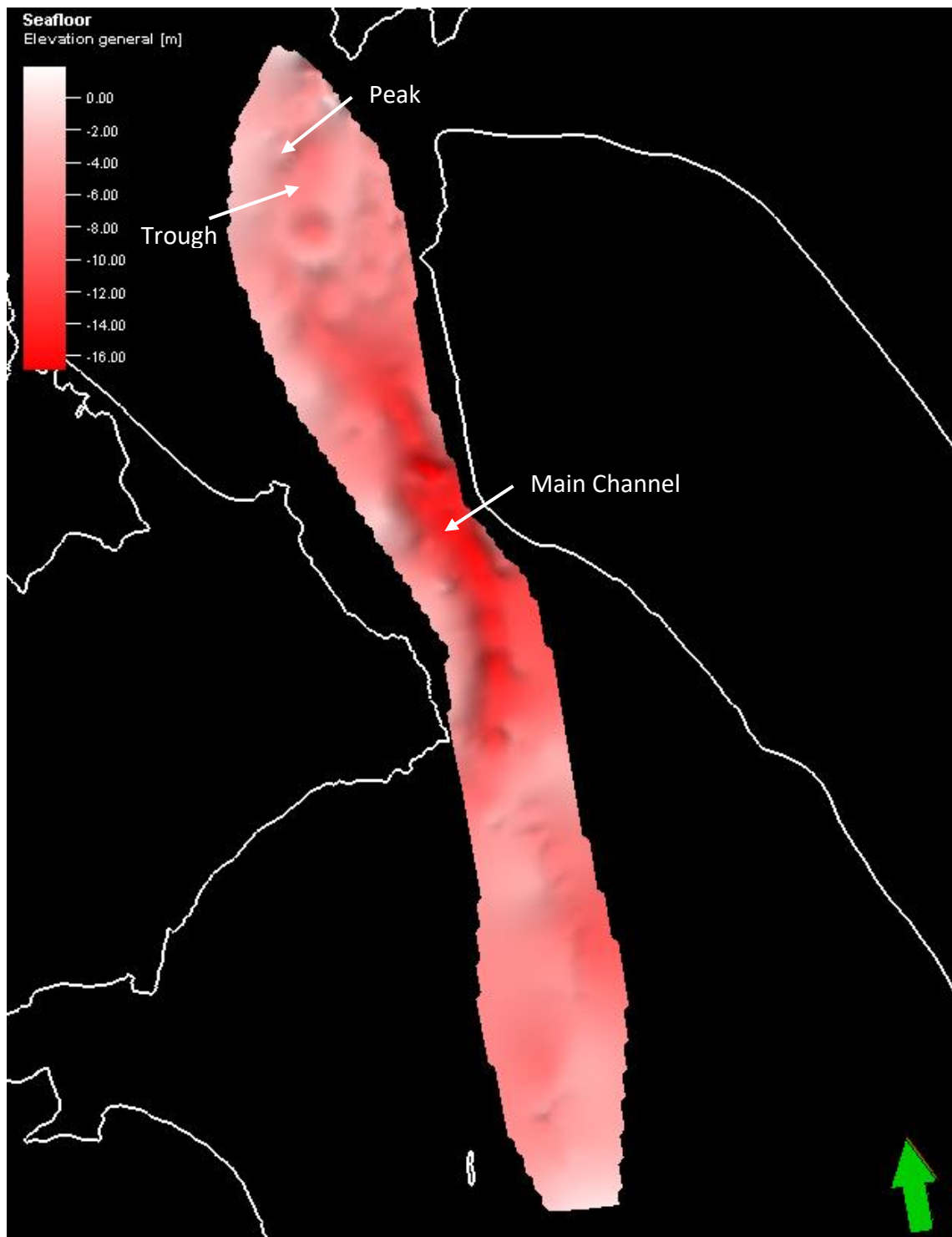


Figure 3.7. Structure contour map of the Seafloor reflector with depth in meters (m).

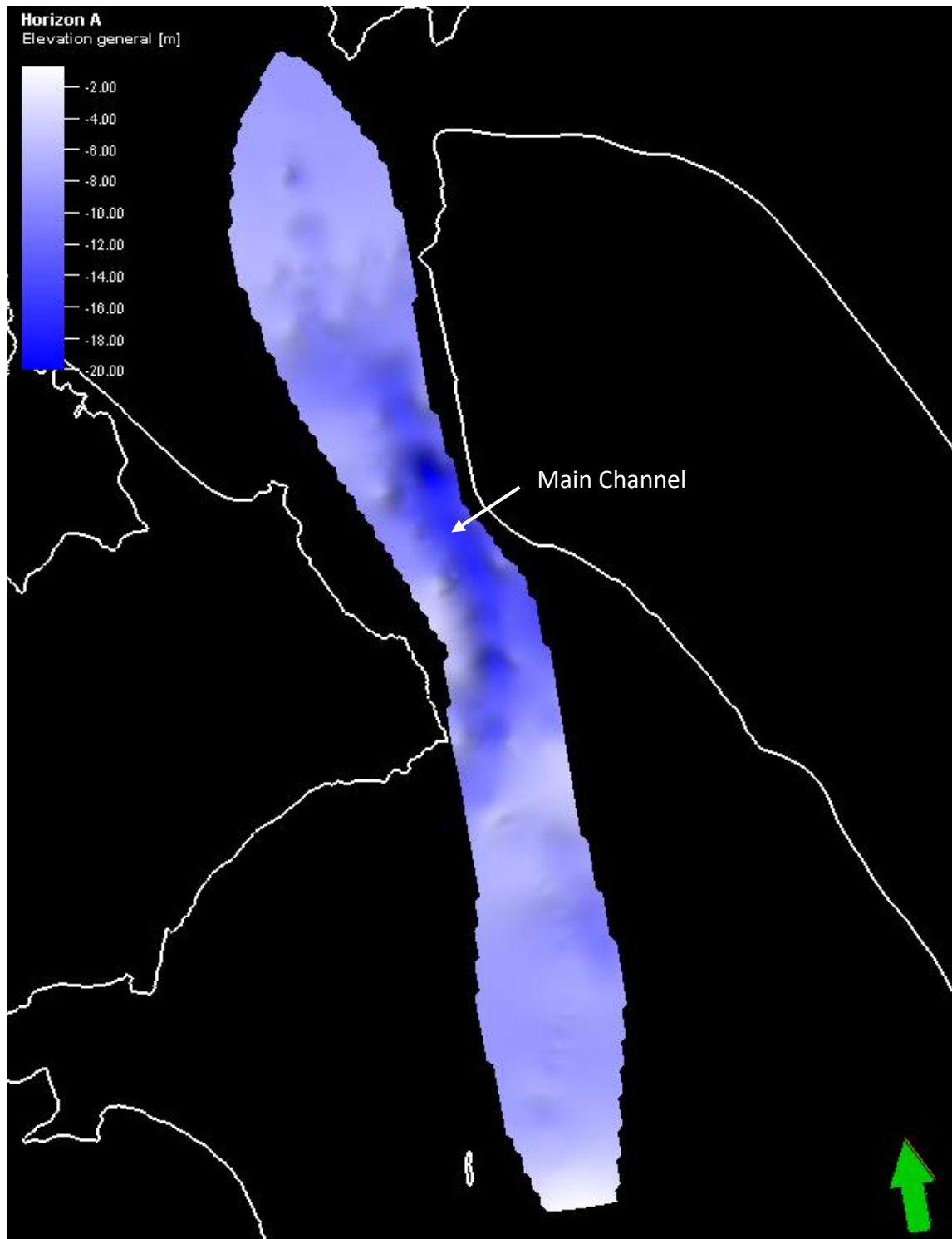


Figure 3.8. Structure contour map of Horizon A with depth in meters (m).

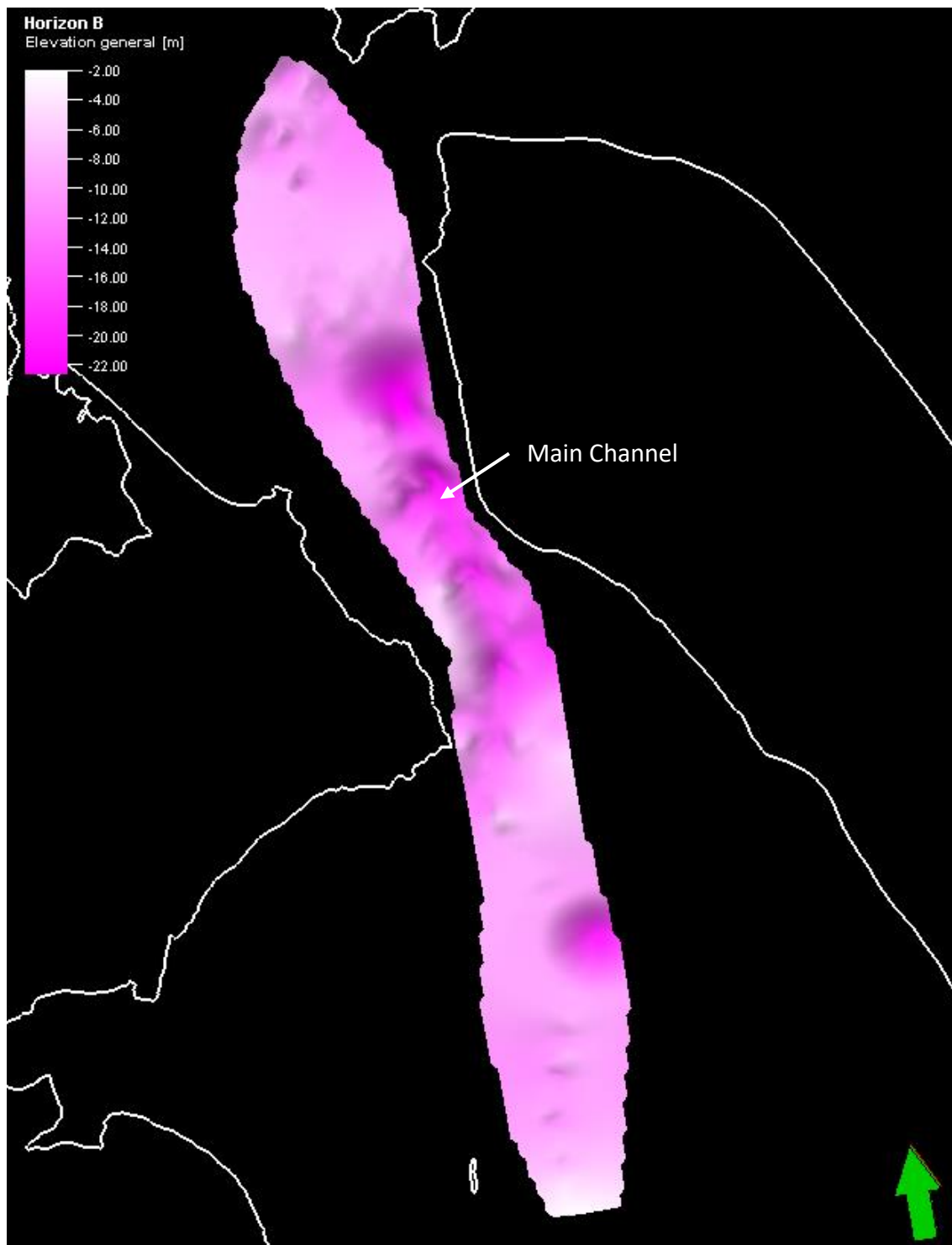


Figure 3.9. Structure contour map of Horizon B with depth in meters (m).

3.6 Isopach thickness Maps

Isopach thickness maps were created between the seismic reflectors identified within the main channel area of the Katikati Basin to determine the thickness of the strata between the three Horizons. Overall, both maps tend to follow a similar trend of thickness.

Seafloor to Horizon A

The isopach thickness map in Figure 3.10 shows that the thickness between the Seafloor Horizon and Horizon A varies from 0.5 m to 3 m. The thinnest areas of about 0.5 m to 1 m are generally located through the central area of the map where the main channel flows. The thicker areas, ranging from 1.5 m to 2.5 m, extend off the boundary off the main channel and also are located in some parts of the central area of the main channel. There are two minor areas that are the thickest at 3 m in the north near the top of the map and in the central south areas.

Horizon A to Horizon B

The isopach thickness map displayed in Figure 3.11 shows that the thickness between Horizon A and Horizon B varies from 0.5 m to 3 m. The thinnest areas of around 0.5 m to 1 m tend to reside in areas where the main channel flows through the basin as well as some areas to the north and the south of the map. The thicker areas, which range from 1.5 m to 2.5 m, extend off the main channel area and are scattered throughout the map. There are also two minor areas that are the thickest at 3 m but they are in different areas than Figure 3.10 where one area is near the central area of the map and one is to the north.

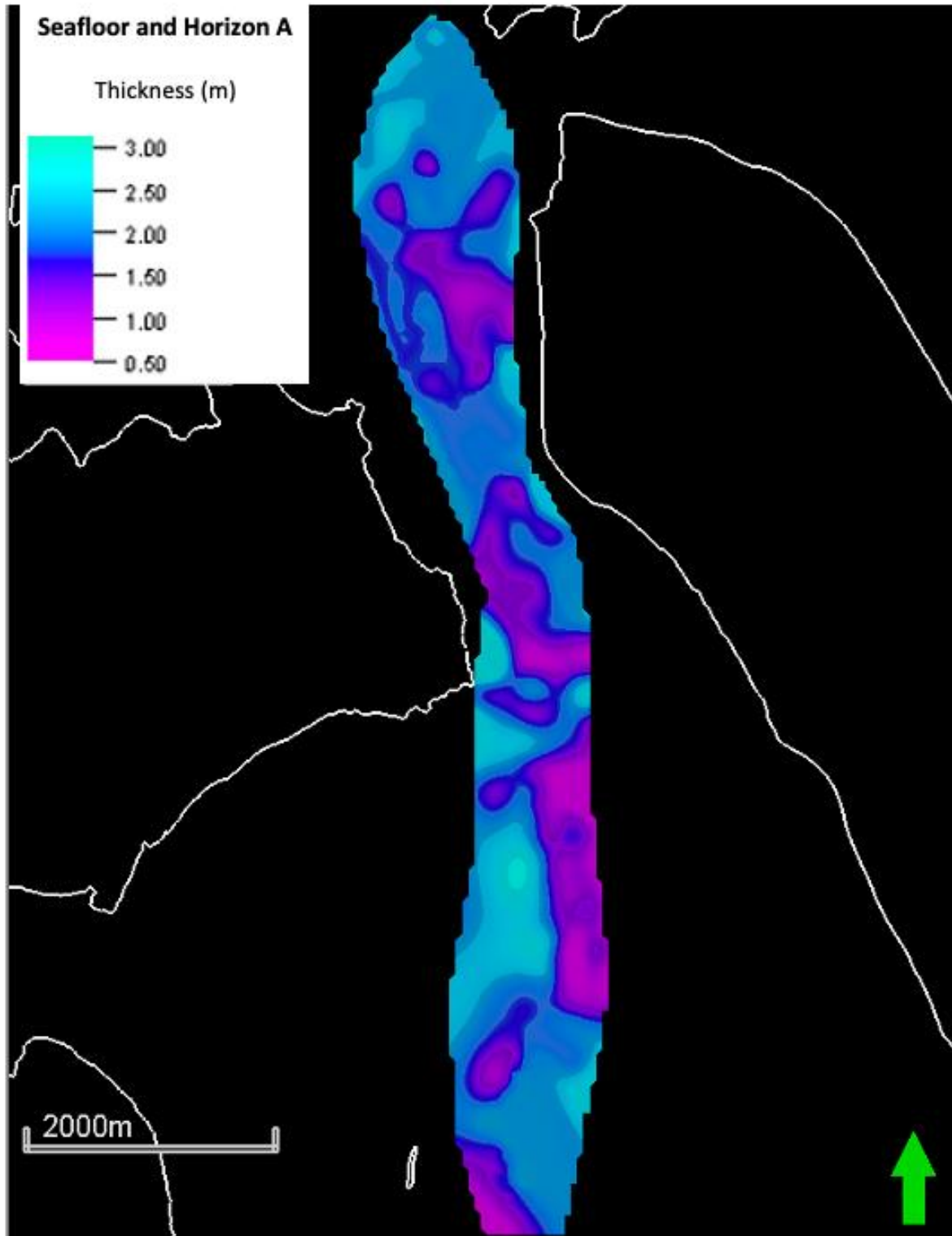


Figure 3.10. Isopach thickness map showing the thickness between the Seafloor Horizon and Horizon A. The contour interval is 0.5 m.

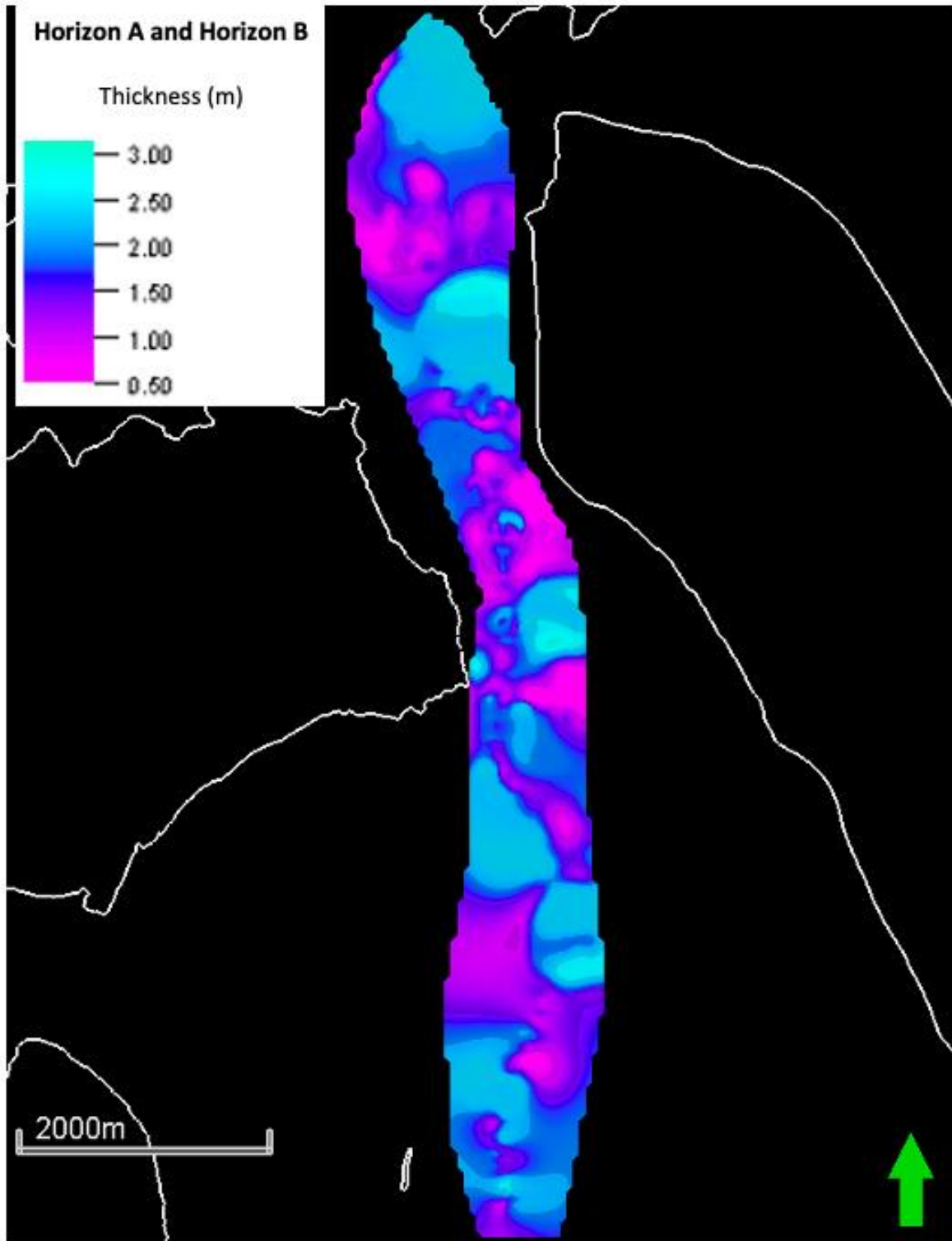


Figure 3.11. Isopach thickness map showing the thickness between Horizon A and Horizon B. The contour interval is 0.5 m.

3.7 Bowentown

The seismic lines surrounding Bowentown displayed in Figure 3.12 show some interesting features. Bowentown is a rhyolite dome tumbolo (Prentice, 2023), therefore the features labeled could have volcanic origin. The sediment mound may be some form of lava flow however (Gudmundsson, 2008) mentions lava flows tend to have layering and there appears to be no evident layering in the sediment mound and its origin or composition is unable to be determined via seismic data alone. Another feature is labelled as boulder/rhyolite dome because it is again unclear what this feature may be. It could be a small rhyolite dome protrusion or a large boulder beneath the surface.

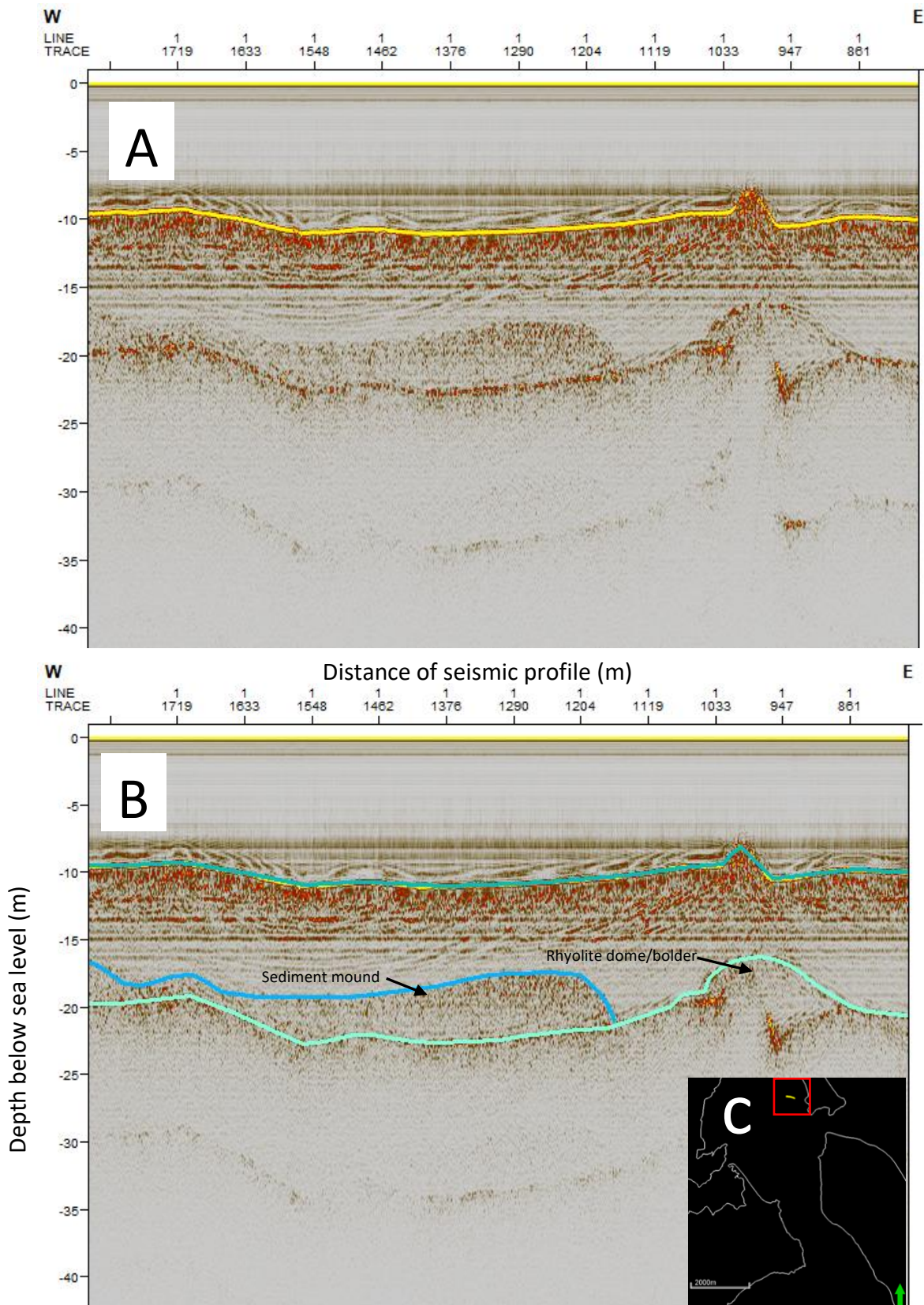


Figure 3.12. A) Uninterpreted portion of seismic line 1400. B) Interpreted portion of seismic line 1400 with the lava flow and rhyolite dome/boulder mapped. C) Location of the seismic line.

3.8 Low Gravity Anomaly Area

As discussed by Stagpoole et al. (2021), there is a low gravity anomaly within the Katikati Basin that is speculated to be a caldera or sedimentary basin. Calderas tend to collapse along ring faults linked to crustal magma chamber processes (Gudmundsson, 2008). Ring faults via calderas are different to faults caused by earthquakes where ring faults form elliptical closed to almost closed ring shapes and earthquake faults are generally straight forming offset segments (Gudmundsson, 2008). Looking at Figure 3.13, there is no clear indication of ring faulting or any obvious evidence of a caldera at all. Majority of the seismic lines in the area near the low gravity anomaly boundary tend to look similar to Figure 3.13, containing a deepening U-shape through the main channel and the three identified reflectors. Calderas are also associated with lava flows (Gudmundsson, 2008). There appears to be no evidence in the seismic data of lava flows. If there is a caldera below the surface in this area it is highly likely to be filled with sediment and calderas are often filled with unconsolidated volcanic material (Stagpoole & Miller, 2021), therefore further analysis is needed to be certain.

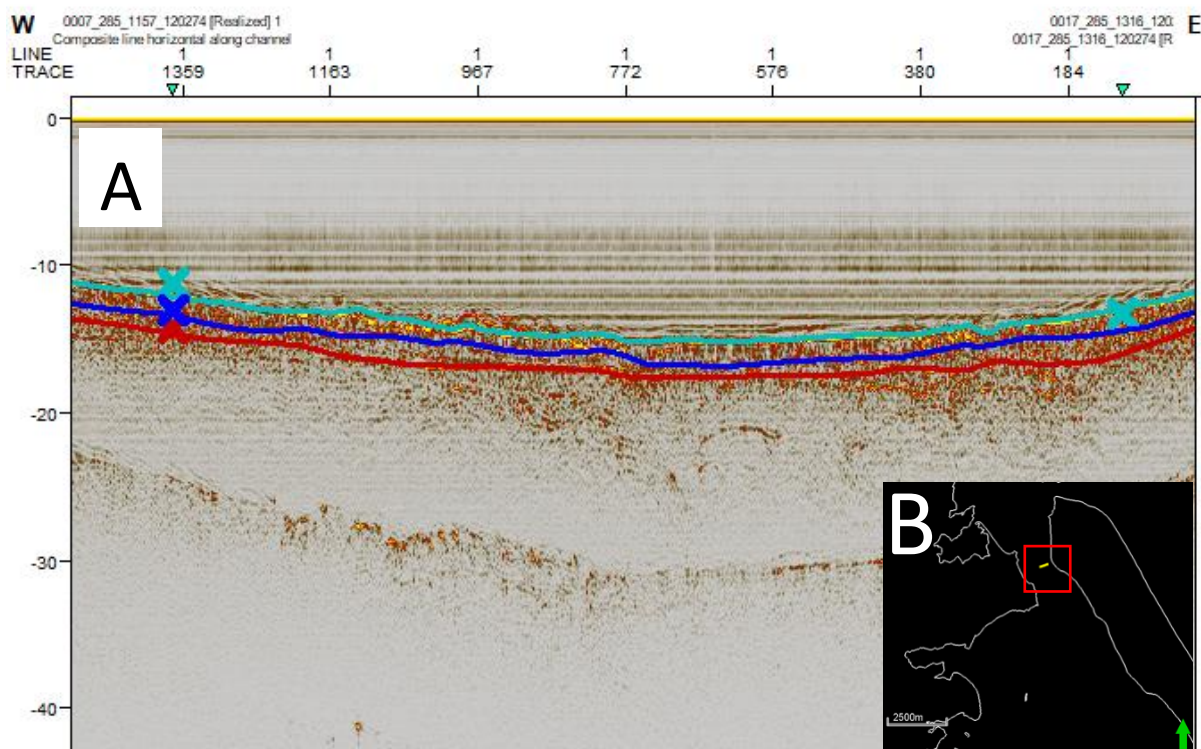


Figure 3.13. A) Interpreted seismic line near the boundary of the low gravity anomaly discussed by Stagpoole et al. (2021). B) Location of the seismic line.

3.9 Summary

In summary, a shallow seismic survey (sub bottom profiling) was conducted within the Katikati Basin of Te Awanui. Three main reflectors were visible in the seismic reflection data including the Seafloor, Horizon A, and Horizon B. These reflectors were mapped through the main channel of the central area of the basin and were interpreted to be of Holocene origin. Structure contour maps were used to determine the geomorphology of the three horizons, and it was found that overall, the three reflectors follow the same geological trend. Isopach thickness maps between the Seafloor and Horizon A, and Horizon A and Horizon B show a similar thickness trend, with units varying between 0.5 m to 3 m thick. No obvious evidence of faulting or a caldera emerged from the seismic data and analysis.

Chapter 4: Historical Air Photographs

4.1 Introduction

This Chapter highlights the changes to the geomorphology of the Katikati Basin including the entrance and Waikoura Point on Matakana Island using historical air photographs and hydrographic charts. The purpose of this chapter is to discuss the changes of the geomorphology and the drivers of these changes which is mainly due to the El Niño Southern Oscillation. It is important to document and understand these changes as weather patterns and threats and periods of erosion and accretion are dependent on periods of El Niño and La Niña.

The changes that may be recorded by the air photographs may be due to natural processes as there has been no recorded dredging activity within the Katikati Basin, and the limited freshwater discharge that could contribute excess sediment due to anthropic activities. Natural changes include changing tidal flows associated with long-period tidal constituents, changes to wave and wind climate linked to climate variability and longer-term climate change, and changes to freshwater discharge linked to changing rainfall patterns.

This chapter will first document the historical changes recorded by air photographs (and hydrographical charts), and then discuss potential drivers and patterns of change.

4.2 Methods

The Historical air photographs were obtained via the Retrolense database (<https://retrolens.co.nz/>). These photographs document changes to the morphology of the harbour channels, shoals, and margins with a higher temporal resolution than the hydrographical charts due to the limited number of hydrographical surveys undertaken. For Te Awanui, the record of Historical air photographs ranges from 1943 – 1999. All images from Retrolense were downloaded as individual jpg files and filtered through via best quality and images from each year that captured the whole of the Katikati Basin including Matakana Island. Images from 1960, 1975, and 1999 were selected as they showed the whole of the Katikati Basin including channels at high enough resolution. The individual images for each year were pieced together to make one whole image using Microsoft word. The images were

then analysed looking at changes to the morphology of the harbour channels, shoals, and margins compared to the present day.

4.3 Historical Air Photographs of the Katikati Basin

Historical air photographs can be used to determine any obvious changes that have occurred overtime within the Katikati Basin. Figures 4.1 – 4.4 demonstrate the changes over a 64-year period from 1960 to the present day. There is a clear main channel running through the basin that branches out into a network of smaller sub channels that flow towards the boundary between the Katikati and Tauranga Basins to the south. Looking at Figures 4.1 – 4.4 the main channel appears to stay relatively the same in shape and thickness through the basin over the years. However, the smaller network of sub channels tend to twist and turn and vary in thickness over time. The main shoal also stays relatively the same size and height above the water with a sub channel flowing around it within the basin. The sand bank at Bowentown in Figure 4.1 during 1960 appears to be more prominent, and slowly declines over time through Figures 4.2 to 4.4. It appears that most of the change within the Katikati basin occurs at the entrance.

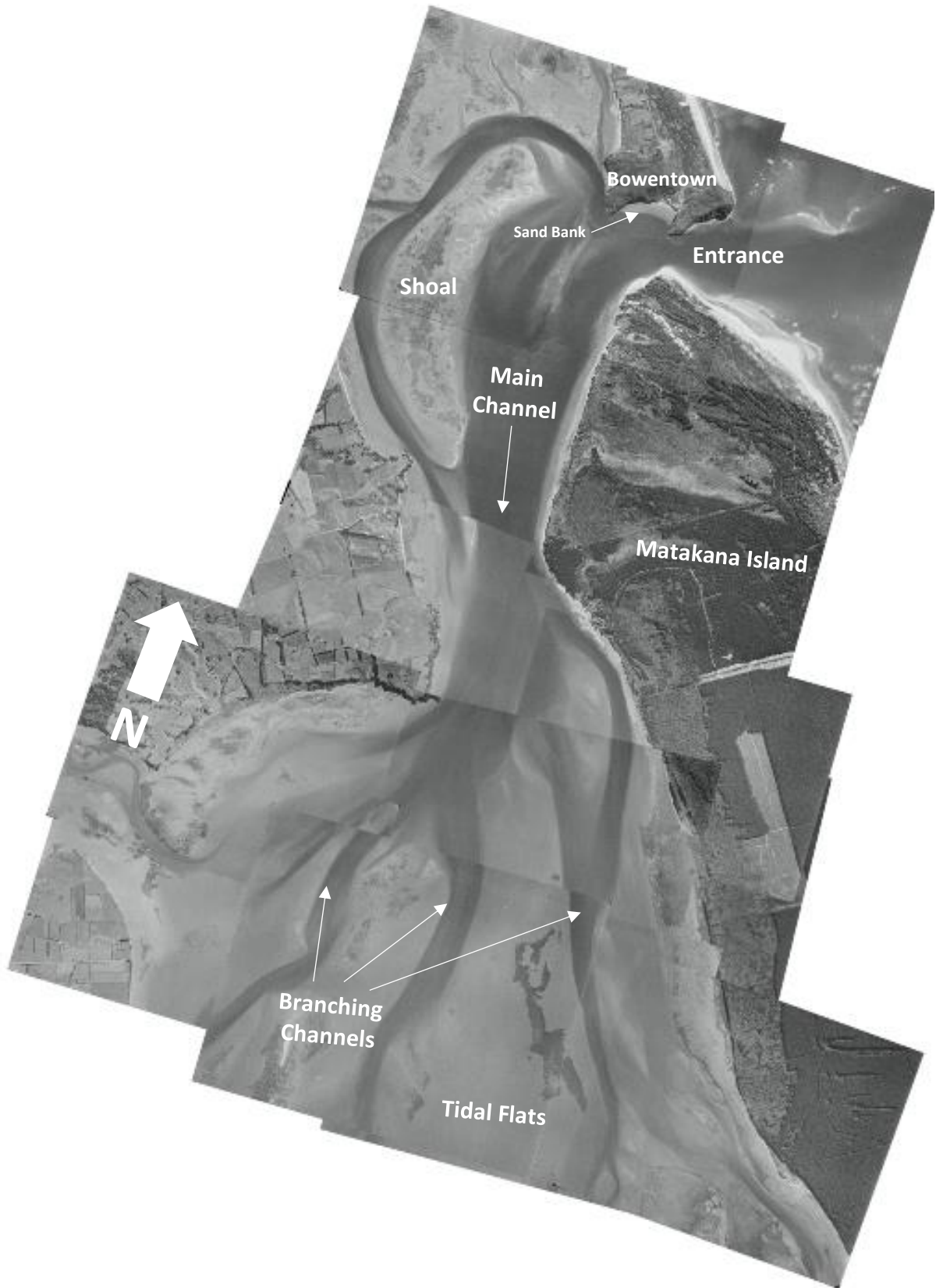


Figure 4.1. Annotated historical air photograph of the Katikati Basin from 1960. (Image source: Retrolense; <https://retrolens.co.nz/>).

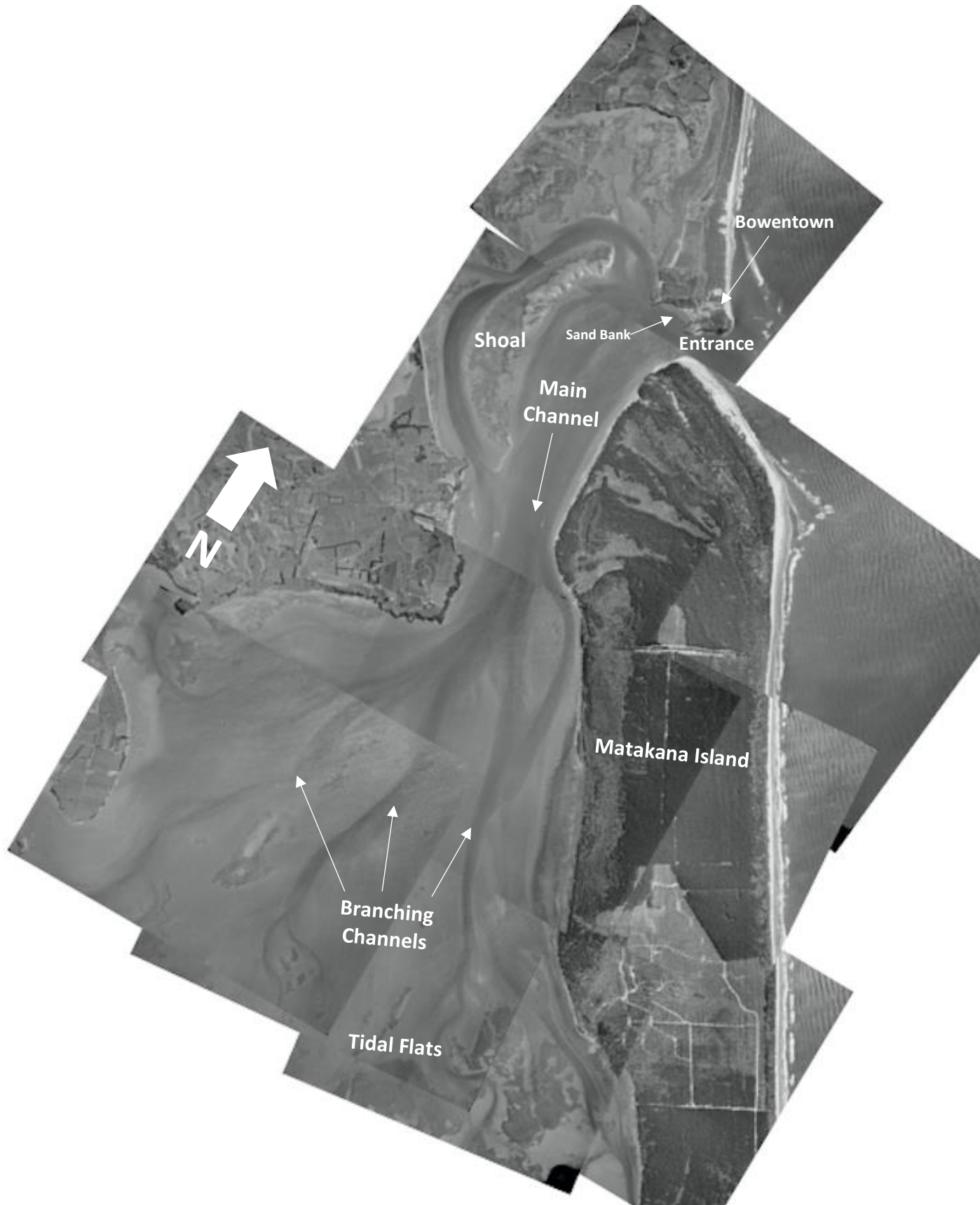


Figure 4.2. Annotated historical air photograph of the Katikati Basin from 1975. (Image source: Retrolense; <https://retrolens.co.nz/>).

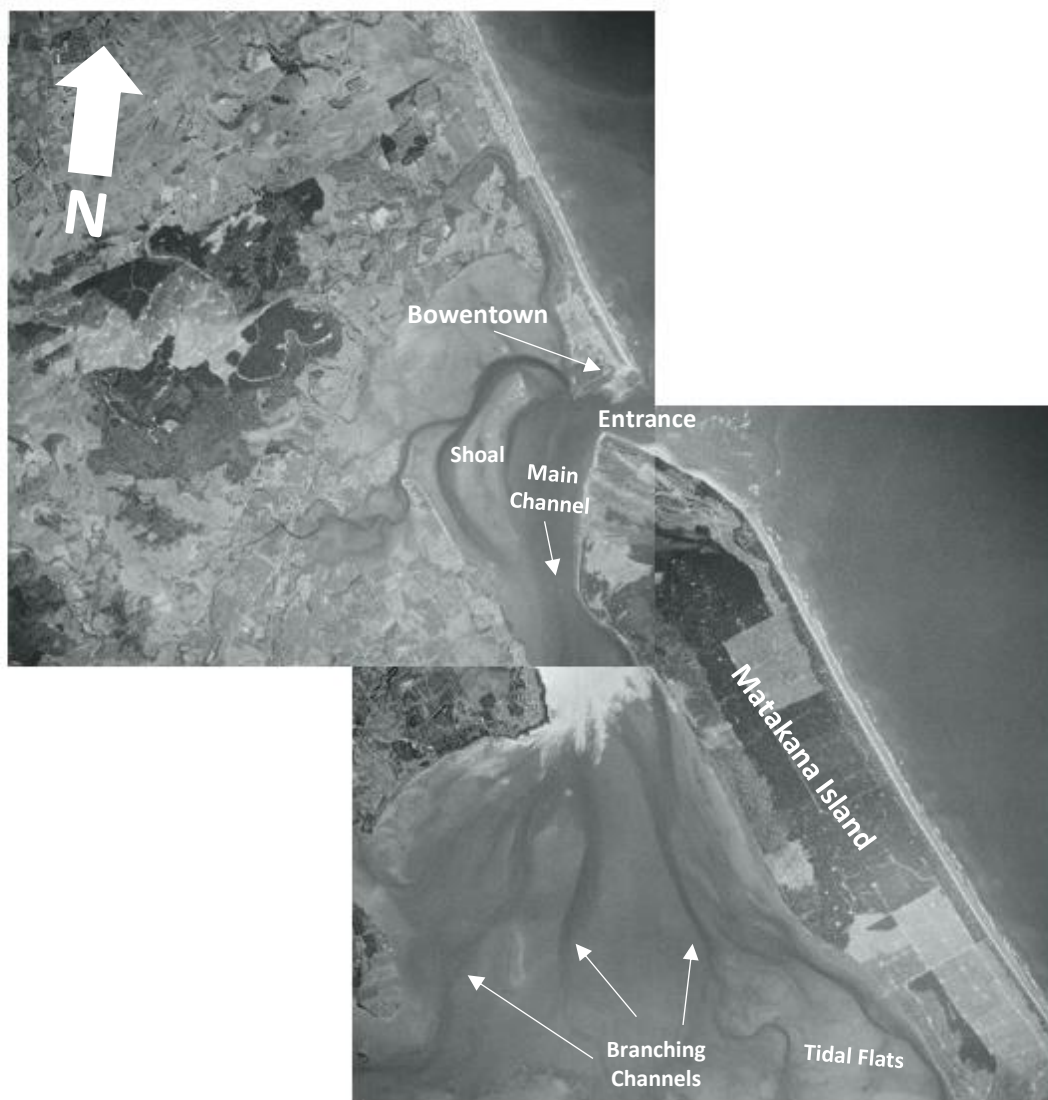


Figure 4.3. Annotated historical air photograph of the Katikati Basin from 1999. (Image source: Retrolense; <https://retrolens.co.nz/>).



Figure 4.4. Katikati Basin in 2024. (Image source: Google Earth).

4.3.1 Historical Air Photographs of the Katikati Entrance

The majority of changes that occur within the Katikati Basin are at the entrance within the tidal inlet and at the spit tip on Waikoura Point, Matakana Island. Triple-dip La Niña events associated with the ENSO cycle can be considered as the main driver of change. Historical air photographs of the Katikati entrance in Figure 4.5 demonstrates the changes during two of the triple-dip events as the other two events are not well documented or imaged.

Erosion of Waikoura Point causes loss of beach and sand dune sediment deposits which in turn generates movement within the channels of the ebb tidal delta. However, channels of the inlet within the harbour side of the entrance are not as affected as they do not migrate or experience any scouring due to the erosional phase (de Lange, 2023).

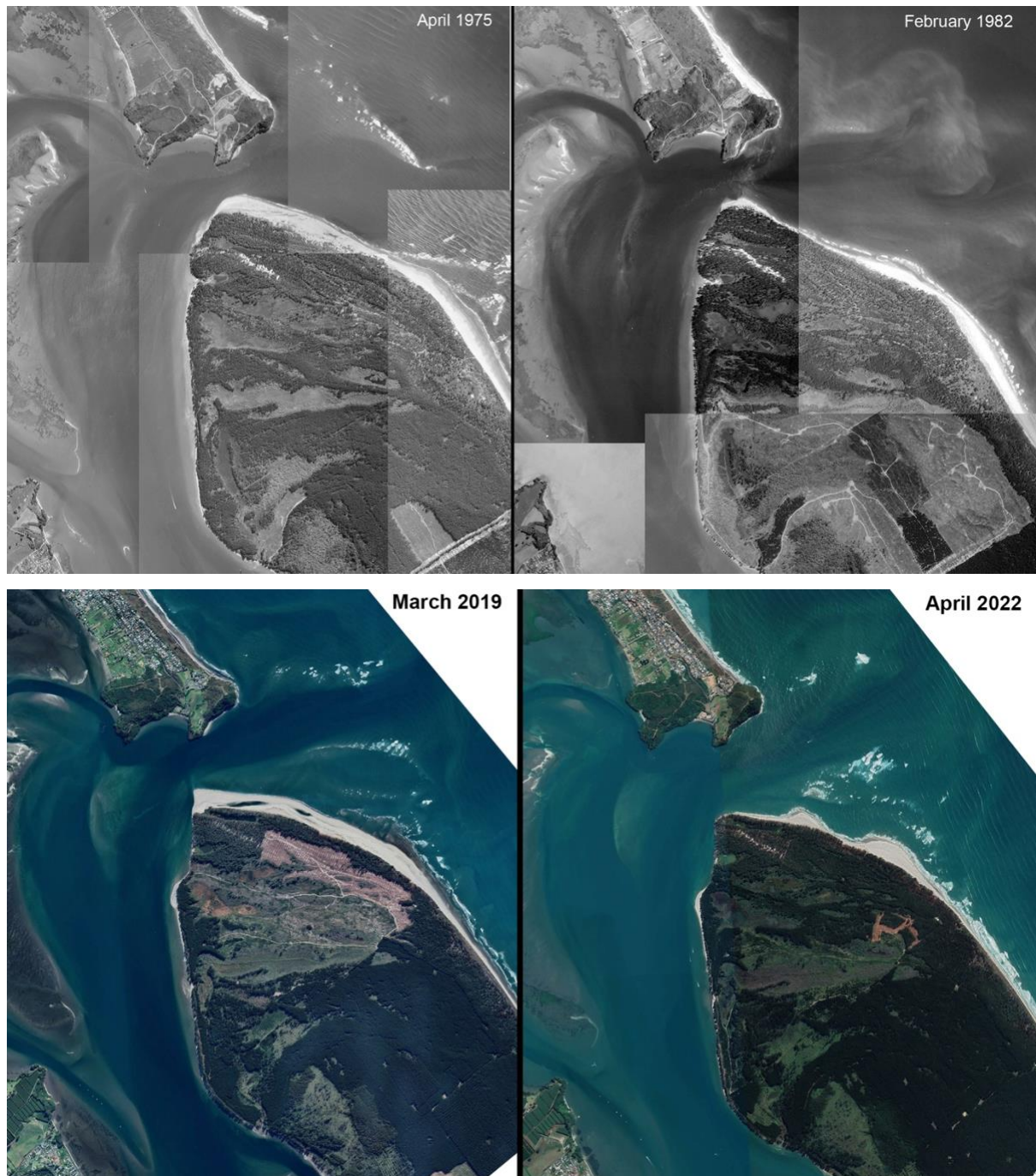


Figure 4.5. Changes to the Katikati Inlet focusing on the shape of Waikoura Point on Matakana Island before and after triple-dip La Niña events during April 1975 to February 1982 and, March 2019 to April 2022 (de Lange, 2023).

4.4 Hydrographical Charts of the Katikati Basin

Historical hydrographical charts for Te Awanui are limited in number. Whereas there are many more available for the adjacent Tauranga Harbour entrance, hydrographical charts from 1976 and 1993 from Katikati Basin can be used alongside historical shorelines to determine patterns and periods of change.

4.4.1 Morphology of the Katikati Basin as Determined from Hydrographical Charts

The hydrographical charts in Figures 4.6, 4.7, and 4.8 show that the Katikati Basin entrance has an asymmetric flood and ebb tidal delta which is joined by a deep, narrow inlet. The Katikati Inlet is armoured by a combination of rock and lag surfaces of shells and boulders and can be categorised as a 'free-form' ebb tidal delta due to minor/unclear offset between the open coast shorelines at the inlet, eroding Waikoura Point on the northern end of Matakana Island from all offshore approach wave directions (de Lange, 2023). 'Free-form' ebb tidal deltas tend to have an asymmetric 'bat-winged shape' which is more obvious in Figure (above) February 1982 compared to the hydrographical charts (Hicks & Hume, 1996). The hydrographical charts also show that the inlet connects to a main tidal channel flowing parallel to Matakana Island which is partially divided to the inlet via shallow shoals that flank the flood tidal delta (de Lange, 2023).

4.4.2 Changes in Morphology of the Katikati Basin as Determined from Hydrographical Charts

The hydrographical charts alone do not give enough information to determine long-term trends of erosion and accretion within the Katikati Basin. Figure 4.9 can be used alongside the hydrographical charts to show that between 1870 and 1974, the Katikati entrance has narrowed due to a period of long-term accretion at the spit tip of Matakana Island and the tidal inlet has deepened in response to the change (de Lange, 2023). The charts demonstrate that the period of long-term accretion of the shoreline between 1870 and 1974 have also ceased and changes to spit morphology occur during cyclic episodes of erosion and accretion (de Lange, 2023).

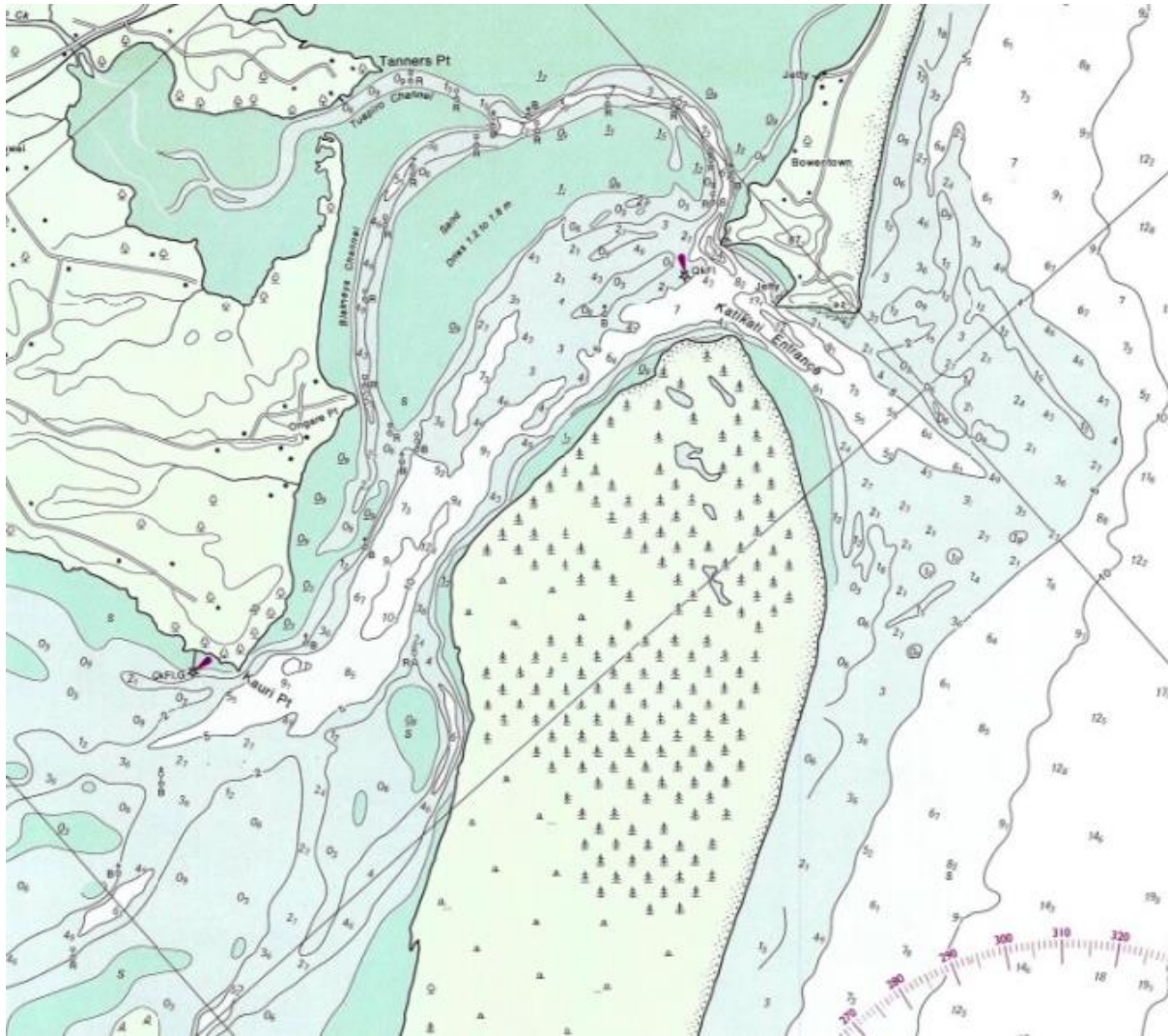


Figure 4.6. Hydrographical chart of the Katikati Basin entrance in 1976. (Data source: <https://paekoroki.tauranga.govt.nz/nodes/view/56207>).



Figure 4.7. Hydrographical chart of the Katikati Basin entrance in 1993. (Data source: <https://onehera.waikato.ac.nz/nodes/view/1625>).

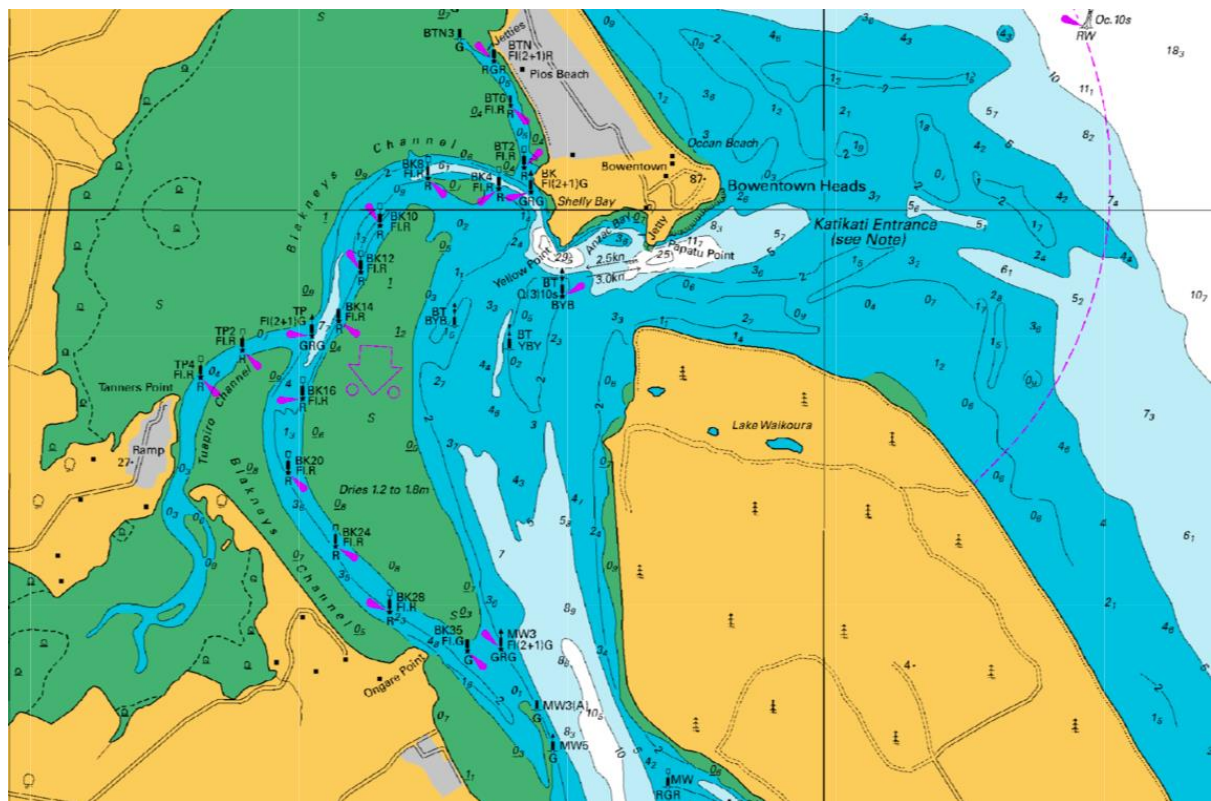


Figure 4.8. Hydrographical chart of the Katikati Basin entrance in 2023. (Data source: hydrographical chart NZ5411).

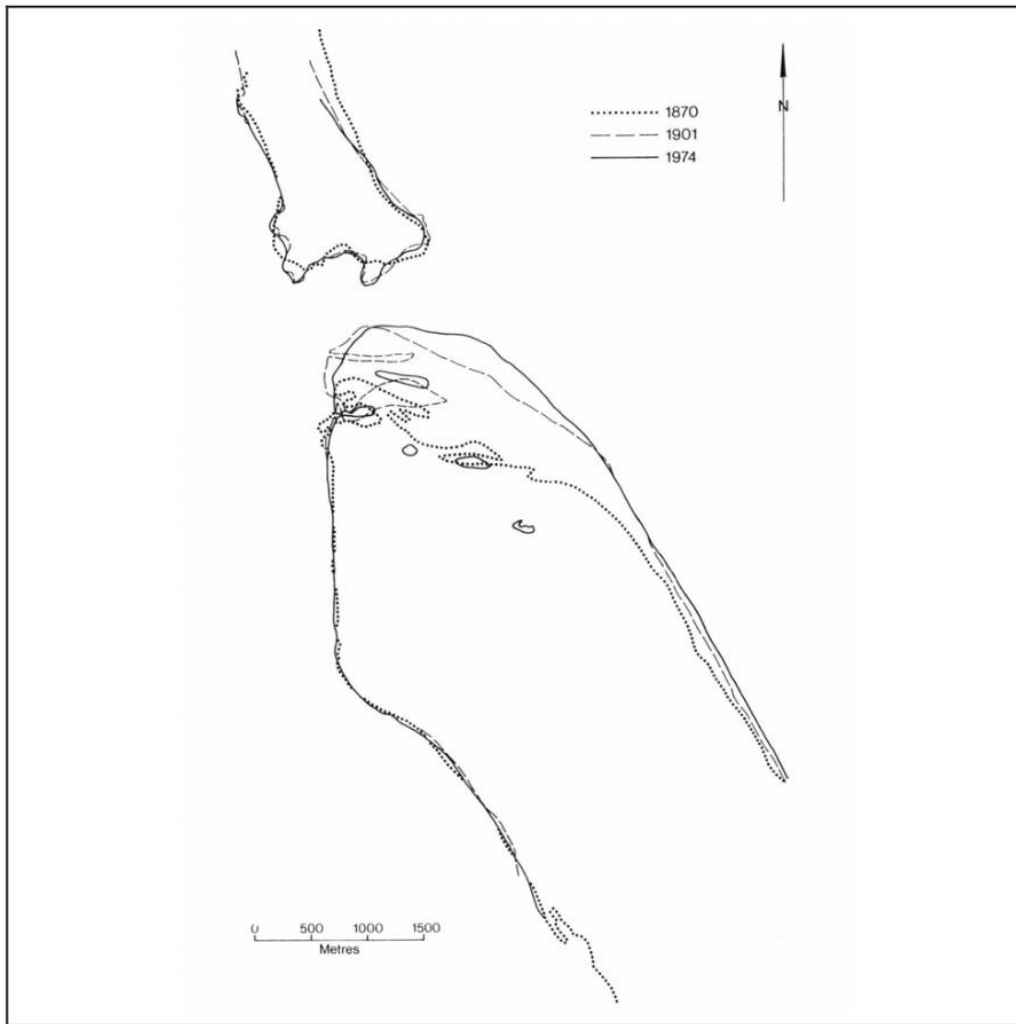


Figure 4.9. Historical shoreline positions of the spit tip of Matakana Island at the Katikati Basin entrance from 1870, 1901 and 1974 (de Lange, 2023).

4.5 Changes in the Ebb Tidal Delta and Barrier Spit

As described by Hansen (1992) a study was conducted of the Katikati ebb tidal delta analysing shoreline changes between 1923 and 1992 from Hinemoa Street at Waihi Beach to Tank Road on Matakana Island. They found changes to the spit tip morphology and the shape of the Katikati Inlet switching between bar bypassing and tidal bypassing (de Lange, 2023; Hansen, 1992). The position of the channel through the ebb tidal delta shifting between more perpendicular to the shore with an east-west orientation and more southerly alignment along the shoreline are associated with the changes to the spit tip (de Lange, 2023).

Hansen (1992) found that the northernmost point of Matakana Island (Waikoura Point) tends to move back, and forth which causes the tidal channel to change between 200 m, 250 m to 450 m. Also, when

the channel widens, the depth of the channel reduces and during a spring tide, the area of the channel below high-water level stays the same (Hansen, 1992).

Three different types of spit tips were identified during the study in Figure 4.10 and re-phrased by (de Lange, 2023):

- A. Broad rounded spit
- B. Rounded spit with notched sides
- C. Narrow spit with a pointed tip

The Type A spit is associated with bar by-passing where sediment travels across the delta and then washed onshore accumulating in the lee of the delta deposit which gives the northern spit the distinguishing rounded shape (Hansen, 1992). The Type B spit is an intermediate form of Type A and C. Type B occurs due to migration of the main channel at the entrance southwards and wave action moves sand across the delta where it deposits on the northern side of the tidal channel (Hansen, 1992). The Type C spit is associated with tidal by-passing where sediment is deposited on the northern spit on Matakana Island via wash over into the channel (Hansen, 1992).

de Lange (2023) shows that Type A spit shape is the most common phase for the northern end of the Matakana spit, but during an erosional period the spit develops into Type B. If the erosional period continues for a long enough time, then the spit will evolve into Type C, then when an accretion period begins the spit evolves back to Type A (de Lange, 2023).



Figure 4.10. Spit tip morphology of Waikoura Point, Matakana Island at the Katikati entrance where A) represents a broad rounded spit, B) rounded spit with notched sides, C) narrow spit with a pointed tip (de Lange, 2023).

4.6 Drivers of Change

The main drivers of change will focus on the ENSO cycle based on the conceptual model of Hansen (1992) as discussed above.

4.6.1 El Niño Southern Oscillation Cycle

The El Niño Southern Oscillation (ENSO) occurs in the equatorial Pacific and is a quasiperiodic climatic cycle averaging over a five-year interval. Sea surface temperature fluctuations within the tropical eastern Pacific and sea level atmospheric pressure fluctuations in the tropical western Pacific characterise ENSO (Tenzer & Wiart, 2014).

ENSO can be divided into neutral, El Niño and La Niña phases. The El Niño phase involves a higher atmospheric pressure in the western Pacific dominated by a warm oceanic phase. La Niña involves a lower atmospheric pressure in the western Pacific and dominated by a cold oceanic phase. The atmospheric component of El Niño is the Southern Oscillation where atmospheric pressure in the lowest troposphere between the tropical eastern and tropical western Pacific Ocean waters (Tenzer & Wiart, 2014).

The Southern Oscillation Index (SOI) describes the intensity of the Southern Oscillation, and the SOI is calculated via differences in the monthly or seasonal fluctuations of atmospheric pressures between Tahiti in the central Pacific and Darwin Australia in the western Pacific. Positive and negative SOI values can be used to determine phases of El Niño and La Niña where, El Niño are negative, and La Niña are positive (Tenzer & Wiart, 2014).

The Pacific Decadal Oscillation (IPO or PDO) involves long-lived periods of El Niño patterns of Pacific climate variability and can last as long as 20-to-30-year cycles and being characterised by warm or cool phases (Mantua & Hare, 2002). Mantua & Hare (2002), described the PDO cool phases occurred during 1890-1924 and 1947-1976 and the warm phases during 1925-1946 and 1977 to the mid 1990's.

The ENSO cycle affects the New Zealand coast (the northeast coast in particular), as fluctuations between El Niño and La Niña extremes can cause changes in weather patterns including storm frequency and severity which affect coastal processes. Since 1973, an open coast tide gauge at Moturiki Island has been operating continuously and gathered data for Te Awanui, which has proven a strong connection between sea level rise and temperatures with the ENSO cycle. During periods of El Niño extreme, lower water temperatures cause a drop in sea level whereas, for La Niña, higher

water temperatures cause a rise in sea level (de Lange, 2001). Although El Niño is associated with a warmer phase, decreased winds due to a decline in the SE to NW pressure gradient causes sea surface temperatures to rise (de Lange, 2001).

de Lange (2001) determined that the ENSO cycle also affects wind directions and the frequency of extratropical cyclones which causes either erosion or accretion on the Tauranga Coast. During El Niño extremes, the wind shifts northwards to a more southwest, offshore direction. This results in lower and smaller waves approaching the northeast coast of Tauranga allowing a cycle of accretion to occur. Periods of La Niña extremes are opposite where the wind shifts southwards to more northwest and northeast with an onshore direction. Coastal erosion of the Tauranga Coast is more prevalent during periods of La Niña extremes due to the rise in sea level and onshore winds pushing larger and steeper waves towards the coast (de Lange, 2001).

Variations in the ENSO cycle affects the tropical cyclone magnitude and frequency for Te Awanui. During a positive phase of the ENSO La Niña conditions with onshore wind in the north-east direction causes positive storm surges and a rise in sea level (de Lange & Gibb, 2000). Therefore, during La Niña conditions there is a higher chance of erosion and storm surge due to tropical cyclones as these conditions favor extra-tropical cyclones to track south towards New Zealand and the Tauranga coast in the bay of plenty (de Lange & Gibb, 2000).

4.6.2 Triple-dip La Niña Events

Triple-Dip La Niña events are rare and occur when the ENSO extreme period lasts longer than average which is around 1-2 consecutive peak summer seasons. These triple-dip extreme La Niña events occur because the conditions are closer to normal than El Niño. Figure 4.11 demonstrates the La Niña events that have occurred on record from 1950 to present noting that there have been 4 events in total approximately every 20-25 years. The four triple dip La Niña events occurred during a negative IPO phase during 1953-1956; 1974-1977; 1998-2001; 2020-2023. The Interdecadal Pacific Oscillation (IPO) can enhance or diminish the ENSO extremes and involves the changes in the mean sea surface temperatures along the Pacific Ocean. Following the negative phase that occurred in 1998, sea surface temperatures have been enhanced strengthening the effects of precipitation and storm generation associated with La Niña events in turn weakening the effects of El Niño events. The negative IPO phase is a contributing factor in increased coastal erosion within the Bay of Plenty region (de Lange, 2023).

Triple-dips in seasonal trends of the Oceanic Niño Index (ONI)

In rare instances, a La Niña can return for three consecutive winters—a so-called 'triple-dip'

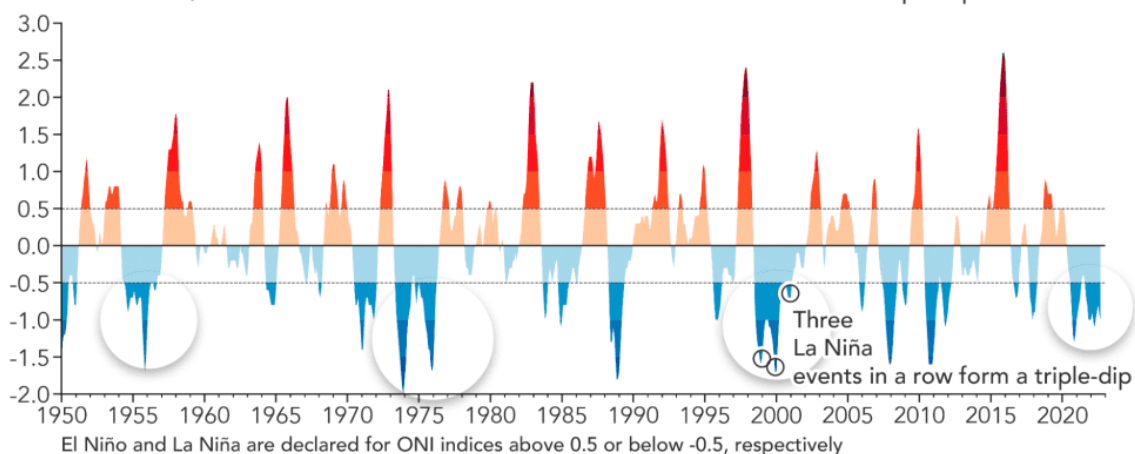


Figure 4.11. Triple-dip La Niña events displayed on a time series graph of the Oceanic Niño Index (ONI), showing a three-month running mean surface temperature anomalies with ENSO (>0.5 = El Niño and <0.5 = La Niña), in the tropical Pacific. This graph was prepared for the northern hemisphere where in the southern hemisphere a triple-dip La Niña event occurs over a four year period over three summers (de Lange, 2023).

4.7 Effects of ENSO on Matakana Island

Research on the effects of erosion and accretion of Matakana Island due to the ENSO cycle tend to be more bias towards the Tauranga entrance at Panepane Point due to dredging and port activities rather than Waikoura Point at the Katikati entrance. Wave activity is a major driver of erosion and accretion of the shoreline on Matakana Island, shaping the spit at each entrance (de Lange, 2022). The shift in wave patterns in particular during ENSO extremes of La Niña and El Niño affects sediment transport at both entrances of Te Awanui on Matakana Island where during periods of accretion at Waikoura Point in Katikati, at the other end at Panepane Point in Tauranga tends to erode at the spit tip (de Lange, 2022).

4.7.1 Changes to the Spit Tip of Matakana Island and Ebb Tidal Behaviour

The ENSO cycle affects the spit tip morphology of Northern Matakana Island at the Katikati entrance. Figure 4.10 demonstrates the erosional and accretional cycle of Matakana Island where a full progression through the cycle of types A, B, and C occur during a triple-dip La Niña event. Whereas during a shorter and normal La Niña event, the spit tip partially evolves from type A to B. During a cycle between all the spit tip types and analysis of volumetric changes, there is minor sediment loss within the harbour. The sediment is predominantly redistributed between the sand dunes and beach

to the ebb tidal delta. The redistribution of sediment to the ebb tidal delta is associated with the switching between spit tip types A and C, bar bypassing and tidal bypassing, as type B is the transitional phase between A and C (de Lange, 2023).

4.8 Summary

Overall, comparing historical air photographs of the Katikati Basin to the present day, suggests that geomorphology of the channels, margins, shoals, and sand banks do not appear change considerably. Due to the lack of historical air photographs of the basin on record and the amount of time that has passed, there is a lack of obvious evidence of major change on the surface. As discussed by Hansen (1992) and de Lange (2023), the major obvious changes observed in the Historical air photographs is on the spit tip at Waikoura Point on Matakana Island due to the effects of the ENSO cycle and particularly the triple dip La Niña events.

Chapter 5: Summary and Discussion

5.1 Introduction

This chapter will discuss the results from the study based on the findings in **Chapter 3: Seismic Reflection Characterisation** and **Chapter 4: Historical Air Photographs**. The stratigraphy, faulting, and low gravity anomaly area from the seismic survey will be discussed and interpreted as well as the geomorphology and effects the ENSO cycle has on the Katikati Basin from the historical air photographs.

5.2 Seismic Interpretation

Stratigraphy

This study mapped three horizons from the seismic data including the Seafloor, Horizon A, and Horizon B. All three reflectors were interpreted to be of Holocene age. The Seafloor Horizon was interpreted as the upper layer of Holocene Sediment, Horizon A was interpreted as the bottom of the upper layer of Holocene sediments of the Seafloor, and Horizon B was interpreted as another layer of Holocene sediments. I interpreted all three reflectors to be of Holocene origin due to another seismic survey conducted through the Stellar Passage within the Tauranga Basin showing similar reflectors at similar depths and they were all identified as Holocene origin after coring was undertaken to prove this (MacPherson, et al., 2017). No coring was obtained for this study so there is only speculation that these sediments are of Holocene origin, but the depth of the seismic survey means it is highly unlikely that any Pleistocene sediments were reached.

The thickest areas of sediment for both isopach thickness maps tend to extend off the main channel at 1.5 – 2.5 m thick. The thinner areas tend to reside in the area of the main channel at 0.5 – 1 m thick for both isopach thickness maps. There are no thickness maps of the Katikati Basin to compare to, therefore the maps generated from this study can be used as a building block to see how the thickness of the sediments change overtime in certain areas of the Basin to understand the processes of sediment deposition and transport further. As some of the data was corrupted when loading into petrel, the whole picture of the southern end of the basin was unable to be mapped. Another seismic

survey through this area could be beneficial to create isopach thickness and contour maps of the entire southern end of the basin including all the sub channels to understand the geomorphology of the area below the surface more.

Faulting

Faults are considered active if they show warping and folding of the ground surface within the last 70,000 – 128,000 years (Van Dissen & Heron, 2023). Research within the Tauranga Basin show evidence of potential active faulting within the last 128,000 years. Podrumac (2016) found evidence of folding, fracturing, and potential faulting within their transects through the western channel of the Tauranga Basin that extended into the Holocene Sediments and used coring to confirm the uplift and downthrow with the sediment contents at each side of the transect near Ōmokoroa. Christophers (2015) found evidence of vertical displacement within the sediments of the cliffs at Ōmokoroa in Te Awanui.

For this research project, there was no obvious evidence of faulting identified within the seismic data of the Katikati Basin. The series of NNE-aligned trending faults that have been identified in the Tauranga region and are associated with the Taupō rift (Villamor et al., 2017) appear to extend into the Tauranga Basin and Ōmokoroa Peninsula (Podrumac, 2016; Christophers, 2015), but not the Katikati Basin.

Low Gravity Anomaly

Calderas are identified as low gravity anomalies on gravity maps as they are filled with low-density volcanic material (Stagpoole & Miller, 2021). A low gravity anomaly has been identified within the Katikati Basin and is speculated to be associated with the Coromandel Volcanic Centre or a sedimentary basin (Stagpoole & Miller, 2021). Christophers (2015) argues that the ridge that marks the boundary between the Tauranga and Katikati Basins made up of Pleistocene sediments from Ōmokoroa to Matakana Island marks the boundary of the caldera/low gravity anomaly and has been infilled by Holocene sediments.

From the seismic data in this study, there was no evidence of a caldera in the upper section of the boundary that passed through northern Matakana Island. This survey appears to not have been deep enough to penetrate any material that could indicate that there may be a caldera present beneath the surface and there was no obvious evidence of ring faulting or lava flows in the seismic data which are generally associated with calderas (Gudmundsson, 2008). This study was only able to reach

potentially Holocene Sediments where if there is a caldera beneath the surface this is the material that has infilled it. Also, the boundary between the Katikati and Tauranga Basin's is quite shallow, and the boat was not able to travel over this section of Te Awanui, so no data was collected for this potential caldera area either. Deeper coring is needed to understand what this low gravity anomaly is whether it is a caldera or sedimentary basin, and further investigation is needed.

5.3 Historical Air Photographs

Geomorphology

Historical air photographs were used alongside hydrographical charts to document changes in the morphology of the channels, shoals, margins, and the spit tip of Waikoura Point on Matakana Island within the Katikati Basin. Photographs from Retrolense.co.nz over a 64-year period during 1960, 1975, and 1999 were used to compare to the present-day basin. What was found was that the main channel through the central area of the basin tended to stay relatively the same shape and thickness from 1960 through to the present day. However, the smaller branching sub channels tended to slightly twist and vary in thickness but overall follow the same trend with three sub channels flowing to the southern end of the basin towards the boundary. Therefore, as a whole there was no obvious changes to the geomorphology of the basin as a whole overtime. There was a prominent sand bank/beach identified at Bowentown during 1960 that slowly declined overtime. It is unclear why this small beach/sandbank on Bowentown has eroded overtime.

It is evident that majority of the changes that have occurred overtime within the Katikati Basin looking at the historical air photographs are at the entrance at Waikoura Point on Matakana Island. The hydrographical charts and historical shoreline positions were used to see if there were changes at the entrance overtime. It is evident in the charts and shoreline positions that from 1870- 1974 that the entrance has narrowed due to a period of long-term accretion at the spit tip of Matakana Island and the tidal inlet in response to the narrowed entrance has deepened (de Lange, 2023). Katikati does not have a port like the Tauranga end of the basin does, so small changes to the entrance like the ones observed have no real effect on shipping and exporting operations.

In comparison to the seismic data, the geomorphology at the surface using the historical air photographs tends to look similar in the seismic data below the surface. There is one main channel through the central region of the basin that branches out into minor sub channels. The main channel was evident throughout the seismic data and the thinner areas in the isopach thickness maps appear

to be in areas that are deeper where the main channel flows and begins to branch into the smaller sub channels, and the shallower areas tend to be thicker.

Effects of the ENSO on the Katikati Basin

What happens to the Katikati Basin, and Te Awanui during the ENSO cycle is that wind patterns, wave patterns, and storm frequency all change during periods of El Niño and La Niña extremes. El Niño extremes cause a warm phase due to a drop in the SE NW pressure gradient creating weaker winds with an offshore direction to the southwest, weakening wave height, dropping the sea level, and therefore allowing a period of accretion to occur on the Tauranga Coast (de Lange, 2001). During La Niña extremes, the wind shifts northwest in the onshore direction causing a rise in sea level and steeper, larger waves towards the Tauranga coast and coastal erosion is more prominent within a La Niña extreme (de Lange, 2001).

Waikoura Point on Matakana Island can face triple-dip La Niña events when the ENSO extreme period lasts longer than average. This causes the spit tip to progress a full cycle of spit tips type A, B, and C where periods of erosion and accretion occur changing the shape of the spit from broad and rounded to rounded with notched sides, and narrow with a pointed tip (de Lange, 2023). These triple-dip La Niña events are not of concern as the spit tip goes through cycles of erosion and accretion meaning that there is minimal to no net loss of sediment.

Tropical cyclone threats for the Tauranga coast are higher during La Niña extremes. The onshore wind direction creates higher storm surges on the coast due to the rise in sea level and conditions are favoured for extra-tropical cyclones to track south towards New Zealand and Tauranga coast threatening erosion (de Lange, 2001; de Lange & Gibb, 2000).

5.4 Limitations

This study faced some limitations. A major limitation was that shallow seismic surveys have never been conducted within the Katikati Basin until now with a bias towards the Tauranga Basin due to dredging activities and the port. This means there is data for comparison to this study and all information found from the seismic data is new. Some of the seismic data was corrupted when entering into Petrel, so the isopach thickness and structure contour maps were only able to show a small section of the basin. Finally, there was no core data analyzed herein, and thus seismic observations did not have ground truth. This was especially relevant to interpreting the age and origin

of seismic reflectors. Nevertheless, this new study of Katikati Basin is the first step to further our knowledge on the Basin and the geological processes that happen within it.

5.5 Summary

Overall, researching the Katikati Basin using seismic surveys and historical air photographs is useful and beneficial for understanding the dynamics within Te Awanui above and below the surface.

Below the surface the seismic surveys found no obvious evidence of faulting. This is a positive outlook for hazard assessment, as known faults in the immediate surrounding areas such as the Tuapiro Fault have not moved in the last 128,000 years and are deemed inactive. Potentially active faults found in other research of the Tauranga Basin show that the NNE-aligned faults associated with the Taupō rift may extend into the Tauranga Basin, but not the Katikati Basin. There was no evidence of a caldera associated with the low gravity anomaly in the Katikati Basin as the survey was not deep enough. Three Horizons were identified and mapped as layers of Holocene sediments as it was unlikely the survey penetrated any Pleistocene sediments at depth. Coring would be beneficial to confirm the faces of the Holocene sediments and investigate the area of the low gravity anomaly boundary further.

Above the surface historical air photographs show changes to the basin geomorphology overtime. This study found that overall, there are no obvious changes to the geomorphology of the Katikati Basin, majority of the changes happen at the entrance and at Waikoura Point which has no effect on the residents and activity of the basin.

Chapter 6: Conclusion

6.1 Summary of Research Findings

This chapter summarizes the main research findings and relates them back to the study aims and objectives. Recommendations for future research are put forward to build on the contents of this thesis.

The aim of this study was to determine the thickness of the Holocene sediments deposited since the flooding of the Katikati Basin by Holocene marine transgression and map any potential faults by undertaking a shallow seismic survey and also investigate the area of the low gravity anomaly that crosses through the Katikati Basin as discussed by (Stagpoole et al., 2021). Also, the historical air photographs were used to discuss the effects of the ENSO cycle on Waikoura point on Matakana Island and any areas of rapid change within the Katikati Basin as a whole. The main objectives and aims of this study were to:

- 1. Determining the thickness of the Holocene sediments.***

Unfortunately, sediment coring was unable to be completed for this project, therefore the true thickness of the Holocene sediments within the Katikati Basin is still unknown. However, based on analysis of seismic reflections through the central area, if these are of Holocene age then they reach depths of 15 m. In comparison to studies of Stella Passage by MacPherson et al. (2017) where the Holocene sediments were found to extend down to 20 m, this study gives reasonable confidence that the seismic reflectors mapped were the Holocene sediments sitting on top of the Pleistocene sediments.

- 2. Map the thickness and structure of the Katikati Basin using data from the shallow seismic survey.***

Structure contour and isopach thickness maps were created for the three horizons identified through the main channel of the Katikati Basin. The structure contour maps generally followed the same geological trends where the main channel was deeper than the surrounding areas and there was some structure in the northern end of the map with peaks and troughs below the surface. Isopach thickness maps were created to determine the thickness between the identified horizons and both maps also

tend to follow a similar trend of thickness. The thinnest areas tend to lie within the main channel at 0.5 – 1 m thick for both maps and the thicker areas tend to extend off the main channel at 1.5 – 2.5 m thick for both maps.

3. *Identify any faults and volcanic features of interest.*

There were no obvious faults discovered in this study. This means that the NNE-aligned faults in the Tauranga region associated with the Taupō rift may extend into the Tauranga Basin and not the Katikati Basin. This seismic survey did not reveal the stratigraphy to a level deep enough to penetrate the low gravity anomaly associated with a caldera or sedimentary basin, so this geological feature is still up for debate and to be researched more.

4. *Determine any areas of rapid change to the geomorphology of the Katikati Basin using historical hydrographical charts and air photographs.*

The historical photographs and hydrographical charts show that there is no obvious change to the Katikati Basin over time, most of the change occurs at the entrance within the tidal inlet and Waikoura Point on Matakana Island. The main channel in the Katikati Basin tends to stay relatively the same shape, where the smaller sub-channels slightly twist and turn overtime. The tidal flat area also appears to stay the same size and depth. Overtime the hydrographical charts have shown that the tidal inlet has narrowed and deepened. The ENSO cycle causes the spit tip at Waikoura Point to change shape and go through periods of erosion and accretion especially during a triple-dip La Niña event.

6.2 Recommendations for Future Work

This study can be used as a building block for future research and it is clear that there is more to discover within the Katikati Basin. Sediment cores would be extremely beneficial to deeper the understanding of sediment dynamics below the surface. Coring was unable to be completed for this study therefore they would reveal the true thickness of the Holocene deposits and potentially find the boundary between the Pleistocene deposits. Although there was no obvious evidence of faulting within the seismic data, coring needs to be done around the basin to rule this out entirely to see if there is any offset between sediment layers. There may be some more deep-seated faults, and if another deeper seismic survey can be done this would be beneficial to rule out if there are any active faults extending into the Holocene sediments that may have been missed within this study. Some of the seismic data was lost when loading into petrel, therefore another round of surveys could help

connect the dots between the layers through the sub-channels in the southern end of the basin. There was also a lot of mobile sediment within the seismic data which made interpretation difficult at times.

More research needs to be done to identify what the low gravity anomaly is within the Katikati Basin if possible, to determine whether it is a sedimentary basin or caldera. The depth of the low gravity anomaly below the surface is not discussed therefore that may make research more difficult but coring can be done to determine what material lies beneath the surface to see if it is unconsolidated volcanic material that is usually deposited within a caldera.

Continuing to monitor changes to the entrance and basin as a whole especially within the ENSO cycle with erosion, accretion, storm surges, sea level height, cyclones etc., to see if there are any areas that are changing and what affects they have on the basin and Te Awanui.

References

- Badesab, F. (2012). *Magnetic mineral enrichment and transport in coastal environments: Tauranga Harbour, Northeastern, New Zealand* (Doctoral dissertation, Staats-und Universitätsbibliothek Bremen).
- Badesab, F., von Dobeneck, T., Briggs, R. M., Bryan, K. R., Just, J., & Müller, H. (2017). Sediment dynamics of an artificially deepened mesotidal coastal lagoon: an environmental magnetic investigation of Tauranga Harbour, New Zealand. *Estuarine, Coastal and Shelf Science*, *194*, 240-251.
- Badesab, F., von Dobeneck, T., Bryan, K. R., Müller, H., Briggs, R. M., Frederichs, T., & Kwohl, E. (2012). Formation of magnetite-enriched zones in and offshore of a mesotidal estuarine lagoon: an environmental magnetic study of Tauranga Harbour and Bay of Plenty, New Zealand. *Geochemistry, Geophysics, Geosystems*, *13*(6).
- Beavan, R. J., & Litchfield, N. J. (2012). *Vertical land movement around the New Zealand coastline: implications for sea-level rise* (p. 41). GNS Science.
- Bell, R. G., Goff, J., Downes, G., Berryman, K. R., Walters, R. A., Chague-Goff, C., ... & Wright, I. C. (2004). Tsunami hazard for the Bay of plenty and eastern Coromandel Peninsula: stage 2. *Environment Waikato Technical Report*, *32*, 70.
- Betts, H. D. (1996). *Late Quaternary evolution of Matakana Island, Bay of Plenty, New Zealand: a thesis submitted in partial fulfilment of the requirements for the degree of Master of Science in Geography at Massey University* (Doctoral dissertation, Massey University).
- Briggs, R. M., Hall, G. J., Harmsworth, G. R., Hollis, A. G., Houghton, B. F., Hughes, G. R., Morgan, M.D., Whitbread-Edwards, A. R. (1996). Geology of the Tauranga Area. Sheet U14 1:50 000.
- Briggs, R. M., Houghton, B. F., McWilliams, M., & Wilson, C. J. N. (2005). ⁴⁰Ar/³⁹Ar ages of silicic volcanic rocks in the Tauranga-Kaimai area, New Zealand: Dating the transition between volcanism in the Coromandel Arc and the Taupo Volcanic Zone. *New Zealand Journal of Geology and Geophysics*, *48*(3), 459-469.
- Burns, D. A., & Cowbourne, A. J. (2003). Engineering geological aspects of the Ruahihi Power Scheme, Tauranga. *Geotechnics on the Volcanic Edge*, 71-80.
- Christophers, A. J. (2015). *Paleogeomorphic reconstruction of the Omokoroa Domain, Bay of Plenty, New Zealand* (Doctoral dissertation, University of Waikato).
- Cole, J. W. (1978). Tectonic setting of Mayor Island volcano (Note). *New Zealand Journal of Geology and Geophysics*, *21*(5), 645–647. <https://doi.org/10.1080/00288306.1978.10424091>.
- Cole, J., & Lewis, K. (1981). Evolution of the Taupo-Hikurangi subduction system. *Tectonophysics*, *72*(1-2), 1-21.
- Cook, E. T. (2016). *Felsic volcanism in the eastern Waihi area; process origins of the Corbett and Ratarua ignimbrites and the Hikurangi Rhyolite* (Doctoral dissertation, University of Waikato).

- Crutchley, G. J., & Kopp, H. (2018). Reflection and refraction seismic methods. *Submarine geomorphology*, 43-62.
- Davis, R. A., & Healy, T. R. (1993). Holocene coastal depositional sequences on a tectonically active setting: southeastern Tauranga Harbour, New Zealand. *Sedimentary Geology*, 84(1-4), 57-69.
- de Lange, W. P. (2001). Interdecadal Pacific Oscillation (IPO): a mechanism for forcing decadal scale coastal change on the northeast coast of New Zealand?. *Journal of Coastal Research*, 657-664.
- de Lange, W. P. (2022). Morphological changes for southeastern Matakana Island (Panepane Point) and Matakana Banks (ebb tidal delta) 2016-22. Report prepared for the Port of Tauranga Ltd. Hamilton, New Zealand: School of Science, Division of Health, Engineering, Computing and Science, The University of Waikato, 15 pp.
- de Lange, W. P. (2023). Morphological changes for south-eastern Matakana Island (Panepane) and Matakana Banks (ebb tidal delta) 2016-23. Report prepared for the Port of Tauranga Ltd. Hamilton, New Zealand: School of Science, Division of Health, Engineering, Computing and Science, The University of Waikato, 27 pp.
- de Lange, W. P., & Gibb, J. G. (2000). Seasonal, interannual, and decadal variability of storm surges at Tauranga, New Zealand. *New Zealand Journal of Marine and Freshwater Research*, 34(3), 419-434.
- de Lange, W. P., Moon, V. G., & Johnstone, R. (2015). Evolution of the Tauranga Harbour Entrance: Influences of tsunami, geology and dredging. In *Australasian Coasts and Ports 2015*. Wellington, New Zealand: IPENZ.
- de Lange, W. P., Moon, V. G., & Fox, B. R. (2014). Distribution of silty sediments in the shallow subsurface of the shipping channels of Tauranga Harbour. (ERI report No 43). Report prepared for the Port of Tauranga Ltd. Hamilton, New Zealand: Environmental Research Institute, Faculty of Science and Engineering, The University of Waikato, 78 pp.
- de Ruiter, P. J., Mullarney, J. C., Bryan, K. R., & Winter, C. (2019). The links between entrance geometry, hypsometry and hydrodynamics in shallow tidally dominated basins. *Earth Surface Processes and Landforms*, 44(10), 1957-1972.
- Gardiner, D.G., 2023. Caldera Collapse Tsunamis: A Study on the Denham Caldera and its Impact on the Bay of Plenty, New Zealand. MSc Thesis, University of Waikato, Hamilton. 139 p.
- Gudmundsson, A. (2008). Magma-chamber geometry, fluid transport, local stresses and rock behaviour during collapse caldera formation. *Developments in Volcanology*, 10, 313-349.
- Hamling, I., Naish, T., Levy, R., Hreinsdottir, S., Bengtson, S., Praveen, K., Kopp, B., & Garner, G. (2024). *New Zealand Vertical land movement and sea rise projections* [Data set]. Zenodo. <https://doi.org/10.5281/zenodo.10976241>
- Hamling, I. J., Wright, T. J., Hreinsdóttir, S., & Wallace, L. M. (2022). A Snapshot of New Zealand's Dynamic Deformation Field From Envisat InSAR and GNSS Observations Between 2003 and 2011. *Geophysical Research Letters*, 49(2), e2021GL096465. <https://doi.org/https://doi.org/10.1029/2021GL096465>

- Hancock, N., Hume, T. M., & Swales, A. (2009). *Tauranga harbour sediment study: harbour bed sediments*. NIWA.
- Hansen, C. J. (1992). *Beach change Matakana Island 1923-1992*. Water Quality Centre, NIWA, NIWA IDR 92/11.
- Hicks, D. M., & Hume, T. M. (1996). Morphology and size of ebb tidal deltas at natural inlets on open-sea and pocket-bay coasts, North Island, New Zealand. *Journal of coastal research*, 47-63.
- Kluger, M. O., Jorat, M. E., Moon, V. G., Kreiter, S., de Lange, W. P., Mörz, T., ... & Lowe, D. J. (2020). Rainfall threshold for initiating effective stress decrease and failure in weathered tephra slopes. *Landslides*, 17(2), 267-281.
- Kluger, M. O., Kreiter, S., Moon, V. G., Roskoden, R. R., & Mörz, T. (2022). Compressibility and permeability of weathered, sensitive volcanic ash (tephra) deposits at the Omokoroa flow slide, New Zealand. *Engineering Geology*, 310, 106885.
- Lee, J., & Villamor, P. (2018). *Interim results on active faults around the Omokoroa-Katikati development sites, Tauranga*. (Report No. CR 2018/52 LR). GNS Science. <https://atlas.boprc.govt.nz/api/v1/edms/document/A3946315/content>.
- Leonard, G. S., Begg, J. G., Wilson, C. J. N., & Leonard, G. S. (2010). *Geology of the Rotorua area*. Lower Hutt, New Zealand: GNS Science.
- Macky, G. H., Latimer, G. J., & Smith, R. K. (1995). Wave climate of the western Bay of Plenty, New Zealand, 1991–93. *New Zealand Journal of Marine and Freshwater Research*, 29(3), 311-327.
- MacPherson, D., Fox, B. R., & de Lange, W. P. (2017). Holocene evolution of the southern Tauranga Harbour. *New Zealand Journal of Geology and Geophysics*, 60(4), 392-409.
- Mantua, N. J., & Hare, S. R. (2002). The Pacific decadal oscillation. *Journal of oceanography*, 58, 35-44.
- Mason, D., Clarke, N., Mills, P. & Barnhill, D. (2023). *Tauranga Landslide Susceptibility Study: Technical Report*. Tauranga City Council.
- Naish, T. R. (1990). *Late Holocene mud sedimentation and diagenesis in the Firth of Thames: Bentonites in the making* (Doctoral dissertation, University of Waikato).
- Nation, T. (2015). *Elders Voices Summit*. Retrieved from: <https://eldersvoicessummit.com/images/EldersVoicesSummitBooklet.pdf>
- Penrose, J. D., Siwabessy, P. J. W., Gavrilov, A., Parnum, I., Hamilton, L. J., Bickers, A., ... & Kennedy, P. (2005). Acoustic techniques for seabed classification. *Cooperative Research Centre for Coastal Zone Estuary and Waterway Management, Technical Report*, 32, 11.
- Pittari, A., Prentice, M. L., McLeod, O. E., Yousef Zadeh, E., Kamp, P. J., Danišik, M., & Vincent, K. A. (2021). Inception of the modern North Island (New Zealand) volcanic setting: spatio-temporal patterns of volcanism between 3.0 and 0.9 Ma. *New Zealand Journal of Geology and Geophysics*, 64(2-3), 250-272.

- Podrumac, A. (2016). *Holocene Evolution of the Upper Western Channel within Tauranga Harbour*. MS Thesis, University of Waikato, Hamilton.
- Prentice, M. L. (2023). *Silicic volcanism of the Tauranga Volcanic Centre and the climactic Waiteariki supereruption at the dawn of the Taupō Volcanic Zone* (Doctoral dissertation, The University of Waikato).
- Rorke, J. (2011). *Matakana Island (Tauranga)*. Retrieved from: <https://paekoroki.tauranga.govt.nz/nodes/view/6574>
- Shepherd, M. J., Betts, H. D., McFadgen, B. G., & Sutton, D. G. (2000). Geomorphological evidence for a Pleistocene barrier at Matakana Island, Bay of Plenty, New Zealand. *New Zealand Journal of Geology and Geophysics*, 43(4), 579-586.
- Shepherd, M. J., McFadgen, B. G., Betts, H. D., & Sutton, D. G. (1997). Formation, landforms and palaeoenvironment of Matakana Island and implications for archaeology. *Science and Research Series*, 102.
- Stagpoole, V., & Miller, C. (2021). The attraction of New Zealand: Gravity anomalies of the Taupo Volcanic Zone. Research Outreach. DOI: 10.32907/RO-124-1540342150
- Stagpoole, V., Miller, C., Caratori Tontini, F., Brakenrig, T., & Macdonald, N. (2021). A two million-year history of rifting and caldera volcanism imprinted in new gravity anomaly compilation of the Taupō Volcanic Zone, New Zealand. *New Zealand Journal of Geology and Geophysics*, 64(2-3), 358-371. <https://doi.org/10.1080/00288306.2020.1848882>
- Stokes, D., Healy, T., & Mason, N. (2009). The benthic ecology of expanding mangrove habitat, Tauranga Harbour, New Zealand. In *Coasts and Ports 2009: In a Dynamic Environment*(pp. 504-511). [Wellington, NZ]: Engineers Australia.
- Tenzer, R., & Wiart, A. (2014). Evidence of the El Niño/La Niña climatic events in New Zealand over the last century. *GSTF Journal of Geological Sciences (JGS)*, 1(2).
- Tonkin and Taylor. (2018). Tauranga Harbour Coastal Hazards Study. *Coastal Erosion Assessment*: Bay of Plenty Regional Council.
- Van Dissen, R., & Heron, D. (2003). Earthquake fault trace survey, Kapiti Coast District. *Institute of Geological & Nuclear Sciences Client Report*, 77.
- Villamor, P., Berryman, K., Ellis, S., Schreurs, G., Wallace, L., Leonard, G., Langridge, R., & Ries, W. (2017). Rapid evolution of subduction-related continental intraarc rifts: The Taupo Rift, New Zealand. *Tectonics*, 36(10), 2250-2272. <https://doi.org/10.1002/2017TC004715>.
- Watson, H. M. (2016). *Potential impacts of wharf extensions on the hydrodynamics of Stella Passage and upstream regions of Tauranga Harbour, New Zealand* (Doctoral dissertation, University of Waikato).
- White, P. A., Meilhac, C., Zemansky, G., & Kilgour, G. (2008). Groundwater resource investigations of the Western Bay of Plenty area stage 1—conceptual geological and hydrological models and preliminary allocation assessment. *GNS Science consultancy report*, 240, 221.